DOKUZ EYLÜL UNIVERSITY

GRADUATE SCHOOL OF NATURAL AND APPLIED SCIENCES

INVESTIGATING THE SWELLING BEHAVIOR OF COMPACTED HIGH PLASTICITY CLAYS

by

Gül BORAN

January, 2017

İZMİR

INVESTIGATING THE SWELLING BEHAVIOR
OF COMPACTED HIGH PLASTICITY CLAYS

A Thesis Submitted to the
Graduate School of Natural and Applied Sciences of Dokuz Eylül University
In Partial Fulfillment of the Requirements for the Degree of Master of Science
in Civil Engineering, Geotechnical Engineering Program
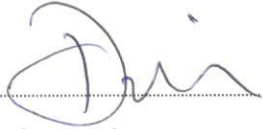
by
Gül BORAN

January, 2017
İZMİR

M.Sc THESIS EXAMINATION RESULT FORM

We have read the thesis entitled **"INVESTIGATING THE SWELLING BEHAVIOR OF COMPACTED HIGH PLASTICITY CLAYS"** completed by **GÜL BORAN** under supervision of **ASSIST.PROF. DR. MEHMET KURUOĞLU** and we certify that in our opinion it is fully adequate, in scope and in quality, as a thesis for the degree of Master of Science.
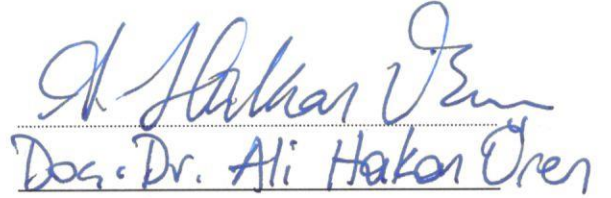
Assist. Prof. Dr. Mehmet KURUOĞLU

Supervisor

Yrd.Doç. Dr. Devrim Erdoğan

(Jury Member)

Doç. Dr. Ali Hakan Ören

(Jury Member)

Prof. Dr. Emine İlknur CÖCEN

Director

Graduate School of Natural and Applied Sciences

ACKNOWLEDGEMENTS

INVESTIGATING THE SWELLING BEHAVIOR OF COMPACTED HIGH PLASTICITY CLAYS

ABSTRACT

Mixtures obtained by adding granular materials to high plasticity clays are used as impermeable soil liners at solid waste landfill sites. When compacted clay mixtures are used as impermeable liners, they are required to have low hydraulic conductivity, high swelling capacity, good self-sealing, and a good radionuclide adsorption. In general, high plasticity clay part is constituted from bentonite, and sand is preferred for the granular part of these mixtures. As an alternative to sand, zeolite is considered for the granular part of the mixtures because Turkey is ranked third place in the world for the zeolite reserve. However, while sand in the mixture is replaced with zeolite, the hydraulic conductivity of compacted clay increases. In order to investigate the cause of the increase in hydraulic conductivity, swelling behavior of zeolite-bentonite mixtures and pure bentonite samples were investigated in this study.

The reason for the difference between the hydraulic conductivities of sand-bentonite mixtures (SBMs) and zeolite-bentonite mixtures (ZBMs) are not completely understood. Researches on that subject have been still under progress. In this study, the swelling behavior of ZBMs was investigated and the results were compared with the swelling behavior of SBMs, the attempt being made to clarify the effect of swelling behavior on hydraulic conductivity. For this purpose, samples of ZBMs with different bentonite contents were prepared and subjected to swelling tests. Samples with three different bentonite contents were prepared: ZBMs with 20% bentonite (80% zeolite + 20% bentonite) and 30% bentonite (70% zeolite + 30% bentonite) contents, and 100% bentonite samples.

First, compaction tests were performed on the samples of the ZBMs with 20% and 30% bentonite contents (20% ZBM and 30% ZBM), and maximum dry unit weight and optimum water content values were determined. Samples of the swelling tests were prepared at the optimum water content values. For swelling tests the samples of two different ZBMs and samples of pure bentonite were prepared and subjected to the tests under different effective vertical stresses (1, 2.5, 5, 12.5, 25, 50, 100 kPa). Besides, in order to investigate the effect of compactive effort on swelling behavior, 100% bentonite samples were prepared in the ring by applying either 25 or 10 blows on the samples. The swelling behavior of ZBMs were investigated depending on the structural, physicochemical, and geotechnical properties of zeolite and bentonite, and according to the bentonite content, final void ratio, swelling strain, and the effect of compactive effort.

Keywords: Swelling behavior, zeolite, bentonite, effective vertical stress, final void ratio, swelling strain, compactive effort.

SIKIŞTIRILMIŞ YÜKSEK PLASTİSİTELİ KİLLERİN ŞİŞME DAVRANIŞININ ARAŞTIRILMASI

ÖZ

Yüksek plastisiteli killere granüler malzeme eklenerek oluşturulan karışımlar, katı atık depolama alanlarında geçirimsiz zemin tabakaları olarak kullanılmaktadırlar. Sıkıştırılmış killi karışımlar geçirimsiz tabaka olarak kullanıldıklarında, bu tabakaların düşük hidrolik iletkenliğe, yüksek şişme kapasitesine, iyi bir kendinden-sızdırmazlık kapasitesine ve iyi bir radyonüklid adsorpsiyona sahip olmaları beklenmektedir. Bu tabakaların genellikle yüksek plastisiteli kil kısmı bentonit, granüler kısmı ise kum olacak şekilde teşkil edilmektedirler. Granüler malzeme için kuma alternatif olarak, dünyadaki rezerv kapasitesi bakımından Türkiye'nin üçüncü sırada olduğu zeolitin kullanılması düşünülmektedir. Karışımda zeolit kumun yerini aldığında, sıkıştırılmış kil tabakasının hidrolik iletkenliği artmaktadır. Hidrolik iletkenliğin artış sebebini şişme davranışı açısından incelemek amacıyla, bu çalışmada sıkıştırılmış kil içeren zeminler olarak zeolit-bentonit karışımlarının ve saf bentonit numunelerinin şişme davranışları incelenmiştir.

Kum-bentonit ve zeolit-bentonit karışımlarının hidrolik iletkenlikleri arasındaki farkın nedeni henüz tam olarak anlaşılamamıştır. Bu konudaki araştırmalar devam etmektedir. Bu çalışmada, zeolit-bentonit karışımlarının şişme davranışı araştırılarak ve literatürde mevcut olan kum-bentonit karışımlarının şişme davranışlarıyla karşılaştırılarak, şişme davranışının hidrolik iletkenlik üzerindeki etkisi aydınlatılmaya çalışılmıştır. Bu amaçla farklı bentonit oranlarında zeolit-bentonit karışım örnekleri hazırlanarak, bunların üzerinde şişme deneyleri gerçekleştirilmiştir. Deneyler için üç farklı karışım oranında; %20 bentonit (%80 zeolit ve %20 bentonit) ve %30 bentonit (%70 zeolit ve %30 bentonit) içeren zeolit-bentonit karışımları ile % 100 bentonitten oluşan numuneler hazırlanmıştır.

Öncelikle, %20 ve %30 bentonit içeren zeolit-bentonit karışımları (%20 ZBM ve %30 ZBM) üzerinde kompaksiyon deneyleri yapılarak, maksimum kuru birim hacim

ağırlık ve optimum su içeriği değerleri belirlenmiştir. Şişme deneylerinde kullanılacak numuneler, kompaksiyon deneyleri sonucunda belirlenen optimum su içeriklerinde hazırlanmıştır. Şişme deneyleri, iki farklı bentonit oranına sahip zeolit-bentonit karışımından oluşan numuneler ile %100 bentonitten oluşan numuneler üzerinde ve farklı efektif düşey gerilmeler altında (1, 2.5, 5, 12.5, 25, 50, 100 kPa) gerçekleştirilmiştir. Ayrıca, sıkıştırma enerjisinin şişme davranışı üzerindeki etkisinin araştırılması amacıyla, %100 bentonit numuneleri ring içerisinde 25 ve 10 darbe uygulanarak iki farklı sıkıştırma enerjisi altında hazırlanmıştır.

Zeolit-bentonit karışımlarının şişme davranışı, karışımı oluşturan zeolit ve bentonitin yapısal, kimyasal ve geoteknik özellikleri ile bentonit içeriği, nihai boşluk oranı, şişme birim deformasyonu ve sıkıştırma enerjisinin etkisine bağlı olarak araştırılmıştır.

Anahtar Kelimeler: Şişme davranışı, zeolit, bentonit, efektif düşey gerilme, nihai boşluk oranı, şişme birim deformasyonu, sıkıştırma enerjisi.

CONTENTS

LIST OF FIGURES

LIST OF TABLES

CHAPTER ONE
INTRODUCTION

1.1 Introduction

Various methods are developed for eliminating the solid wastes by using appropriate techniques. For this purpose, regular solid waste landfill sites are constructed by selecting suitable areas in the cities. The most important problem in the regular landfill sites is the infiltration of leachate to ground water through the soil. In order to avoid that infiltration, soil layers with high impermeabilities are needed at the sites. The objective for the impermeable liner used at solid waste landfill sites is to prevent any leachate infiltration to ground water or to reduce infiltration to a minimum. The most important parameter to be considered in line with that target is hydraulic conductivity. The value of hydraulic conductivity must not exceed $1.0x10^{-9}$ m/s (Kayabalı and Kezer, 1998). In soils, the most appropriate impermeability values can be provided by clays. Because clay in the soil absorbs water, it creates a tendency to lower the hydraulic conductivity of the soil layer (Ören 2007). Impermeability characteristics are related to high swelling capacity. While clayey soil swells by absorbing water, its hydraulic conductivity decreases. Therefore, examination of the swelling behavior of the impermeable soil liners containing clay to be used at solid waste landfills has great importance.

High plasticity clays have low hydraulic conductivity, high swelling capacity and high adsorption capacity. At solid waste landfill sites where liners containing high plasticity clays are used, the desirable impermeability can be obtained. The radioactive materials can be retained within the liner due to the cation exchange capacity of clay minerals (Komine and Ogata, 1999).

It is possible to use HDPE (high density polyethylene) liners or other polymer liners as impermeable layers at solid waste landfill sites instead of clay liners. Although the synthetic liners could be an appropriate solution to the infiltration problem they degrade in time and at some point they lose their function and become

unable to prevent the leakage of leachate. On the other hand, clay liners are natural materials, they are cheap and easy to obtain, and they are able to resist for longer periods (Cho et al., 1999).

Clay soils swell when they absorb water and conversely shrink when the water dries up; this is one of the main characteristics of the clay soils. If the soil shrinks more than it had swelled, cracks occur in the soil and as a result the impermeability is damaged and the leachates infiltrate through those cracks and flow into ground water. Liners made up of pure clay soils which do not contain granular materials are not resistant and swelling-shrinkage behavior leads to cracks in a short time. In order to avoid formation of cracks, granular materials are mixed with clay soils (Kayabalı, 1997). In mixtures prepared in the said way, the granular part controls volumetric shrinkage while the clay part controls hydraulic conductivity.

When preparing bottom liner for solid waste landfill sites, generally sand employed for the granular part and bentonite is employed for the clay part because of void-filling capacity by swelling. Among the different types of clay, bentonite is the one with the lowest hydraulic conductivity for filling voids in the mixture by its swelling capacity. SBMs are able to provide the desired hydraulic conductivity. But due to the lack of the adsorption capacity of sand, sand-bentonite mixtures cannot afford to prevent leachates from flowing into ground water (Kleppe and Olson, 1985).

In order to eliminate this disadvantage, zeolite, which is another material with granular structure, has in the recent times begun to be used as an alternative to sand. Zeolite is charged with negative ions and has a high cation exchange capacity. Thanks to this characteristic, it can act as a chemical sieve that retains polluants within itself. Consequently, the substitution of zeolite for sand yields a desirable result by preventing radioactive materials from infiltrating through the liner. Another advantage for using zeolite is its abundancy in Turkey. There are rich zeolite reserves, notably in Bigadiç, Ankara Polatlı Mülk Oğlakçı Region, Şaphane, Gediz,

2

Emet and Gördes locations (Kaya and Durukan, 2004). Turkey is ranked third among countries having the largest zeolite reserves in the World.

Although a limited number of the studies have been made on ZBMs, the test conditons of those studies differ within each other (Kayabalı and Kezer, 1998, Kayabalı and Mollamahmutoğlu, 2000). Additionally, field conditions may not coincide with the test conditons, completely (Kayabalı, 1997). In those studies the hydraulic conductivity of ZBMs is higher than that of sand-bentonite mixtures (Ören et al., 2011). There has not yet been any study in the literature about the change of the swelling behavior by using zeolite instead of sand. That is why this study's aim is to make contribution with findings to the literature. The attempt is also here made to make the effect of swelling on hydraulic conductivity more understandable.

In the research on literature about ZBMs, only hydraulic conductivitiy tests and volumetric shrinkage tests had been made. When tests on swelling behavior are researched, it is seen that the swelling tests on SBMs and pure bentonite are remarkable. If the swelling behavior of ZBMs is questioned it is seen that the mechanism causing swelling behavior is not revealed, precisely. Therefore an aim of this study is to make a significant contribution by rendering swelling behavior of ZBMs and the mechanism leading to swelling more comprehensible.

1.2 Background

1.2.1 Hydraulic Conductivity of ZBMs and SBMs

Mollins et al. (1996) applied hydraulic conductivity tests and swelling tests to pure Na-Bentonite samples and SBMs with different bentonite contents (having 5%, 10% and 20% bentonite). In order to determine the hydraulic conductivities of the samples, the clay void ratio calculation was made. When pure bentonite reaches the final step of swelling, it is observed that the void ratio-effective vertical stress curve gets closer to horizontal. Swelling of SBMs is expressed in terms of "clay void ratio". Swelling amount of the mixtures differs from pure bentonite above a certain

value of effective vertical stress. That threshold value changes with change of the bentonite content in the mixture. Clay in the mixture under the threshold value is able to swell and by swelling it separates the sand grains from each other for reaching the same clay void ratio. That behavior is shown in Figure 1.1. For the applied stress values higher than the threshold value, the material reacts in a way to compensate that excess, in such a case the clay void ratio becomes greater and the clay tries to fill in the voids of sand grains while they are contacted with each other completely or partially. The threshold stress value decreases as the clay content of the mixture decreases. Hydraulic conductivity of SBMs can be estimated with the help of the bentonite ratio, sand porosity and applied effective vertical stress. Bentonite in the mixtures with very low bentonite content is dispersed in a disordered array and consequently a higher hydraulic conductivity value is obtained.
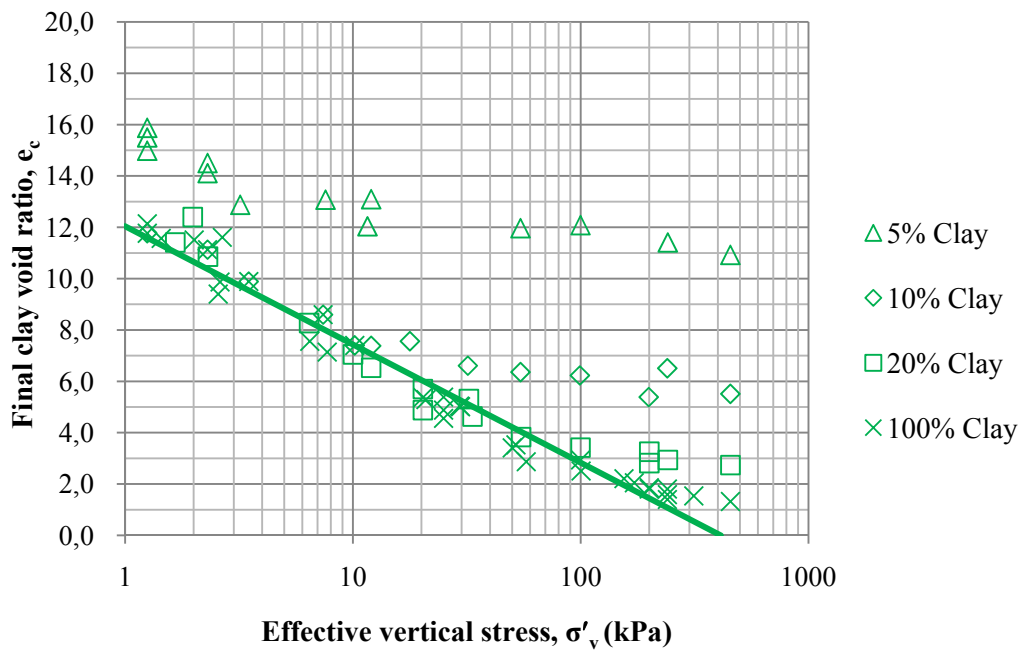
Figure 1.1 Final clay void ratio after swelling of the sand-bentonite mixtures (Mollins et al., 1996)

In another study, seven ZBMs with different bentonite contents (5%, 10%, 15%, 20%, 26%, 33%, 40%) were prepared at optimum water contents, and hydraulic conductivity tests were conducted on them (Kayabalı, 1997). The hydraulic conductivity value (k) of the ZBMs containing more than 5% bentonite varies in the range of 2×10^{-8} - 4×10^{-8} cm/s. Owing to their low hydraulic conductivity values, the

ZBMs with 5% - 10% bentonite contents are suitable for an ideal impermeable liner. Utilization of ZBMs for constructing landfill liners as an alternative to clay liners will result in the decrease of the thickness of the liner employed for preventing groundwater pollution. Increasing the bentonite content does not affect the hydraulic conductivity of the mixture, significantly. The hydraulic conductivity value of the mixture with the lowest bentonite content is 1×10^{-8} cm/s. The coefficient of permeability values of ZBMs stay within the limits of the values required for impermeable layers.

In their study, Kayabalı and Mollamahmutoğlu (1999) conducted tests on the effects of hazardous liquid wastes on the permeability of the six different mixtures. Sand or natural zeolite was used in the granular part of the mixture and bentonite or microcement was used in the clay part or as an additive. Only two mixtures showed a good performance against chemical effects in the applied tests.

The following results can be deduced from the studies on the permeabilities of the mixtures subjected to the effects of chemicals:

- The effect of chemicals of high acidity on SBMs increases as the bentonite content of the mixture increases.

- A SBM containing 15% bentonite and a ZBM containing 10% bentonite are more resistant to the chemicals with high acidity than others included in the sample group on which tests were applied (bentonite/sand ratio: 0.05, 0.10, 0.15; bentonite/zeolite ratio: 0.10; microcement/sand ratio: 0.10; and microcement/zeolite ratio: 0.10). The coefficient of permeability of the ZBM containing 10% bentonite was found in the range 10^{-8}-10^{-7} cm/s.

- The desired hydraulic conductivity cannot be obtained when the microcement is mixed with sand or zeolite.

The aim of the study of Komine (2004) was to find the hydraulic conductivities of SBMs with various bentonite contents (5-50%), and different dry unit weights (1.43-1.79 Mg/m^3) through experiments. Furthermore, the relationship between hydraulic conductivity and the bentonite content was investigated through the swelling behavior of bentonite. The study stated that hydraulic conductivity is an important parameter for volumetric swell deformation of montmorillonite. According to the test results, the hydraulic conductivity of SBMs with 5-20% bentonite content is in the range 2.66×10^{-10}- 4.85×10^{-12} m/s, and that of the mixtures with 30-50% bentonite content is in the range 6.87×10^{-12} -1.21×10^{-12} m/s.

In the study of Kaya and Durukan (2004), adsorption characteristics of Na-bentonite and Ca-bentonite; cation exchange capacities of Na-bentonite and natural zeolite; volumetric shrinkages, compaction characteristics, and hydraulic conductivities of ZBMs (with 10%-20% bentonite contents) were determined. Both of the hydraulic conductivity values of ZBMs with 10% and 20% bentonite contents were lower than 1×10^{-9} m/s. That value is within the limits required for impermeable liners. When compaction characteristics of ZBMs are considered, the dry unit weight is found less than those of the other mixtures containing clays. While the dry unit weight of ZBM varies from 12.7 kN/m^3 to 12.0 kN/m^3, when bentonite content of ZBMs increases from 3% towards 20%. As the bentonite content of the mixture increases, the dry unit weight decreases and optimum water content increases. According to the shrinkage results, the optimum water content of ZBMs prepared with 3-5% wet of optimum water content should be less than 4%. This value of 4% is the upper limit for the barrier materials. The hydraulic conductivity value of the ZBM with 10% bentonite content is lower than 1×10^{-9} m/s. That value is accepted by most public institutions. Based on the laboratory results, it can be said that ZBMs are superior to SBMs because of the high adsorption capacity of zeolite. The higher adsorption capacities of ZBMs compared to those of SBMs provide an advantage for using them as impermeable barriers.

In the study of Ören et al. (2011), hydraulic conductivity tests were conducted on ZBMs, SBMs, and zeolite-sand-bentonite mixtures (ZSBMs) with unique bentonite

content. When the ZBMs and the SBMs with the same bentonite content were compared it was seen that the hydraulic conductivity value of ZBMs was higher than that of SBMs. Furthermore the hydraulic conductivity value of the ZBM with 30% bentonite content was higher than that of the SBM with 10% bentonite content. The higher value of the hydraulic conductivity of the ZBM compared to the SBM is due to the porous structure of zeolite. Zeolite grains constitute a network frame in the ZBM. This network helps the flow of water into the mixture. Besides, compaction characteristics of ZBMs were investigated also in the study. The obtained results were compared with those of SBMs. The results of compaction tests revealed that maximum dry unit weights of ZBMs are less than that of SBMs for each bentonite contents. On the contrary, optimum water contents of ZBMs are more than those of SBMs. It can be inferred from these facts that optimum water content of SBMs increases with the addition of zeolite grains, whereas maximum dry unit weight decreases. According to the hydraulic conductivity tests, it was determined that the hydraulic conductivity value of ZBMs with 10% bentonite content is 22 times higher than that of SBMs with 10% bentonite content. While the hydraulic conductivity value of ZSBMs is less than that of ZBMs, it is higher than that of SBMs. When another sample was examined it was determined that the hydraulic conductivity value of a ZBM with 20% bentonite content is 28 times higher than that of a SBM with the same bentonite content. Increasing the bentonite content of a ZBM decreases the hydraulic conductivity value to some extent. However, the hydraulic conductivity value of a ZBM with 30% bentonite content is higher than than that of a SBM with 10% bentonite content. Hydraulic conductivity values of ZBMs are higher than than those of SBMs for all the bentonite percentages, because water shows tendency to flow through the zeolite network.

Bentonite water content calculations for ZBMs and SBMs were made by considering the SBM model. That model was suggested by Kenney et al. (1972). In the suggested model it was assumed that the sand portion did not take the water. Some modifications were made in the model because of the relationship of zeolite with water in Ören et al. (2011). When the bentonite water content calculation was made according to the modified model and by taking the bentonite content of the

mixture into consideration it was seen that the bentonite water content of a ZBM is less than that of a SBM. This is because of the fact that the volume of voids between the bentonite particles is larger in ZBMs. The increase of the volume of voids in ZBMs makes the water flow easier not only through the zeolite network but also through the voids between the bentonite particles. In the study of Ören et al. (2011), the hydraulic conductivity value of ZBMs was found higher than those found in the previous studies.

In the study of Ören et al. (2014), hydraulic conductivity values of SBMs were compared with those of ZBMs. While the hydraulic conductivity values of SBMs are not affected by compaction water content and bentonite content, those of the ZBMs are affected by those parameters. The hydraulic conductivity value of a ZBM with 10% bentonite content decreases gradually as the compaction water content increases towards the optimum water content and tends to decrease rapidly when the water content exceeds optimum. In contrast, the hydraulic conductivity value of a ZBM with 20% bentonite content sharply decreases at the early stages of compaction water content (i.e. on the dry side of optimum water content). However, there is at least one order of magnitude difference between the hydraulic conductivities of ZBMs and SBMs, supporting the zeolite network model as suggested in previous studies.

1.2.2 Swelling of SBMs

In the study of Cui et al. (2012), swelling tests were conducted on GMZ SBMs with different sand contents (0%, 10%, 20%, 30%, 40%, and 50%). In the examination of the test results it was seen that swelling took place at three stages: Primary swelling, secondary swelling and swelling deformation following a sigmoid relationship with time. In that study, it was found that with constant initial dry unit weight, the maximum swelling pressure presents an exponential increase and the maximum swelling deformation increases linearly. As the sand content increases, the maximum swelling pressure decreases exponentially while the maximum swelling strain follows a quadratic decrease. It is seen that an increase of initial dry unit weight increases the swelling characteristics of GMZ SBMs. Furthermore, an

increase of sand content affects the maximum swelling pressure more than maximum swelling deformation. In order to evaluate the relationship between the effective clay density and swelling characteristics, new equations were suggested in the study. The method suggested for compacted GMZ SBMs was supported by a combination of the effective clay density expressions and new equations. The feasibility of that method was investigated by comparison of the curves showing the relationship between the swelling deformation and the swelling pressure that were drawn according to the test results of GMZ SBMs. Experimental data showed satisfactory results, so these equations can predict the swelling characteristics of GMZ SBMs with various sand contents and initial dry unit weight within a certain numeric area.

In the study of Sun et al. (2013) swelling tests were conducted in order to investigate swelling characteristics of pure GMZ bentonite and SBMs by using distilled water. The test results showed that the relation between the void ratio and the swelling pressure of fully saturated and compacted GMZ SBMs is independent of the initial conditions (such as the initial dry unit weight and initial water content) and dependent on the bentonite/sand ratio. An empirical equation was suggested to calculate the swelling deformation and swelling pressure of the mixture. The swelling capacities of GMZ, Kunigel-V1 and MX-80 bentonite types were discussed in the study. Swelling tests under constant vertical stress were applied on twenty-seven samples. The samples had different bentonite/sand ratios: 100/0%, 70/30%, 30/70%, 20/80%, and 10/90%. The initial dry unit weight and initial water content of each sample were different. Swelling deformation due to wetting depends on the bentonite content and initial density of the mixture. When the bentonite content of the mixture is high (bentonite/sand ratio: 100/0%, 70/30%, etc.), the relationship between effective vertical strain and the void ratio is determined by bentonite content. Under the same vertical stress, the mixture with higher bentonite content gets a higher final void ratio. The final void ratio is the void ratio at which deformation of the saturated samples is stable. The final void ratio-vertical stress relationship is linear on a logarithmic scale without regarding initial dry unit weight and initial water content. Therefore, under a certain stress, the void ratio of the fully saturated mixture is independent of the initial conditions (such as the initial dry unit

weight and initial water content). In that case the void ratio of the mixture depends on the bentonite content of the mixture. When the bentonite content is low, the sand skeleton structure could be the determinative in the void ratio-vertical stress relationship. This phenomenon can be explained in the way that the vertical stress is borne mainly by the sand skeleton. Intergranular voids in the skeleton are wide enough to freely allow bentonite swell. Swelling of bentonite fills up the voids while the mixture taking water but does not lead to the swelling of the sample. The void ratio-vertical stress relationship of the samples with low bentonite contents is shown in Figure 1.2. The void ratio under the vertical stress changes slightly as the bentonite ratio decreases. In other words the swelling potential of bentonite disappears in the voids between the grains. That is why the swelling characteristics of the sample cannot be understood precisely.
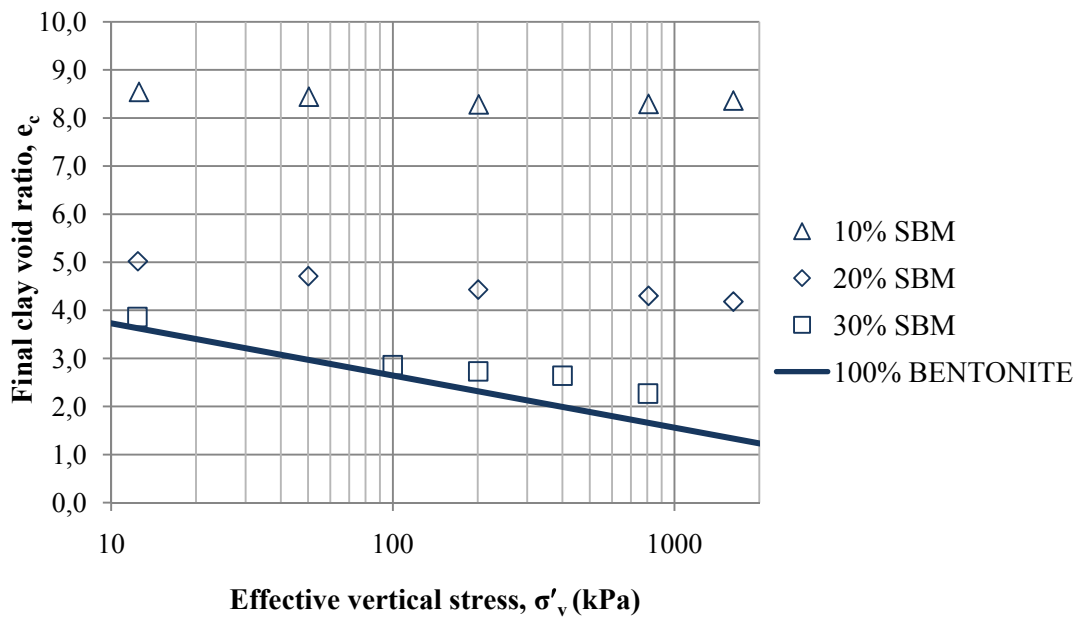
Figure 1.2 e_c-σ'_v relationship of GMZ SBMs with low bentonite contents at full saturation
(Sun et al., 2013)

The curve illustrating the final clay void ratio-effective vertical stress relationship shows that the compactibility of the mixture decreases as the sand content increases. The compactibility of the mixtures with low bentonite content (e.g. a bentonite/sand ratio of 10/90%) is low just at is the case for pure sand. Therefore the final clay void

ratio-effective vertical stress relationship in the mixtures with low bentonite content is dependent on the inital density of the mixture.

1.3 Scope of The Study

It is known that there is a distinctive difference between hydraulic conductivity of ZBMs and that of SBMs. That difference is due to the void structure of the mixtures. In order to understand the void structure, swelling tests are made. Because of its high swelling capacity, bentonite has a significant effect on swelling behavior. Bentonite contained in zeolite-bentonite mixtures and sand-bentonite mixtures tries to fill the voids in the mixtures. The mixture with fewer voids will swell more with the effect of bentonite. In order to understand thoroughly the void structures of ZBMs, this study attempted to investigate the swelling behavior of ZBMs with different bentonite contents.

With this in mind, the swelling tests were conducted on the samples of ZBMs with different bentonite contents and the pure bentonite samples under different effective vertical stresses. Swelling tests were made in the Soil Mechanics Laboratory of Civil Engineering Department, Dokuz Eylül University. They were made by placing compacted wet mixtures into the cells and left for swelling under the effective vertical stress range 1-100 kPa, and the swelling amounts of the two different ZBMs (20% and 30% bentonite contents) and that of the pure bentonite (100% bentonite) were determined. The findings of the tests of the ZBMs with 20% bentonite content were compared with the findings of the tests of the SBMs with 20% bentonite content, which were previosly made in another research in the same laboratory. The same bentonite sample supplied by the same firm was used in both the ZBMs of 20% bentonite content and the SBMs of 20% bentonite content - besides that zeolite and bentonite shows similar grain size distribution. Thus the aim was to determine the mixture in which the swelling capacity of bentonite operated better. Graphs showing the void ratio-effective vertical stress relationships of ZBMs and SBMs were drawn. In case of the pure bentonite tests, the samples were

compacted by applying 25 and 10 blows and so the effect of the compactive effort on swelling behavior was investigated.

1.4 Outline of The Thesis

This thesis is composed of seven chapters. In the first chapter, the "Introduction" indicates the purpose and scope of the study, and the subtitle "Background" discusses the journal articles gleaned from the literature that helped the understanding of the subject. The second chapter explains the geotechnical properties of soil materials used in this study, soil mechanics laboratory tests conducted within the scope of this study, and the preparation of soil mixture samples, test equipment, and procedures. The third chapter discusses the swelling behavior of pure bentonite, the effect of effective vertical stresses on the swelling behavior, and the investigation of the presence or absence of the effect of the compactive effort applied on the pure bentonite samples while they are being prepared in the rings. Swelling behavior of the pure bentonite samples under the effective vertical stresses 1, 2.5, 5, 12.5, 25, 50, and 100 kPa are examined in detail. The fourth chapter examines the swelling behavior of ZBMs with respect to the bentonite contents of the mixtures and the effective vertical stresses. The samples of ZBMs were prepared with 20% and 30% bentonite contents. These samples were subjected to swelling tests under the effective vertical stresses 1, 2.5, 5, 12.5, 25, 50, and 100 kPa. The fifth chapter interprets the swelling behavior of SBMs and ZBMs. The compared SBMs were prepared with 10% and 20% bentonite contents. The sixth chapter discusses the results of the conducted tests. The seventh and last chapter gives the obtained results and suggestions for future studies.

CHAPTER TWO
MATERIALS AND METHODS

This chapter first addresses the physical properties, chemical compositions and general geotechnical characteristics of the soil materials used in this study. Then the test equipment of the soil mechanics laboratory, test methods, and preparation of soil samples are explained.

2.1 Materials

2.1.1 General Properties of Zeolite and Bentonite Materials

The tests conducted in this study used ZBMs having 20% and 30% bentonite content. The bentonite used in the ZBMs is Na-bentonite, which is composed of Na-smectite (77%), minor cristobalite (10%), plagioclase (6%), quartz (4.5%), and illite (2.5%). The zeolite was supplied by Rota Madencilik A.Ş., the bentonite was supplied by Karakaya Bentonit Sanayi ve Ticaret A.Ş. The physical properties of bentonite are given in Table 2.1 and its chemical components are given in Table 2.2.

The physical properties, chemical components, and mineral compositions of zeolite are given in Tables 2.3, 2.4 and 2.5, respectively.

Table 2.1 Pysical Properties of Bentonite (Karakaya,n.d.)

600 d/d reading value on fann 35 viscometer	30 min.
Filtration amount	12.5cc max.
Yield	80 bbl. min.
Humidity	2.5% max (by weight)
Wet screen analysis 200 Mesh (75 mic.) oversize	10% max (by weight)
Yield point plastic viscosity ratio (YP/PV)	1.5 max.
Dispersed plastic viscosity (conditioned by adding 5 ml sodium hexametaphosphate of 10% content to the 350 ml mixture at room temperature.)	10 cp min.
Ratio of the conditioned YP*/PV*'nin tol normal YP/PV (the conditioning was made under pressure of 200 psi and dynamic conditions at 3450 F during 16 hours and the mixture was cooled at room temperature)	1.5 min.
Ratio of Normal YP/PV to dispersed YP**/PV** (**dispersed values were measured in the mixtures prepared with 3% H_2O_2 content)	3 max

Table 2.2 Chemical composition of bentonite (Karakaya, n.d.)

Component	Ratio
SiO_2	61.28%
Al_2O_3	17.79%
Fe_2O_3	3.01%
CaO	4.54%
Na_2O	2.70%
MgO	2.10%
K_2O	1.24%

Table 2.3 Physical properties of the zeolite (Rota Madencilik, n.d.)

Appearance	Ivory white	Oil Absorption (ml/100g)	57	Solubility	None
Smell	None	Wear (mg/100g)	87	Plasticity	Minor
Porosity	45-50%	Single point surface area	39 m^2/g	Softening	1150 ^{0}C
Hardness	2-3 Mohs	Micropore Area	11 m^2/g	Melting	1300 ^{0}C
Sludging	None	Mesopore Area	29 m^2/g	Mass density	650-850 kg /m^3
Water Absorption	42-50%	Efficient Pore Diameter	4 Angstrom	pH	7.0-8.0

Table 2.4 Chemical composition of the zeolite (Rota Madencilik (G.T), July 15, 2016, data was obtained from the website)

SiO_2	65 – 72 %	Fe_2O_3	0.8 – 1.9 %	MnO	0 – 0.08 %
Al_2O_3	10 – 12 %	MgO	0.9 – 1.2 %	Loss on ignition	% 9 - 12
CaO	2.5 – 3.7 %	Na_2O	0.3 - 0,65 %		
K_2O	2.3 – 3.5 %	TiO_2	0 – 0.1 %	SiO_2/Al_2O_3	5.4 – 6.0 %

Table 2.5 Mineral contents of the zeolite (Rota Madencilik, n.d.)

Clinoptilolite	58 %	Montmorillonite	2 – 5 %	Muscovite	0 – 3 %
Feldspar	3 – 5 %	Cristobalite	0 – 2 %		

Table 2.6 gives the specific gravity, consistency limits (liquid limit and plastic limit), plasticity index and mineralogical properties of the zeolite and bentonite. While the liquid limit of bentonite is 405%, zeolite is a non-plastic material. On the other hand, when it is examined with respect to mineralogy it is seen that the smectite ratio in zeolite is negligible. A low smectite ratio and non-plastic behavior can be interpreted as an indicator of the absence of the clay properties in zeolite.

Table 2.6 Comparison of zeolite's and bentonite's properties

Properties	Zeolite	Bentonite
Specific gravity	2.31	2.71
Atterberg Limits		
Liquid limit (BS 1377)	Non-plastic	405%
Plastic limit	-	57%
Plasticity index	-	348%
Mineralogy		
Smectite ($^\beta$)	1%	77%
Cristobalite	-	10%
Quartz	-	4.5 %
Illite	-	2.5 %
Clinoptilolite	58%	-
Mordenite	41%	-

2.1.1.1 Zeolite

Zeolite is a member of the micro-porous solids group, a structure also described as "molecular sieves" (Blanchard et al., 1984; Zamzow and Murphy, 1992; Trgo and Peric, 2003; Ören and Kaya, 2006). Zeolite has a porous structure. Water, cations and various minerals can pass through the pore openings of zeolite easily (Jacobs & Förstner, 1999). Although zeolite takes in water while wetting as clay does, its

volume does not change due to the porous structure. In other words zeolite does not show swelling behavior while wetting.

The mineral structure has the shape of three dimensional cages that are assimilable to a honeycomb (Blanchard et al., 1984; Zamzow and Murphy, 1992; Trgo and Peric, 2003; Ören and Kaya, 2006). Zeolite consists of linked frameworks and channelles. Cages in the zeolite structure enable water to flow through the honeycomb-like structure easily. Also Al^{3+} ions, which can be exchanged by Si^{4+} ions, are present in the frameworks. Due to its cation exhange capacity, negative charge can be generated in the zeolite structure. The high exchange capacity enables zeolite to accommodate heavy metals in its structure and to act as a filter (Zamzow and Murphy, 1992). Zeolite types can be arranged as follows in the increasing order of cation exchange capacity, from the lowest to the highest:
mordenite < clinoptilolite < erionite < chabazite <philipsite (Zamzow and Murphy, 1992).

In Figure 2.1 the general formula of zeolite and the formula of the clinoptilolite type are given and its structure illustrated.
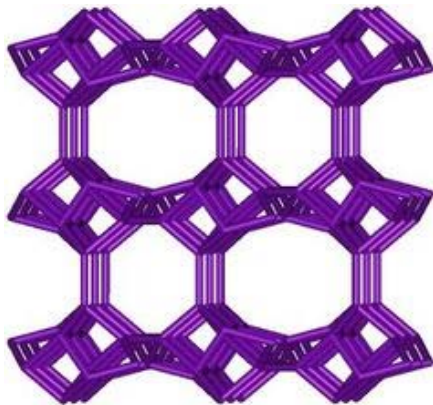
General formula: $M_{2/n}O.Al_2O_3.xSiO_2.yH_2O$

Clinoptilolite: $(Ca,K_2,Na_2,Mg)_4.Al_8Si_{40}O_{96}.24H_2O$

Figure 2.1 Zeolite structure, general formula of zeolite and formula of the clinoptilolite type of zeolite

2.1.1.2 Bentonite

Bentonite is natural clay consisted of montmorillonite minerals. It is a member of the smectite group. It has a large surface area (100-800 m^2/g), a net negative charge, and exchangeable surface ions. These are the advantages of montmorillonite. There are water and weak cation bonds between the silica and alumina sheets. Therefore bentonite can absorb water easily. A disadvantage of bentonite in use is its sensitivity to water: due to its chemical properties bentonitie swells when it is wetted and shrinks when it dries. Bentonite structure is shown in Figure 2.2.
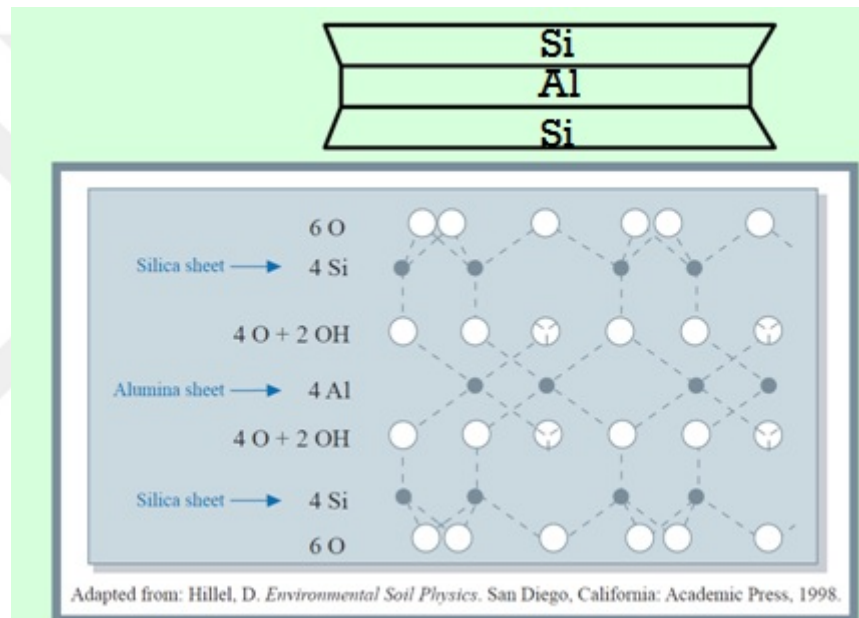
Figure 2.2 Bentonite structure

2.2 Method

ZBMs were prepared in the determined compositions (20-30%) and the planned tests of this thesis were conducted. The tests aimed to determine the geotechnical properties of the ZBMs. All the tests were made in the Soil Mechanics Laboratory of Civil Engineering Department at Dokuz Eylül University. The test procedures followed in all the tests were those described by the American Society for Testing and Materials (ASTM). Below, the sieve analysis, soil classification according to

USCS, and the findings of the compaction and swelling tests are presented, respectively.

2.2.1 Sieve Analysis

Grain size distribution curves of zeolite and bentonite are given in Figure 2.3. When those curves are examined it is seen that zeolite conforms to a grain distribution of coarse-grained soil and bentonite conforms to a grain size distribution of fine-grained soils.
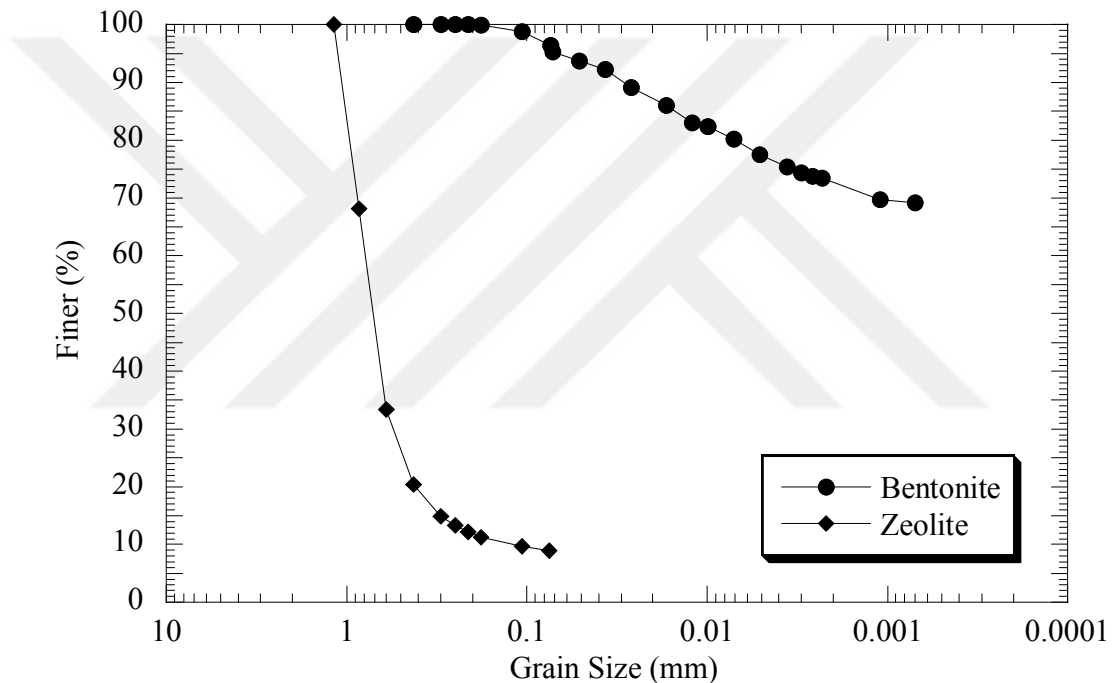
Figure 2.3 Grain size distribution curves of zeolite and bentonite

Zeolite

According to the grain size distribution curve, which is given in Figure 2.3, and the Unified Soil Classification System (USCS), zeolite material is classified as "SP-SM: Poorly Graded Sand and a little silt". The details of classification are given in the Appendix-A.

Bentonite

According to sieve analysis it was determined that 95% of bentonite material passed through a No.200 (0.076 mm) sieve. Bentonite has the characteristics of fine-grained soils (-No.200>50%) and according to the Unified Soil Classification System (USCS) it is classified as "CH: High Plasticity Clay" The details of classification is given in the Appendix-A.

2.2.2 Compaction Test

ZBMs were prepared at optimum water contents with 20% and 30% bentonite contents. Optimum water contents were determined by the compaction tests conducted in the soil mechanics laboratory. In order to investigate the compaction characteristics of the ZBMs with 20% and 30% bentonite contents, a Standard Proctor Compaction Test was applied to the samples of the mixtures in conformity to ASTM D698 Procedure. In order to obtain the mixtures with homogenous water contents, water was added to the initially dry samples by spraying. In order to keep their water contents, the wet samples were placed in plastic bags for 24 hours and the next day they were compacted by applying Standard Proctor Compaction Energy (593 kJ). With the Standard Proctor Compaction Tests, compaction values of the zeolite-bentonite mixtures (maximum dry unit weight and optimum water content) were obtained. Compaction curves of 20% ZBM and 30% ZBM are given in Figure 2.4.
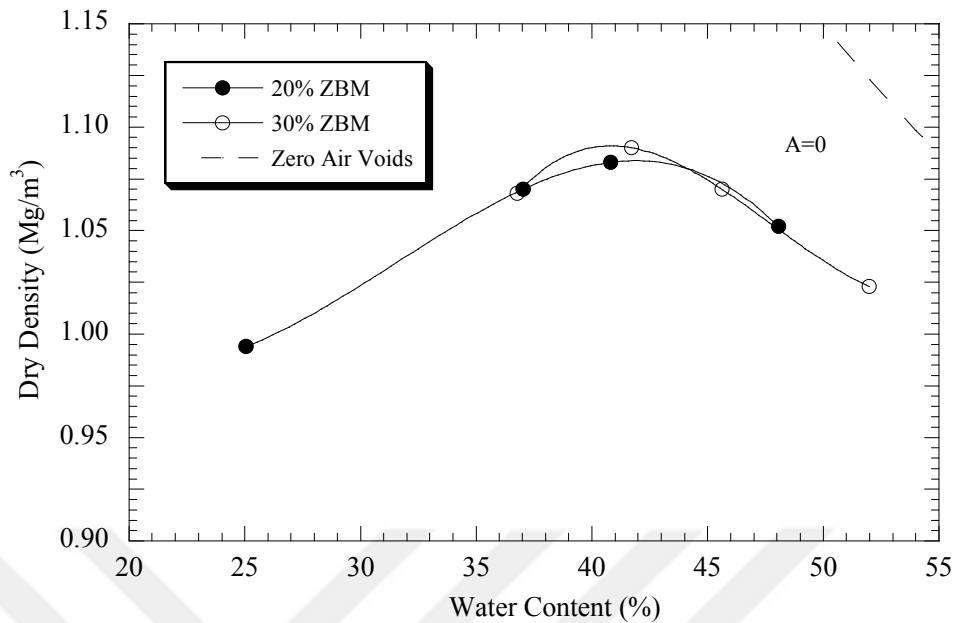
Figure 2.4 Compaction curves of zeolite-bentonite mixtures

According to Figure 2.4, the maximum dry density of 20% ZBM is 1.083 Mg/m^3 and its optimum water content is 42%, whereas the maximum dry density of 30% ZBM is 1.09 Mg/m^3 and its optimum water content is 41%. When the data of the compaction tests reported in the literature were examined, it was seen that the obtained compaction values were in accordance with those in the literature.

By using the maximum dry unit weight and optimum water content data of ZBMs in the literature a linear relationship was given in Figure 2.5 (Ören et al., 2014). While the upper part of the linear curve represents SBMs, the lower part represents ZBMs. That is to say, sand-bentonite mixtures have higher maximum dry unit weights and lower optimum water contents. The obtained results of ZBMs may indicate that zeolite has a porous structure. Location of the data representing compaction values of 20% and 30% ZBMs used in this study according to the linear curve obtained from the literature findings were shown in Figure 2.5. When the compaction values of ZBMs are examined in relation with the positioning of the linear curve in Figure 2.5 it is seen that they are in compliance with the linear curve; in other words they are similar to the ZBM values reported in the literature.

According to the Figure 2.4 and Figure 2.5, it can be seen that maximum dry unit weight of a ZBM with 30% bentonite content is a little higher than that of a ZBM with 20% bentonite content whereas its optimum water content is a little lower than the other. An increase of bentonite content does not cause a significant difference in the compaction values. The obtained compaction curves and compaction values are quite close to each other.
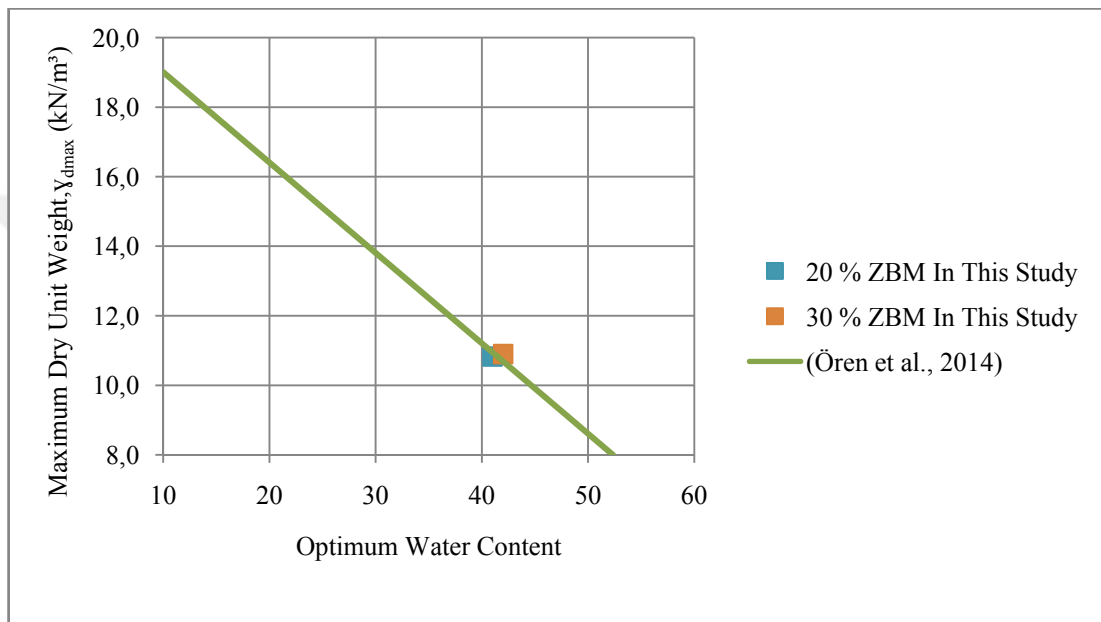
Figure 2.5 Positions of the compaction values of zeolite-bentonite mixtures with respect to the linear curve drawn with the data in the literature.

2.2.3 Swelling Tests

Three samples with different bentonite contents, 20% ZBM, 30% ZBM and 100% bentonite, were prepared for the swelling tests. The samples of 20% ZBM and 30% ZBM were prepared at optimum water content and they were placed in rings with 19 mm in height. In order to determine the effect of compactive effort on the swelling behavior, 100% bentonite samples were placed by applying 25 and 10 blows on samples. Because their swelling capacities are high, 100% bentonite samples were prepared in a way to ensure that their height would be 3 mm in the ring. Then they were subjected to swelling tests under 1, 2.5, 5, 12.5, 25, and 50 kPa effective

vertical stresses. In addition to these values, 100 kPa was applied to 100% bentonite. Swelling tests were conducted according to ASTM D2435 procedure.

In order to prepare 20% ZBM and 30% ZBM, first zeolite and bentonite were mixed in dry condition. The coarse-grained zeolite and fine-grained bentonite are shown in Figure 2.6. In order to obtain homogeneity, zeolite and bentonite were mixed in their dry states as shown in Figure 2.7. Optimum water content was reached by spraying tap water into the mixture. In order to check whether optimum water content was reached, some samples were taken from the prepared mixture. These samples were kept at 105 ^{0}C in the oven for 24 hours. Thus, water contents of the mixtures were verified.

(a)   (b)
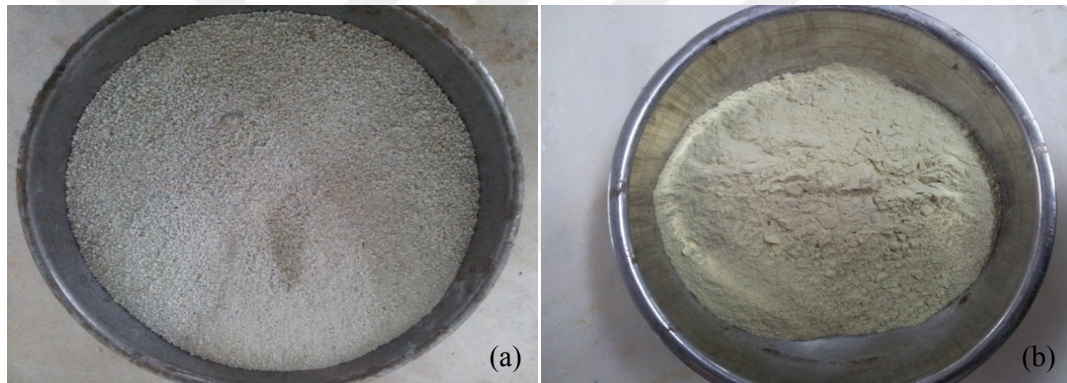
Figure 2.6 General views of samples: a) Zeolite sample, b) Bentonite sample

Figure 2.7 Dry mixing of zeolite and bentonite

The water was added to the mixtures by spraying as shown in Figure 2.8. In order to ensure homogenous distribution of water, the mixture was kneaded carefully.

23

Figure 2.8 Kneading the mixture (a) Dry kneading, (b) Wet kneading

The mixture was placed into the ring with the help of a mallet as shown in Figure 2.9.a. After placing the samples in the rings, their surfaces were smoothed with help of a spatula (Figure 2.9.b). Before putting in the oedometer cell, mixture samples were weighed and the weights of the wet samples and rings were recorded for determination of water content. In order to apply the swelling test, the ring containing the sample was put in the cell as shown in Figure 2.10.a. Upper and lower porous stones and filter papers were placed above and below the sample as shown in Figure 2.10.b.

Figure 2.9 a) Placing the sample in the ring with help of mallet, b) Sample placed in the ring
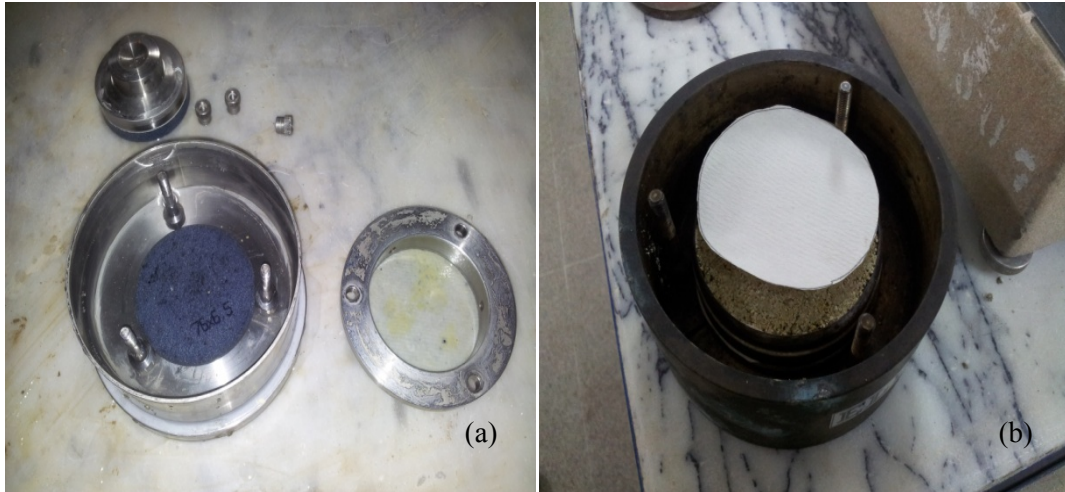
Figure 2.10 a) Cell components, b) Filter paper on the upper surface of the sample

The cell was placed into the oedometer frame, a loading plate was placed onto the ring and the ring was fixed with the help of nuts (Figure 2.11 and 2.12). Tap water was filled into the cell up to the loading plate level. Weights designed for application of the effective vertical stresses were placed onto the rod holding the weights of the oedometer (Figure 2.11).

After starting the test, the values of dial readings were recorded at regular time intervals (Figure 2.12). The swelling data and curves showing the swelling amount-time relationship obtained from the swelling tests conducted on the samples are given in Appendix B.

Figure 2.11 One dimensional consolidation test apparatus

When the difference between dial readings becomes negligibly small, the test was terminated. Then the sample was taken out of the cell (Figure 2.13.a) and it was weighed for determination of the water content (Figure 2.13.b).

Figure 2.12 General view of the cell at the end of the swelling test

Figure 2.13 ZBM sample taken out of the cell and weighing for determination of water content
a) ZBM sample after the test, b) Weighing the sample for water content

The time needed to complete the test for ZBMs was longer for the effective vertical stresses less than 12.5 kPa. At vertical stresses more than 12.5 kPa, consolidation was observed in the samples. Swelling tests of those samples ended in a shorter time. States of a sample after tests (wet condition) and after drying in the oven are shown in Figure 2.14.

Figure 2.14 ZBM samples after completion of swelling (a) wet sample (b) dry sample

The preparation process of the 100% bentonite sample was different from that of the ZBM samples. Since the swelling capacity of 100% bentonite is higher than that of the ZBMs, the samples were placed in the ring in 3 mm height as shown in Figure 2.15.a and Figure 2.16. In order to investigate the effect of compactive effort, 10 and 25 blows were applied on the samples (Figure 2.15.b). As with ZBMs, the bentonite samples in the rings were placed in the oedometer frame and dial readings under the same effective vertical stresses were recorded. The time of the swelling test for 100% bentonite samples was longer than that of ZBMs because of the high swelling capacity of bentonite.
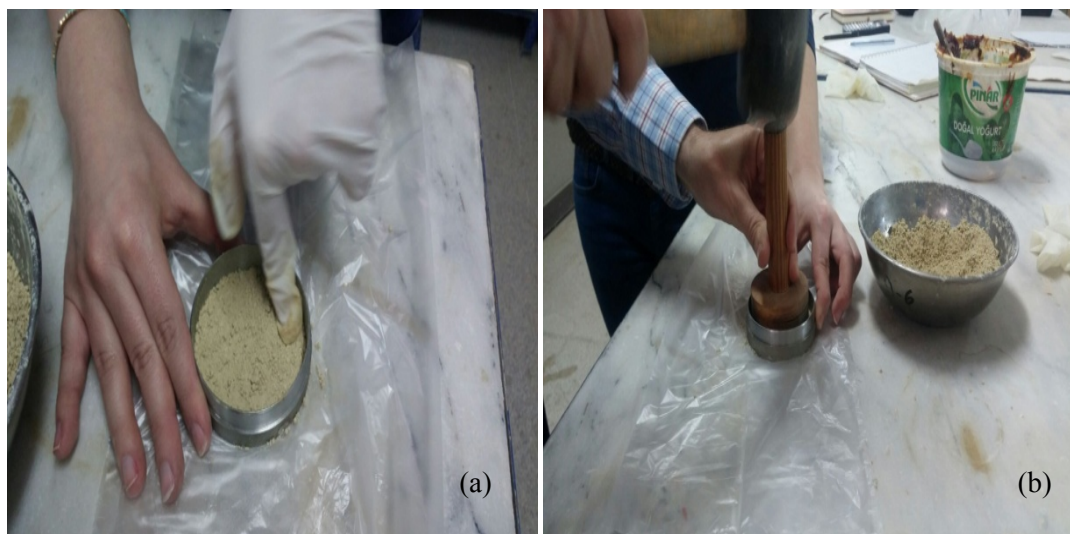
Figure 2.15 a) Placing the pure bentonite sample into the ring, b) Applying blows on the sample

Figure 2.16 Pure bentonite sample prepared in height of 3 mm in the ring

When the swelling ceased, the 100% bentonite was removed from the ring and dried in an oven at 105^0 C (Figure 2.17).
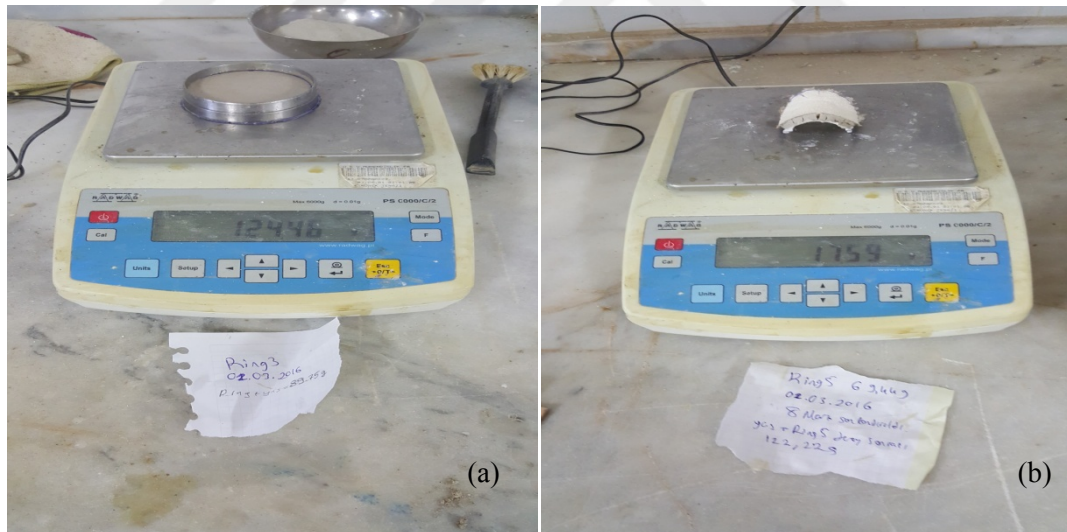
Figure 2.17 After completion of the swelling test of the pure bentonite sample:
(a) wet sample, (b) dry sample

More information about measurements of the samples before (initial state) and after (final state) the tests is given in Appendix C.

CHAPTER THREE
SWELLING BEHAVIOR OF BENTONITE SAMPLES

This chapter examines the swelling of 100% bentonite samples. The swelling capacity of bentonite samples was examined under the effective vertical stresses applied during the tests and with respect to the effect of the compaction effort applied while placing samples into the rings.

3.1 Swelling of Bentonite in terms of Compactive Effort

Investigating compaction effort on the swelling capacity of 100% bentonite samples was one of the objects of this thesis study. The samples were placed in the rings having a 3 mm height by applying 10 or 25 blows on them. The initial height of 3 mm was measured from the edge of the ring with the help of a vernier caliper but the height of the middle part of the sample could not be measured sensitively. In order to eliminate uncertainties originating from that condition it is appropriate to make an apparatus adjustable to the diameter of the ring to measure the heights of the 100% bentonite samples precisely.

Because bentonite has a high swelling capacity, the swelling tests of the bentonite samples lasted for about 2-8 weeks. The swelling amounts and sample height-time relationships of all bentonite samples compacted with 10 or 25 blows under all the effective vertical stress values (1, 2.5, 5, 12.5, 25, 50, and 100 kPa) is given in Figure 3.1.
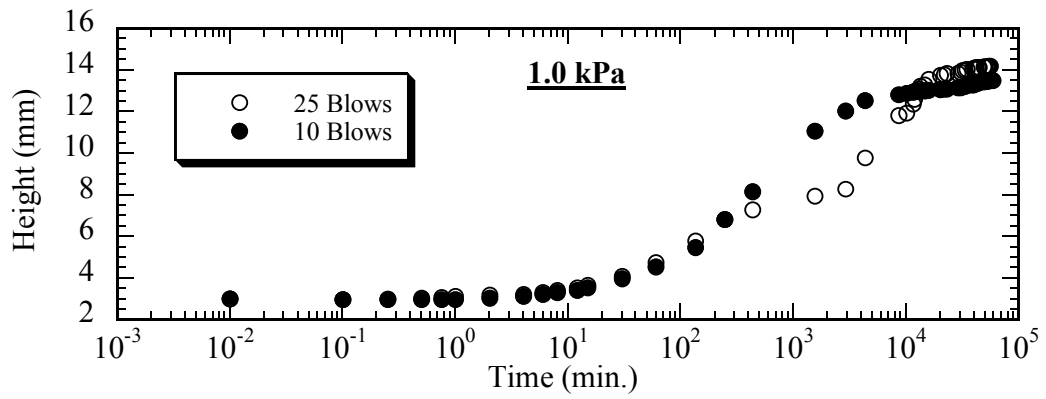
(a)
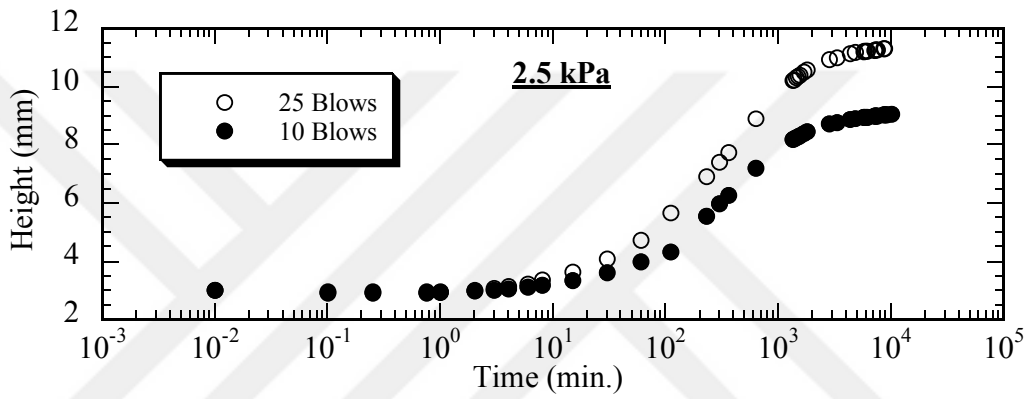
(b)
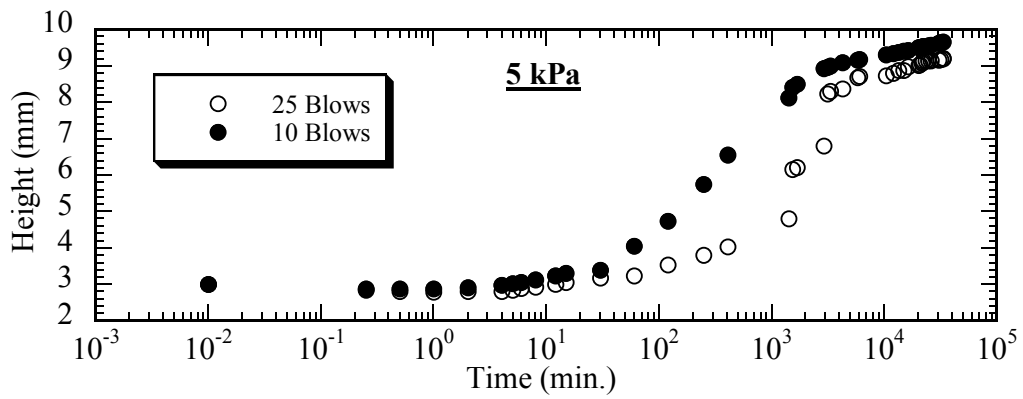
(c)

Figure 3.1 Swelling-time curves of the bentonite samples compacted by different number of blows:

a) 1 kPa, b) 2.5 kPa, c) 5 kPa
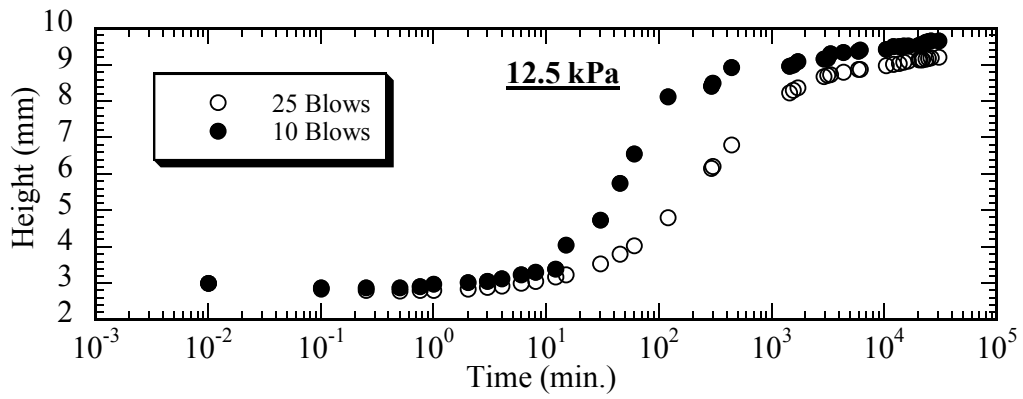
(d)
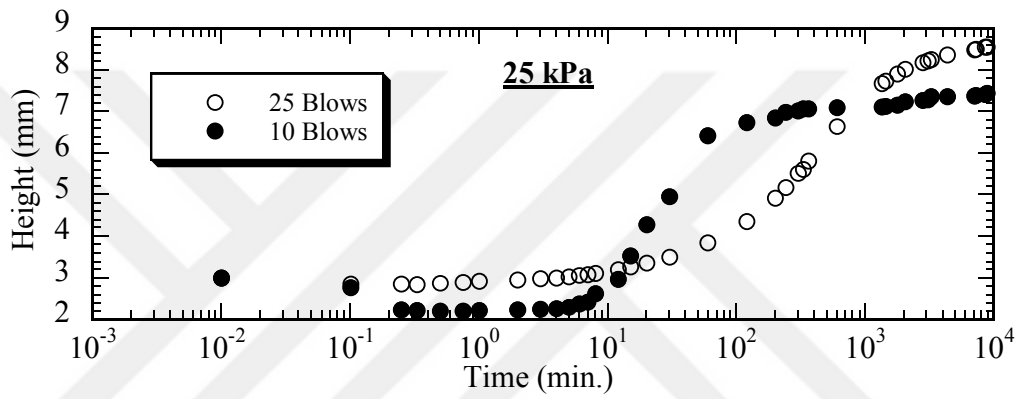
(e)
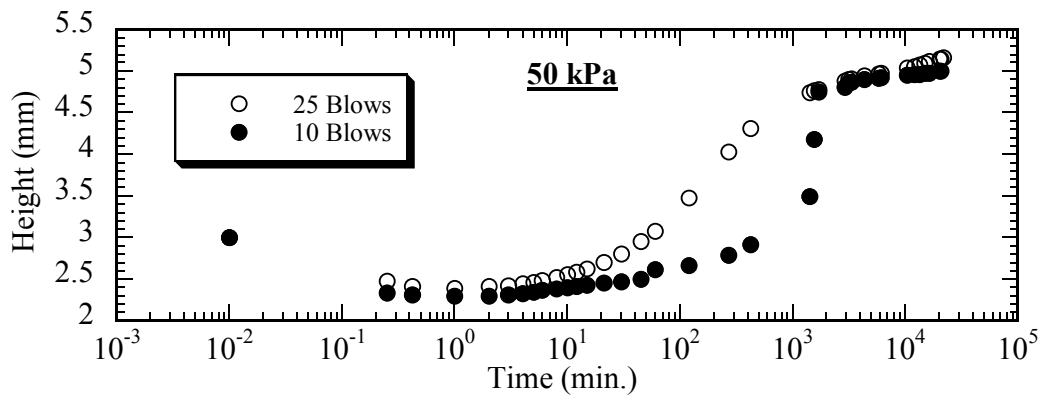
(f)

Figure 3.1 Swelling-time curves of the bentonite samples compacted by different number of blows (continued): d) 12.5 kPa, e) 25 kPa, f) 50 kPa

31
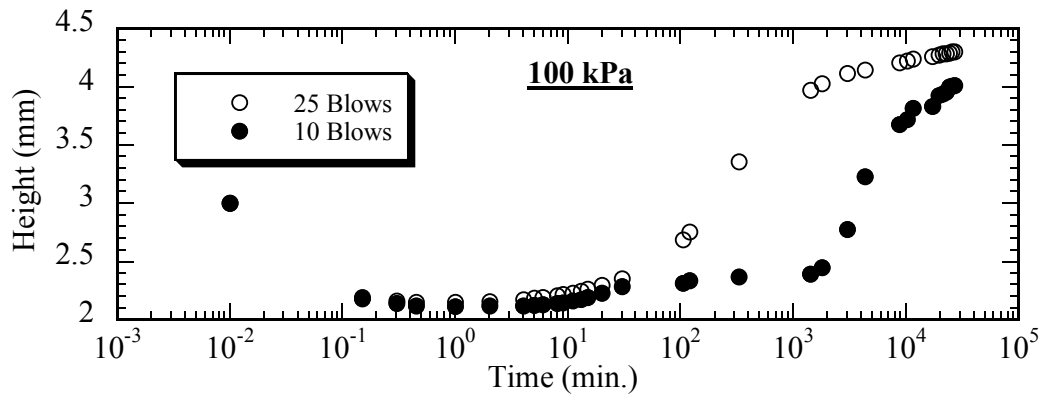
(g)

Figure 3.1 Swelling-time curves of the bentonite samples compacted by different number of blows (continued): g) 100 kPa

Figure 3.1 shows that there is no significant difference between the swelling amounts of the samples compacted by 10 or 25 blows under all effective vertical stress values. As a result, it is possible to deduce from the graphs that applying different compaction effort on bentonite samples has no significant effect on the amount of welling.

It was observed that the samples swelled slightly more under 25 blows than 10 blows. It can be seen that the increase was caused by getting closer of the grains due to the increase in the number of blows. More closely placed grains are able to absorb more water which leads to more swelling of the mixture.

3.2 Swelling of Bentonite in terms of Effective Vertical Stress

Figure 3.2 shows the curves of the change of swelling amounts and swelling strains with time for samples prepared by applying 10 blows in the ring under different effective vertical stresses. Similarly, the curves of the change of swelling amounts and swelling strains with time for samples prepared by applying 25 blows in the ring under different effective vertical stresses is shown in Figure 3.3. Figures 3.2 and 3.3 reveal that swelling occurs rapidly at the beginning of the test (in the first 24 hours) then slowed as time passed. In the 1-5 kPa small effective vertical stress

32

range, the sample height rose to threefold or fourfold of its initial value (swelling strain reaches the values 200%-350%). On the other hand, as the effective vertical stress increased the swelling amount decreased. Under 100 kPa effective vertical stress, the sample height rose from 3 mm to 4 mm and swelling strain increased by 33%. Swelling occured under all the vertical stress values.

Samples compacted by applying 10 or 25 blows in the rings showed similar swelling behavior. In the study of Mollins et al. (1995) it is seen that the compaction method does not affect the swelling behavior, significantly. Similar behavior of the samples prepared in the ring by applying 10 blows or 25 blows in this study also supports that finding. In the study of Cui et al. (2012), it was reported that bentonite samples do not show any swelling or compression under 400 kPa effective vertical stress, and they show some compression under 1600 kPa effective stress. In this thesis, it was revealed that the bentonite samples swelled by 33% under 100 kPa effective vertical stress.
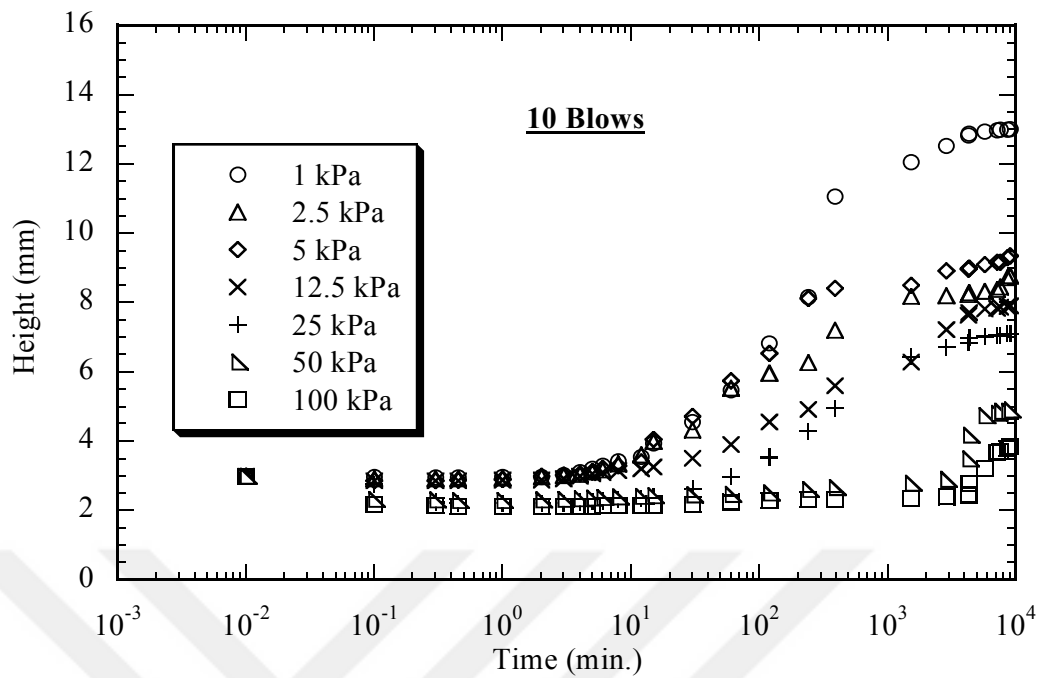
(a)
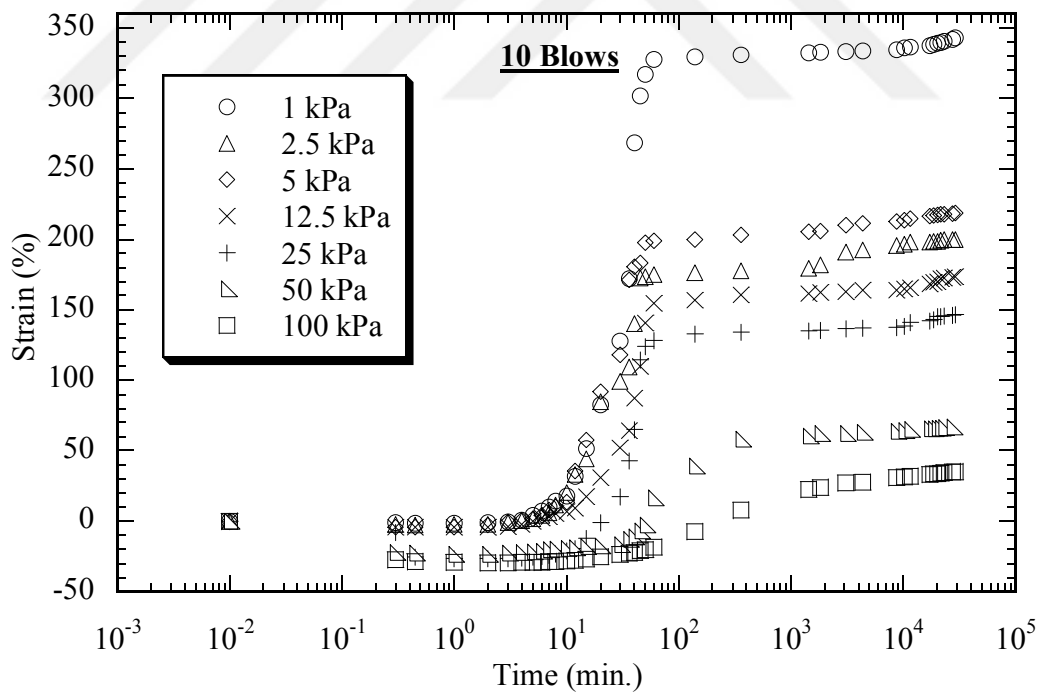
(b)

Figure 3.2 Swelling capacities of bentonite samples prepared by applying 10 blows under different effective vertical stresses: a) Sample height (mm) b) Strain (%)

34
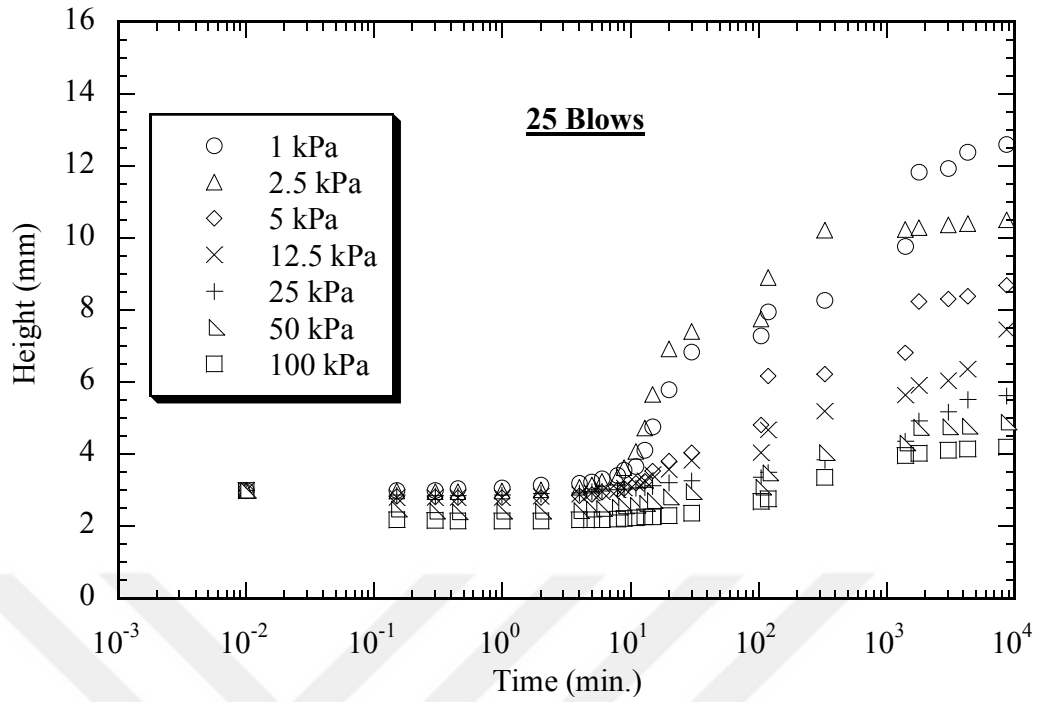
(a)
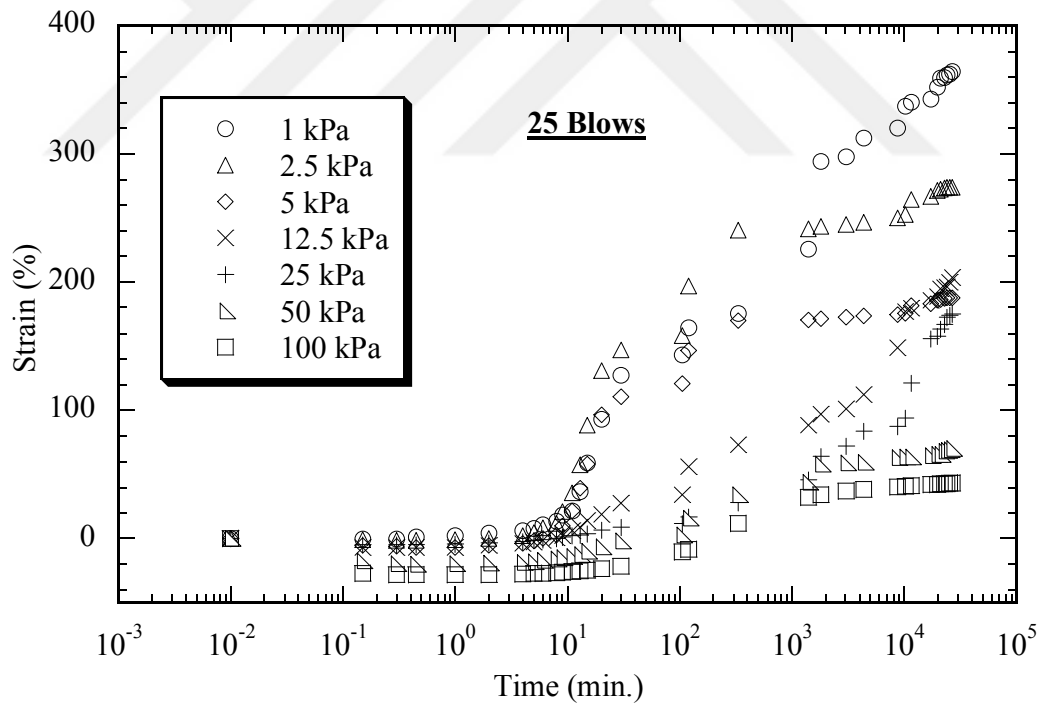
(b)

Figure 3.3 Swelling capacities of bentonite samples prepared by applying 25 blows under different effective vertical stresses: a) Sample height (mm) b) Strain (%)

Final void ratios of the bentonite samples were calculated and their relationship with effective vertical stress is illustrated in Figure 3.4. The final void ratio-effective vertical stress relationship of the bentonite samples used in this study represents a parallel linear relation with the final void ratio-effective vertical stress relationship of the bentonite samples used in the study of Mollins et al. (1995). The cause of that parallellism is the use of close liquid limit values in both studies; the liquid limit value in this study is 405% and it was 407% in the study of Mollins et al (1995). On the other hand, the final void ratio-effective vertical stress relationship of the bentonite samples used in the study of Sun et al. (2013) showed a non-linear relation.
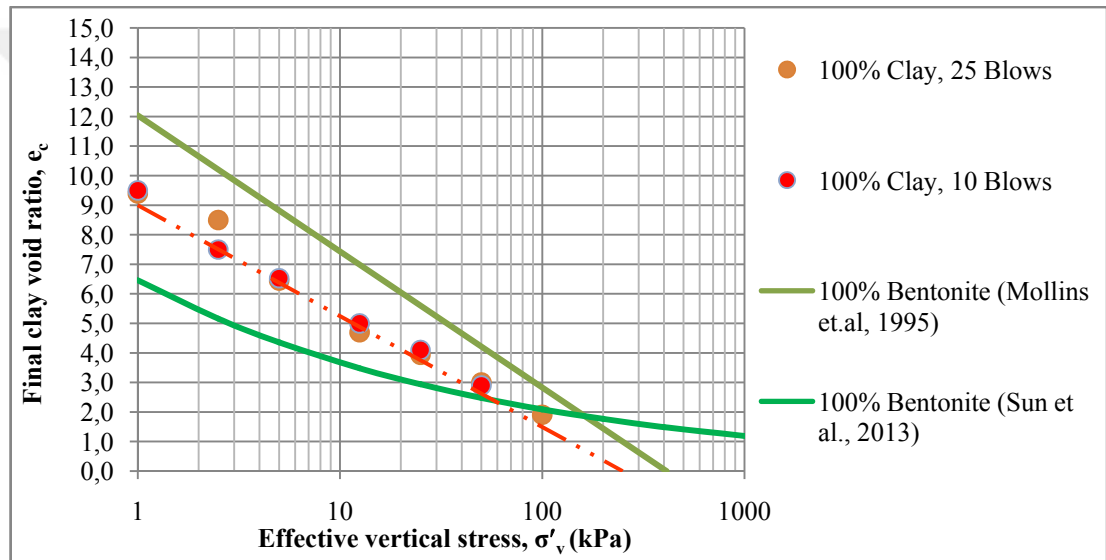
Figure 3.4 Final clay void ratio and effective vertical stress (e_c–σ'_v) relation of bentonite samples at full saturation and comparison with that of the literature

CHAPTER FOUR

SWELLING BEHAVIOR OF ZEOLITE-BENTONITE MIXTURES

In this chapter, the information about swelling tests conducted in order to determine swelling behavior of ZBMs with 20% and 30% bentonite contents and findings of these tests are examined.

4.1 Swelling of ZBMs in terms of Bentonite Content

The swelling amounts of 20% ZBM and 30 % ZBM samples under each effective vertical stress are shown in the sample height-time curves given in Figure 4.1.
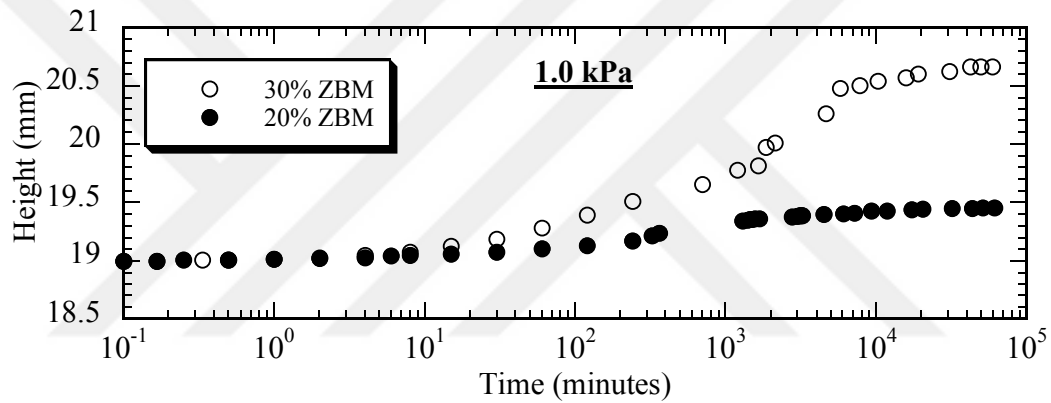
(a)
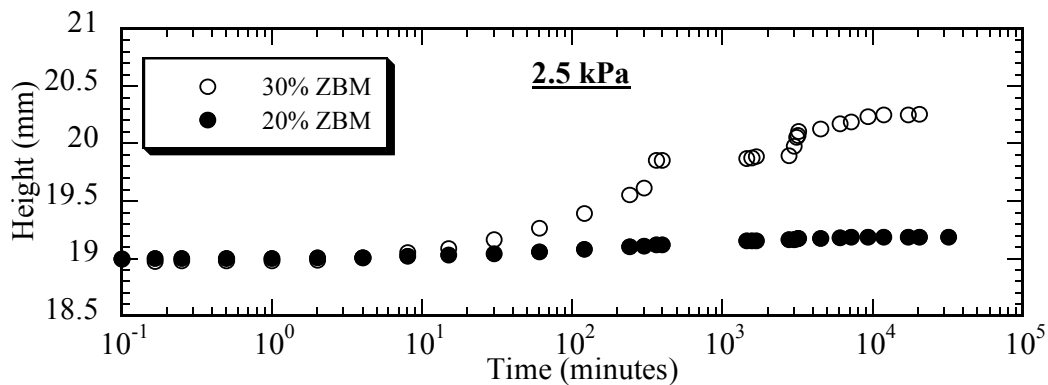
(b)

Figure 4.1 Swelling-time curves of the ZBM samples: a) 1 kPa, b) 2.5 kPa
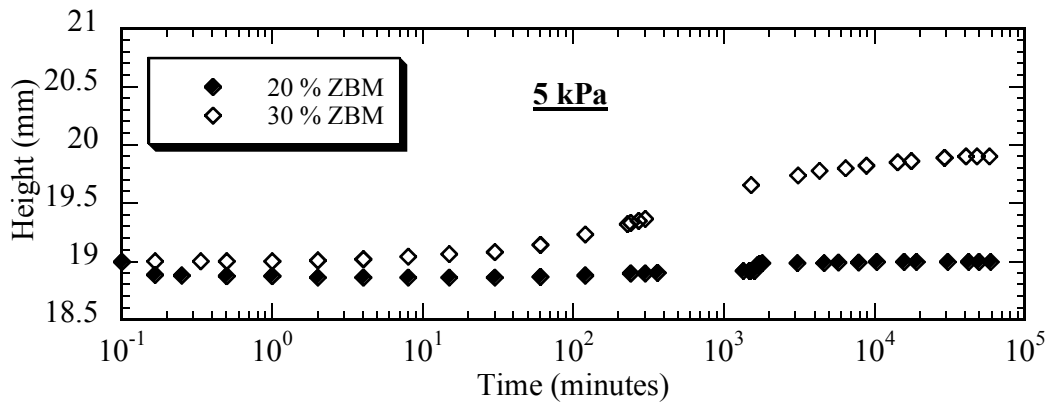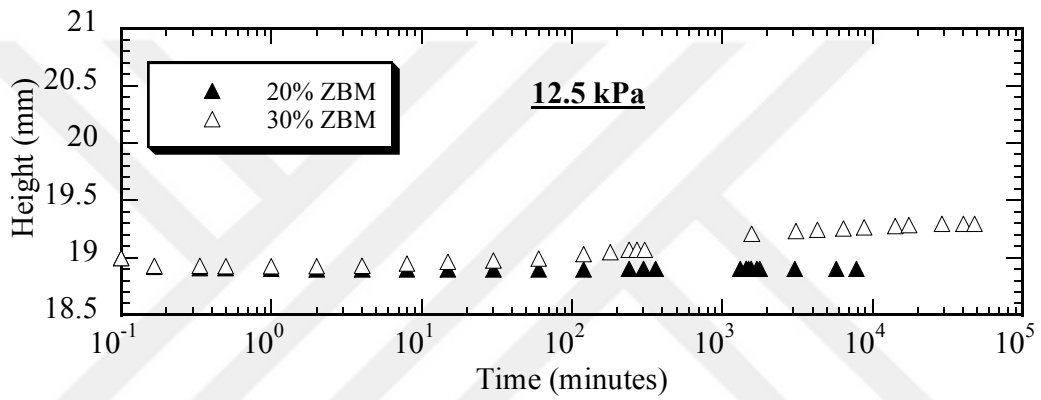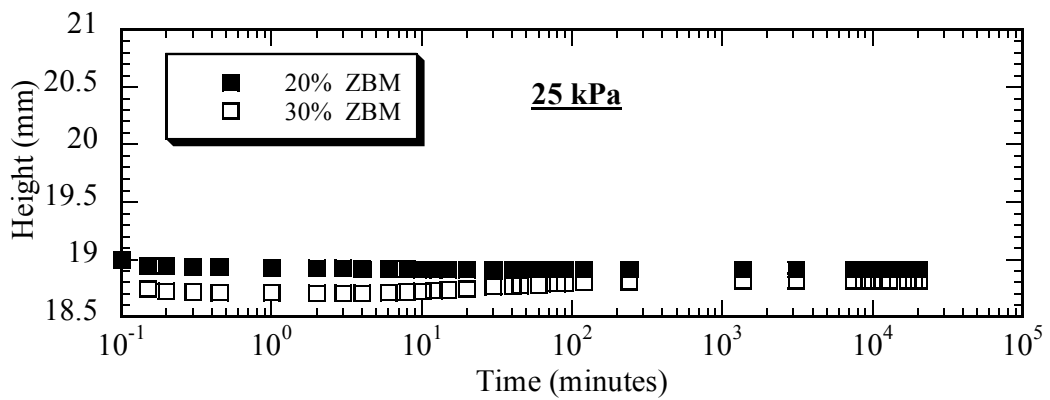
Figure 4.1 Swelling-time curves of the ZBM samples (continued):

c) 5 kPa, d) 12.5 kPa, e) 25 kPa
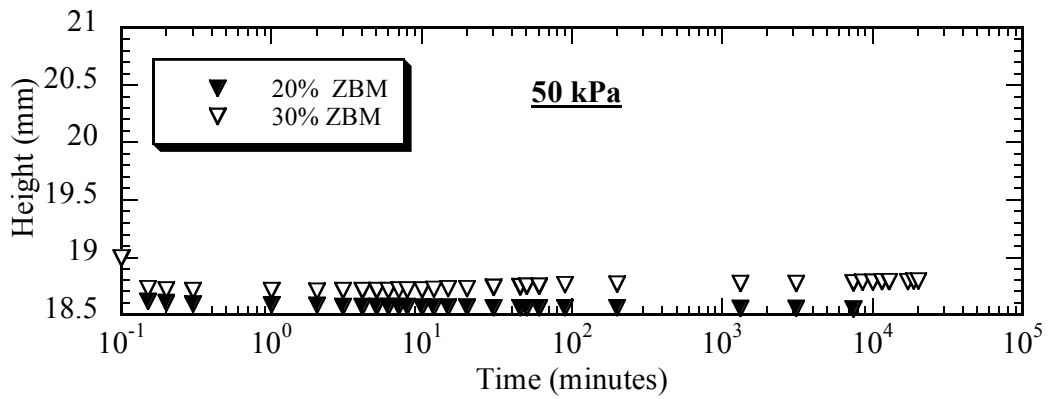
Figure 4.1 Swelling-time curves of the ZBM samples (continued): f) 50 kPa

The swelling-time curves show that the swelling amount of the ZBMs with 30% bentonite content is more than that of the ZBMs with 20% bentonite content. As the bentonite content increases, the swelling capacity of the ZBMs increases. While the ZBMs with 30% bentonite content shows swelling up to 12.5 kPa effective vertical stress, the ZBM with 20% bentonite content does not show swelling exceeding 5 kPa effective vertical stress. When the swelling capacity of pure bentonite is compared with that of ZBM, under all the effective vertical stress values it is seen that the 100% bentonite samples have higher swelling capacities. When Figure 4.1 is examined it is possible to say that the bentonite content is the primary factor affecting the swelling capacity.

4.2 Swelling of ZBMs in terms of Bentonite Content and Vertical Stress

The swelling-time curves of 20% ZBM and 30% ZBM samples under different effective vertical stresses are given in Figures 4.2 (a) and (b). The swelling strain-time relationships of 20% ZBM and 30% ZBM samples under different effective vertical stresses are shown in Appendix B (Figures B.1.a and b). Swelling-time curves and data recorded during the test and calculations of void ratio are given in Appendix B and Appendix C, respectively.

39
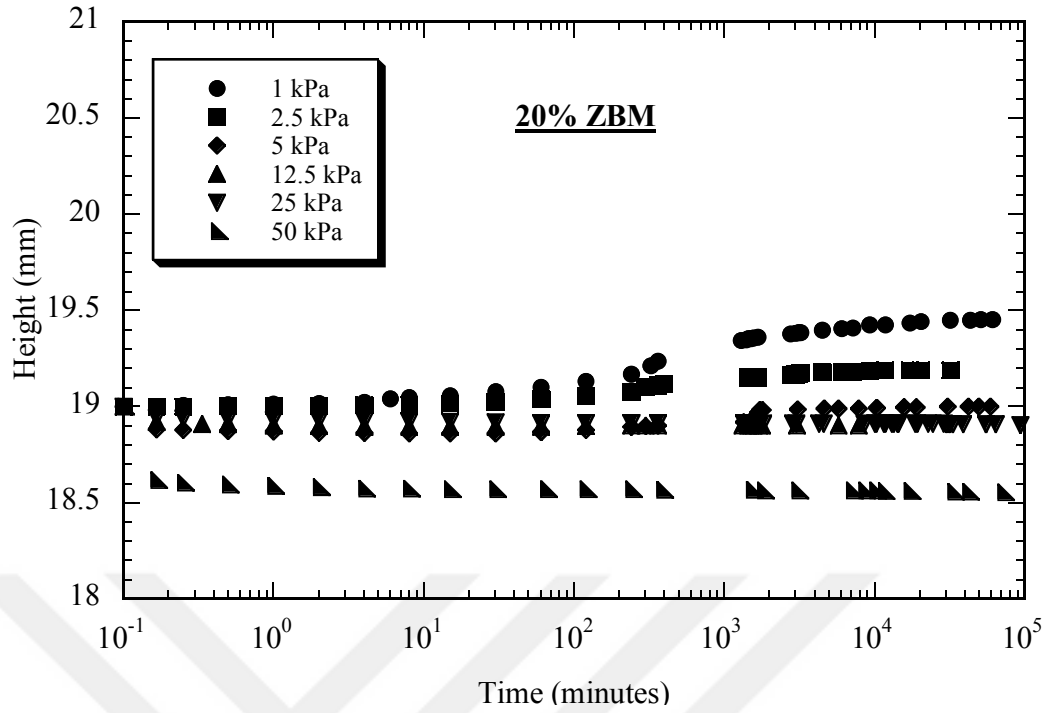
(a)
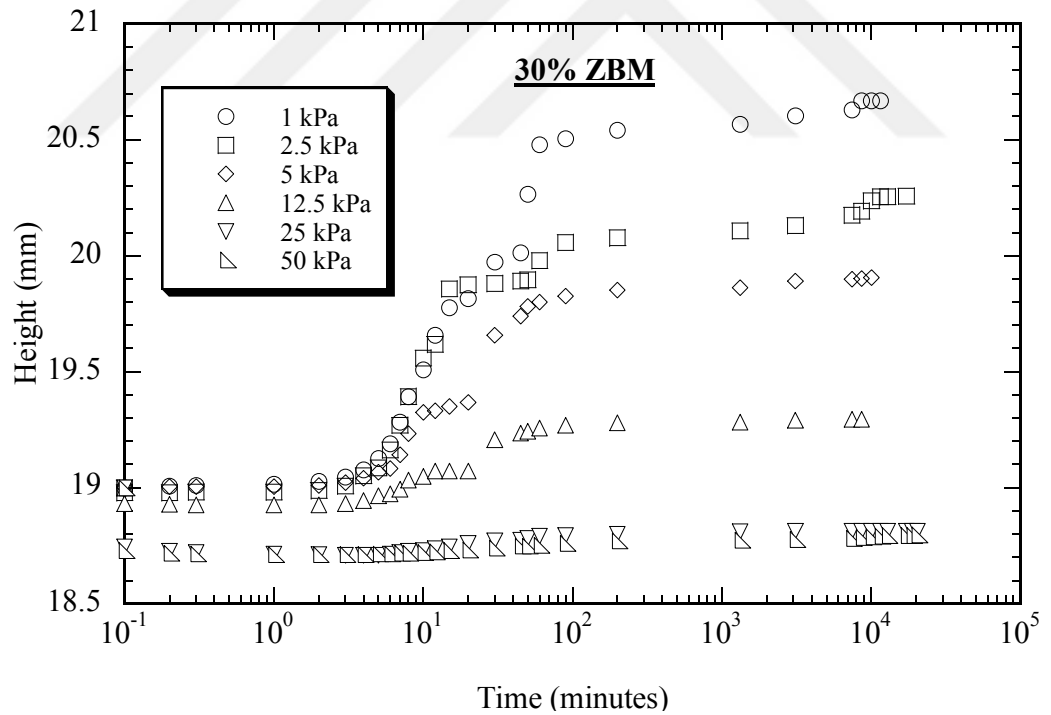
(b)

Figure 4.2 Swelling-time curves of ZBMs under different effective vertical stresses:

a) 20% ZBM, b) 30% ZBM

When the swelling-time curves of 20% ZBMs are compared with those of 30% ZBMs, which are given in Figure 4.2, it is clearly seen that the swelling amount increases with the increase of bentonite content of the mixture. When the effective vertical stress is low, bentonite can enter the voids between zeolite grains easily; hence the swelling amount is increased. Conversely, when the effective vertical stress is high, it is estimated that the bentonite could penetrate into the grains harder and fill the voids less well because the grains in the mixture are in close contact with each other.

The 20% ZBMs showed swelling under the effective vertical stresses 1 and 2.5 kPa, whereas the 30% ZBMs showed swelling under the effective vertical stresses 1, 2.5 and 5 kPa. When 20% ZBMs were tested under the effective vertical stress 5 kPa, and 30% ZBMs were tested under the effective vertical stresses 12.5, 25 and 50 kPa, although the samples were compressed at the first moments of the test, they swelled because of water uptake of bentonite as time passed and the test was completed with some swelling. The 20% ZBMs did not swell under the effective vertical stresses 12.5, 25 and 50 kPa because bentonite could not dislocate the grains.

According to the approach stated in the study of Graham et al. (1986) the internal stress distribution in SBMs is a combination of osmotic pressure and intergranular forces between sand grains. Osmotic pressure decreases as the void ratio of clay increases. Clay in the mixture subjected to low effective vertical stresses provides swelling by separating sand particles from each other in order to reach the same void ratio. But under high effective vertical stresses the sand grains are in contact completely or partly, and bentonite particles are not able to dislocate sand grains. It is possible to say that there is similar mechanism takes place for ZBMs.

CHAPTER FIVE
COMPARISON OF SWELLING BEHAVIOR OF ZEOLITE-BENTONITE
MIXTURES AND SAND-BENTONITE MIXTURES

5.1 Swelling of ZBMs and SBMs in terms of Bentonite Content

Findings of the previous swelling tests of SBMs made in the Soil Mechanics Laboratory of Civil Engineering Department of Dokuz Eylül University were compared with the test results of the ZBMs obtained in this study. Bentonite material used in the SBMs is the same as the material included in the ZBMs and the grain size distribution of the sand is similar to that of the zeolite. Swelling-time curves of the ZBMs with 20% and 30% bentonite contents and the SBM with 20% bentonite content are shown in Figure 5.1.

(a)
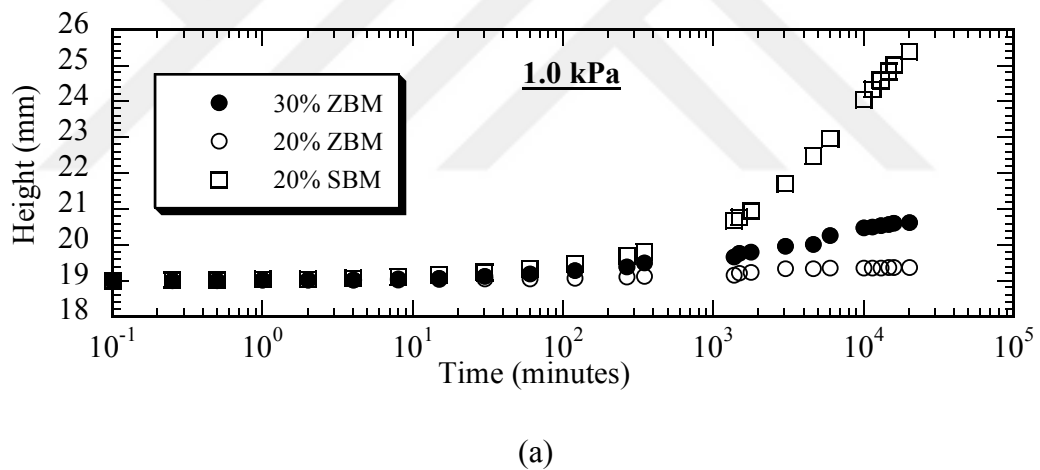
Figure 5.1 Swelling-time curves of zeolite-bentonite and sand-bentonite mixtures: a) 1 kPa
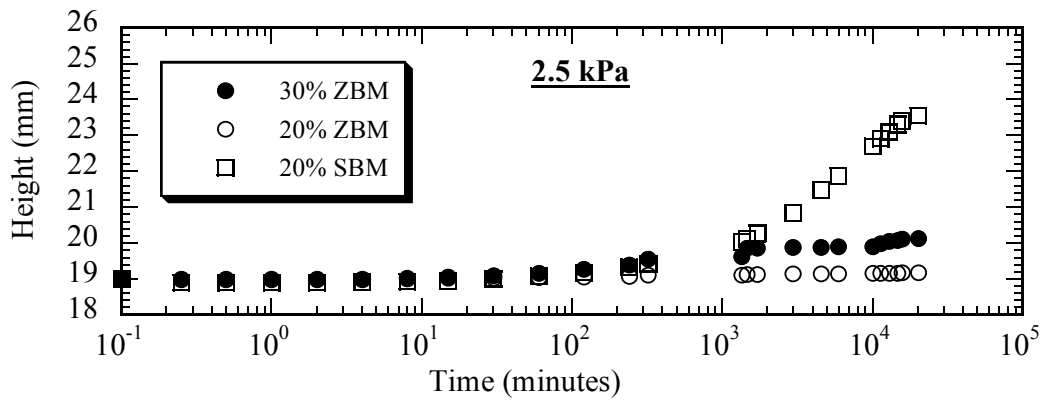
(b)
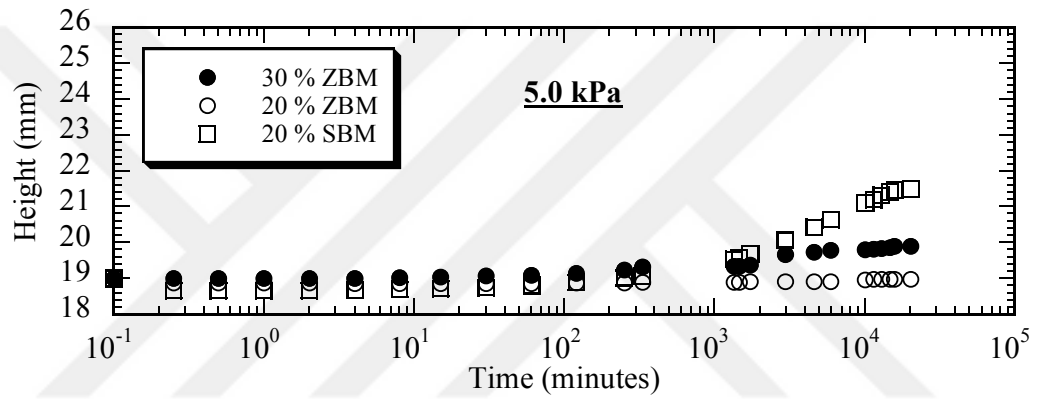
(c)
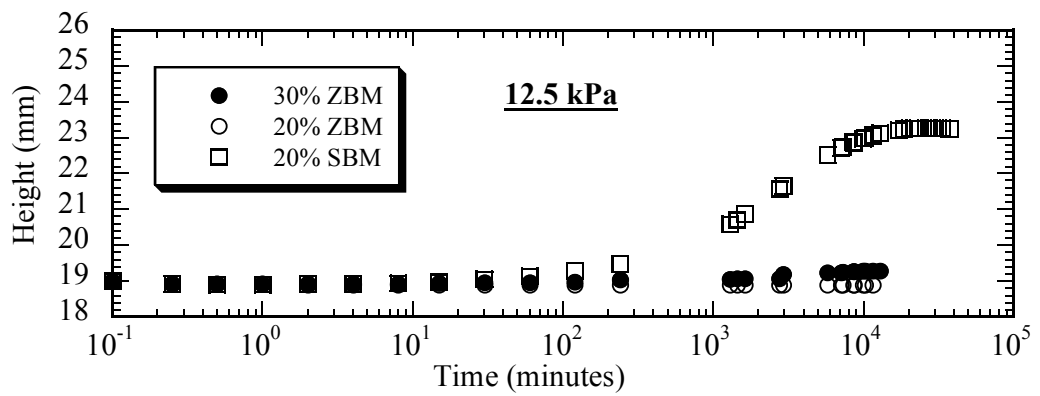
(d)

Figure 5.1 Swelling-time curves of zeolite-bentonite and sand-bentonite mixtures (continued):
b) 2.5 kPa, c) 5 kPa, d) 12.5 kPa
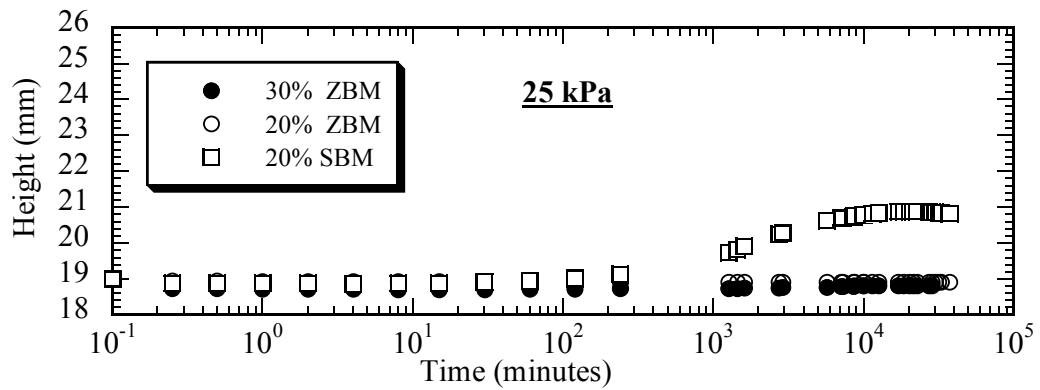
(e)
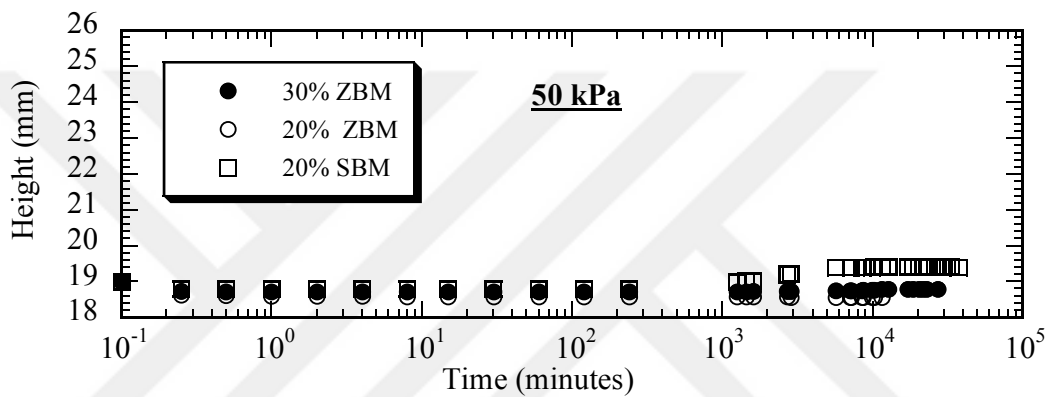
(f)

Figure 5.1 Swelling-time curves of zeolite-bentonite and sand-bentonite mixtures (continued):
e) 25 kPa, f) 50 kPa

When the swelling graphs of ZBMs and SBMs under different effective vertical stresses were examined, it was seen that SBMs swelled more than ZBMs. While the ZBMs showed swelling behavior under the effective vertical stresses 1, 2.5, 5 and 12.5 kPa, whereas, they showed compression behavior under the effective vertical stress values of 25 kPa and 50 kPa. On the other hand, it was determined that the SBM with 20% bentonite content continued to swell even under the effective vertical stress of 50 kPa (Figure 5.1.f). Although bentonite content is an important factor for controlling the swelling behavior, it can be said that it is not the only factor. Less swelling amount of the ZBM with 30% bentonite content than the SBM with 20% bentonite content can be explained by the porous structure of zeolite. The channels and honeycomb-like crystalline structure of zeolite allow water to flow through the

44

zeolite grains and accommodate a considerable amount of water. This characteristic affects the swelling behavior, significantly.

In ZBMs and SBMs the components constituting the solid phase are sand/zeolite and clay, and liquid phase is water. The situation of bentonite in the mixtures can be described with the clay void ratio parameter. In the study of Mollins et al. (1996), the idealized soil prism of the SBM is given in Figure 5.2. When the prism is examined, it is seen that the sand did not take water and the water filled the voids between the sand grains.
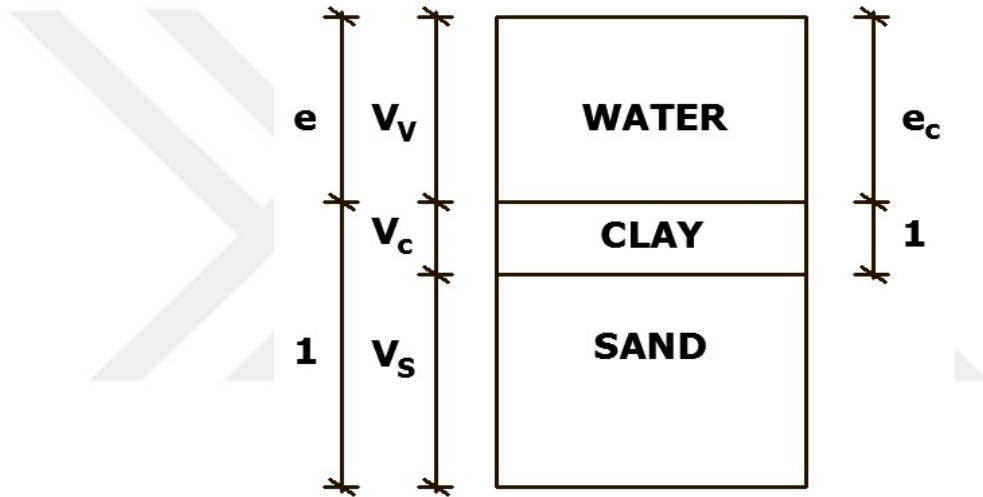
Figure 5.2 Idealized soil prism for sand-bentonite mixtures:
V_v: volume of voids, V_c: volume of clay, V_s: volume of sand (Mollins et al., 1996).

While the sand in the SBM does not take water and the water fills the intergranular voids, the case is different for the ZBM. Due to its porous structure, zeolite absorbs some water because of channels formed in its crystalline structure. This explains the lower swelling behavior of the ZBM than that of the SBM with the same bentonite content. The granular structure of zeolite affects the swelling behavior of the mixture, significantly.

A soil prism similar to that developed for the SBM in the study of Mollins et al. (1996) was developed for the ZBM used in this study (Figure 5.3). When the prism of the ZBM prism is examined it is seen that the water is shared by clay and zeolite.
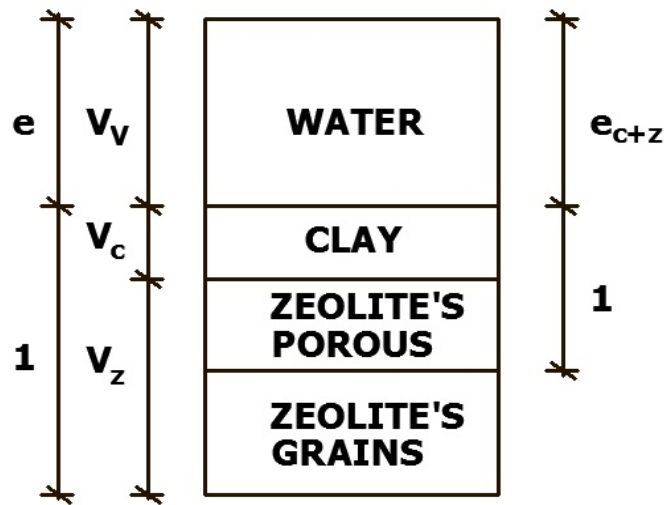
Figure 5.3 Soil prism developed in this study for zeolite-bentonite mixtures:
V_v: volume of voids, V_c: volume of clay, V_z: volume of zeolite

The linear graph obtained by sketching the data of swelling tests of 100% bentonite samples and the clay final void ratio-effective vertical stress graphs of the ZBM samples with 20% and 30% bentonite contents are shown in Figure 5.4. In their study Mollins et. al (1996) showed that the SBMs follows the linear graph of 100% bentonite until some threshold values of effective vertical stresses. After exceeding the threshold values, the clay final void ratio-effective vertical stress graph gets closer to the horizontal. The threshold value of effective vertical stress varies in relation to the bentonite content of the SBM. The calculations of SBMs were made with the assumption of the absence of voids in the sand. Also when the prism in Figure 5.4 was developed, it was assumed that there were no intragranular voids in the zeolite. The montmorillonite void ratio formula used in the study of Sun et al. (2013) was used for the ZBMs in this study. When Figure 5.4 is examined, it is seen that the formula applied to the sand-bentonite structure in the literature did not produce the same result for ZBMs. This is because zeolite has a porous microstructure.
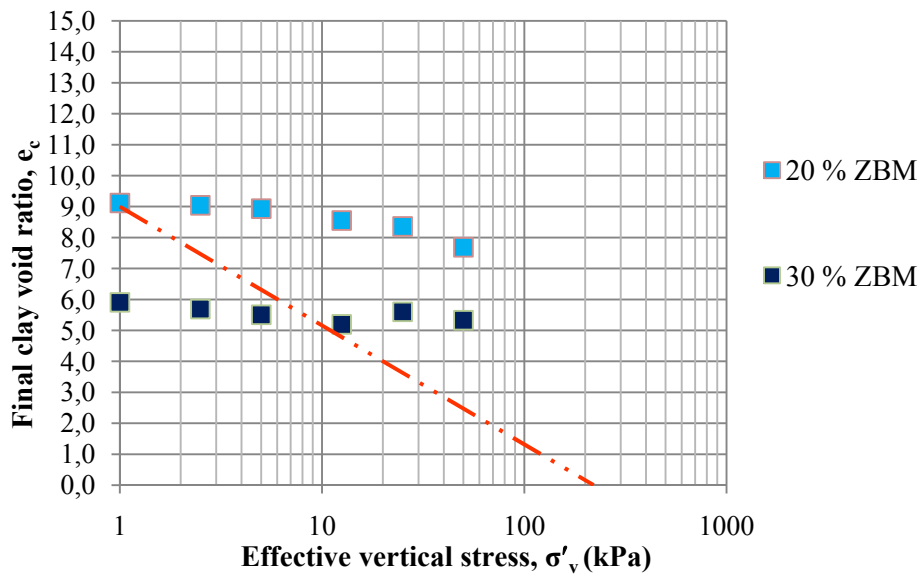
Figure 5.4 e_c-σ'_v relationship for 20% ZBM and 30% ZBM samples

This case can be explained by following approach: The SBMs and ZBMs with the same bentonite content may have different volumetric bentonite contents. As a result, the swelling amount of bentonite might be insufficient for filling the voids in the ZBMs (Durukan, 2013).

Intergranular voids of the ZBMs cannot be filled by bentonite because the low bentonite content is not sufficient for filling the intergranular voids. For this reason the void ratio of bentonite does not vary significantly under the effective vertical stresses applied to the ZBMs. On the other hand, the intergranular voids in the sand of the SBMs with the same bentonite content are filled with bentonite and the mixtures show swelling behavior. That difference originates from the microstructure of zeolite. Under low effective vertical stresses, the clay in SBMs swells easily under the effect of stress and dislocate the grains of sand to reach the same void ratio (Mollins et al., 1996). But when bentonite content is low, the bentonite cannot dislocate zeolite particles and the bentonite void ratio does not vary in ZBMs with increase of vertical stress as expected. Because the zeolite in the mixture has a porous microstructure containing channels, it absorbs some part of the water.

CHAPTER SIX
CONCLUSIONS

This thesis aimed to find out mechanisms affecting the swelling behavior of ZBMs. Bentonite content has a significant effect on the swelling behavior. In order to prove that effect scientifically, swelling tests were applied to ZBM samples of 20% and 30% bentonite contents. After the swelling tests, the swelling-time curves of the ZBMs were drawn; the findings of the tests were compared to the results of studies in the literature as well as to the findings of the previous swelling tests of SBMs using the same bentonite material and made in the same laboratory conditions. Additionally, the swelling behavior of 100% bentonite was investigated and the effect of compaction effect on the swelling behavior was investigated.

.   The following conclusions are drawn from the findings of the tests:

- The optimum water content values of ZBMs are almost the same as those of the ZBMs reported in the literature, and they are 2.5 times higher than those of SBMs. On the other hand, maximum dry unit weights of ZBMs are almost the same as those of the ZBMs reported in the literature, and they are 1.5 times lower than those of SBMs. The difference between the compaction values of ZBMs and SBMs can be explained by the following factors: lower specific gravity of zeolite than sand, the porous crystalline structure of zeolite, and water uptake of zeolite.

- The swelling amount of ZBM increases as the bentonite content increases. The principal factor affecting the swelling behavior of high plasticity clays is the clay content in the mixture.

- Swelling was observed at all stress levels for 100% bentonite samples, which were prepared by applying 10 or 25 blows (1, 2.5, 5, 12.5, 25, 50, and 100 kPa). Although effective vertical stress was increased to 100 kPa, the 100% bentonite sample continued to swell in a decreased amount. The difference

48

between the swelling amounts of the samples subjected to 10 blows and 25 blows vary within the range of 0.3-2.0 mm. The samples subjected to 25 blows swelled a little bit more than the samples subjected to 10 blows. The difference can be explained by the increase of the interactions of the grains with the increase of the number of blows. When more blows applied, the grains get closer and can absorb more water and so the mixture swells more.

- The results of the swelling tests of the ZBMs with 20% and 30% bentonite contents were compared with those of the previous swelling tests of the SBM with 20% bentonite content. The SBM was prepared with the same bentonite material. The sand had with the same grain size distribution with zeolite. The swelling amount of 20% SBM is 1.3 times higher than that of 20% ZBM under 1 kPa effective vertical stress. The 20% ZBM swelled only under the effective vertical stresses 1, 2.5 and 5 kPa, whereas, 20% the SBM swelled under all effective vertical stresses (1, 2.5, 5, 12.5, 25, and 50 kPa). The 30% ZBM swelled more than the 20% ZBM under any effective vertical stress, however, it swelled less than the 20% SBM.

- Although the bentonite content of ZBM is higher than that of SBM, it swelled less than SBM and it showed compression behavior under high values of the effective vertical stresses. Although bentonite content is the principal factor affecting the swelling behavior there are some other factors. Less swelling of ZBM can be explained by distribution of the absorbed water between zeolite and bentonite. The water in SBMs is absorbed only by bentonite. But the case is different for ZBMs. Zeolite retains some water inside of the grain. Since water retained in the porous structure of zeolite, little amount of water can be used by bentonite. This is one of the most important findings of this study. Less swelling of ZBMs than SBMs was stated also in the study of Ören (2007).

- In the study of Mollins et al. (1996), the graph of the final clay void ratio-effective vertical stress relationship is linear for 100% bentonite. SBMs separate from that linear graph at the threshold values of effective vertical stresses and follow a horizontal tendency. The threshold stress values of the SBMs with low bentonite contents are lower than those of the mixtures with high bentonite contents because the sand skeleton formed in the SBMs with low bentonite contents counterbalanced the applied stress. It might be expected that there is a similar skeleton formation in the mixtures containing zeolite. But this study revealed that zeolite behaves in a different way. ZBM does not conform to the load counterbalance mechanism described above because the void ratio of ZBM is higher than that of SBM with the same bentonite content. The reason is the porous structure of zeolite in contrast with sand.

REFERENCES

ASTM D 422 (2007). *Standard test method for particle-size analysis of soils.* The American Society for Testing and Materials, West Conshohocken, USA.

ASTM D 698 (2003). *Standard test methods for laboratory compaction Characteristics of Soil UsingStandard Effort (12,400 ft-lbf/ft^3(600 kN-m/m^3))[1].* The American Society for Testing and Materials, West Conshohocken, USA.

ASTM D 2435 (2002). *Standard test methods for One-Dimensional Consolidation Properties of Soils Using Incremental Loading.* The American Society for Testing and Materials, West Conshohocken, USA.

Blanchard, G., Maunaye, M., & Martin, G. (1984). Removal of heavy metals from waters by means of natural zeolites. *Water Research, 18(12),* 1501-1507.

Cho, W.J., Lee, J.O.,& Chun, K.S. (1999). The temperature effects on hydraulic conductivity of compacted bentonite. *Applied Clay Science, 14,* 47-58.

Craig, R.F. (2004). *Craig's soil mechanics.* London & New York: Spon Press, Taylor and Francis Group.

Cui, S., Zhang, H., & Zhang, M.(2012). Swelling characteristics of compacted GMZ bentonite-sand mixtures as a buffer/backfill material in China. *Engineering Geology, 141–142,* 65–73.

Gurtug, Y. & Sridharan, A. (2004). Compaction behavior and prediction of its characteristics of fine grained soils with particular reference to compaction energy. *Soils and Foundations, 44,* 27-36.

Holtz, R.D. & Kovacks, W.D. (1981). *An introduction to geotechnical engineering,* New Jersey: Prentice-Hall, Inc.

Jacobs, P.H. & Förstner, U. (1999). Concept of subaqueous capping of contaminated sediments with active barrier systems (ABS) using natural and modified zeolites. *Water Resources, 33 (9)*, 2083-2087.

Kaya, A. & Durukan, S. (2004). Utilization of bentonite-embedded zeolite as clay liner. *Applied Clay Science, 25*, 83-91.

Kayabalı, K. (1997). Engineering aspects of a novel landfill material: Bentonite amended natural zeolite. *Engineering Geology, 46,* 105-114.

Kayabalı, K. & Kezer, H. (1998). Testing the ability of bentonite amended zeolite (clinoptilolite) to remove heavy metals from liquid waste. *Environmental Geology, 34*, 95-102.

Kayabalı, K. & Mollamahmutoğlu, M. (2000). The influence of hazardous liquid waste on the permeability of earthen liners. *Environmental Geology, 39*, 201-210.

Kleppe, J. H. & Olson, R.E. (1985). Desiccation cracking of soil barriers. *ASTM Special Technical Publication, 874*, 263-275.

Komine, H. (2004). Simplified evaluation on hydraulic conductivities of sand-bentonite mixture backfill. *Applied Clay Science, 26*, 13-19.

Komine, H. & Ogata, N. (1999). Experimental study on swelling characteristics of sand- bentonite mixture for nuclear waste disposal. *Soils and Foundations, 39 (2),* 83-97.

Lambe, T.W. (1958). The engineering behavior of compacted clay. *Journal of the Soil Mechanics and Foundations Division, 84*, 1-35.

Lee, J.O., Cho, W.J. & Chun, K.S. (1999). Swelling Pressures of a Potential Buffer Material 518 for High-Level Waste Repository. *Journal of the Korean Nuclear Society, 31,* 139-150.

Mollins, L.H., Stewart, D.I., & Cousens, T.W. (1996). Predicting the properties of bentonite-sand mixtures. *Clay Minerals, 31*, 243-252.

Ören, A.H. (2007). *Engineering investigation of zeolite-bentonite mixtures for landfill liners.* PhD Thesis, Graduate School of Natural and Applied Sciences, Dokuz Eylül University, Izmir.

Ören, A.H. & Kaya, A. (2006). Factors affecting adsorption characteristics of Zn2+ on two natural zeolites. *Journal of Hazardous Materials, 13(1-3),* 59–65.

Ören, A.H. & Kaya A. (2013). Compaction and volumetric shrinkage of bentonitic mixtures. *Proceedings of Institution of Civil Engineering - Geotechnical Engineering.*

Ören, A.H., Durukan S., & Kayalar A.Ş. (2014). Influence of compaction water content on the hydraulic conductivity of sand-bentonite and zeolite-bentonite mixtures. *Clay Minerals, 49*, 109-121.

Ören, A.H., Kaya, A., & Kayalar, A.Ş. (2011). Hydraulic conductivity of zeolite bentonite mixtures in comparison to sand bentonite mixtures. *Canadian Geotechnical Journal, 48* (9), 1343-1353.

Sridharan, A., Pandian, N.S., & Srinivas, S. (2001). Compaction behavior of Indian coal ashes. *Ground Improvement, 5,* 13-22.

Stewart, D.I, Cousens, T.W., Studds, P.G., & Tay, Y.Y. (1999). Design parameter for bentonite enhanced sand as a landfill liner. *Proceedings of Institution of Civil Engineering - Geotechnical Engineering, 137* (4), 189-195.

Sun, D., Zhang, Jin, Zhang, Junran, & Zhang, L. (2013). Swelling characteristics of GMZ bentonite and its mixtures with sand. *Applied Clay Science, 83-84,* 224-230.

Tay, Y.Y., Stewart, D.I., & Cousens, T.W. (2001). Shrinkage and dessication cracking in bentonite-sand landfill liners. *Engineering Geology, 20*, 263-274.

Trgo, M. & Peric, J. (2003). Interaction of the zeolitic tuff with Zn containing simulated pollutant solutions. *Journal of Colloid and Interface Science, 260(1),*166-175.

Zamzow, M.J. & Murphy, J.E. (1992). Removal of metal cations from water using zeolites. *Separation Science and Technology, 27(14),* 1969–1984.

APPENDICES

APPENDIX A

SOIL CLASSIFICATION
(ZEOLITE AND BENTONITE MATERIALS)

Zeolite

$$No. \ 200 \cong 9\% < 50\% \ => Coarse - grained \ soils$$

$$No. \ 4 \cong 100\% > 50\% \ => Sand$$

$$5\% < No. \ 200 \cong 9\% < 12\% \ => Dual \ symbols$$

$$D_{60} \cong 0{,}78 \ mm, \qquad D_{30} \cong 0{,}55 \ mm, \qquad D_{10} \cong 0{,}11 \ mm$$

$$C_u = \frac{D_{60}}{D_{10}} = 7{,}09 > 6 \ and \ C_c = \frac{D_{30}^2}{D_{10}D_{60}} = 3{,}52 \ => SP - SM$$

$$SP - SM => Poorly \ graded \ sand \ and \ a \ little \ silt$$

Bentonite

$$No. \ 200 \cong 95\% > 50\% \ => Fine - grained \ soils$$

$$Liquid \ Limit : 405\%$$

$$Plastic \ Limit : 57\%$$

$$Plasticity \ Index : 348\%$$

$$CH => High \ Plasticity \ Clay$$

APPENDIX B

THE SWELLING DIAGRAMS AND TABLES:
DIAL READINGS AND SAMPLE HEIGHTS
(20%-30% ZBMs and 100% BENTONITE SAMPLES)
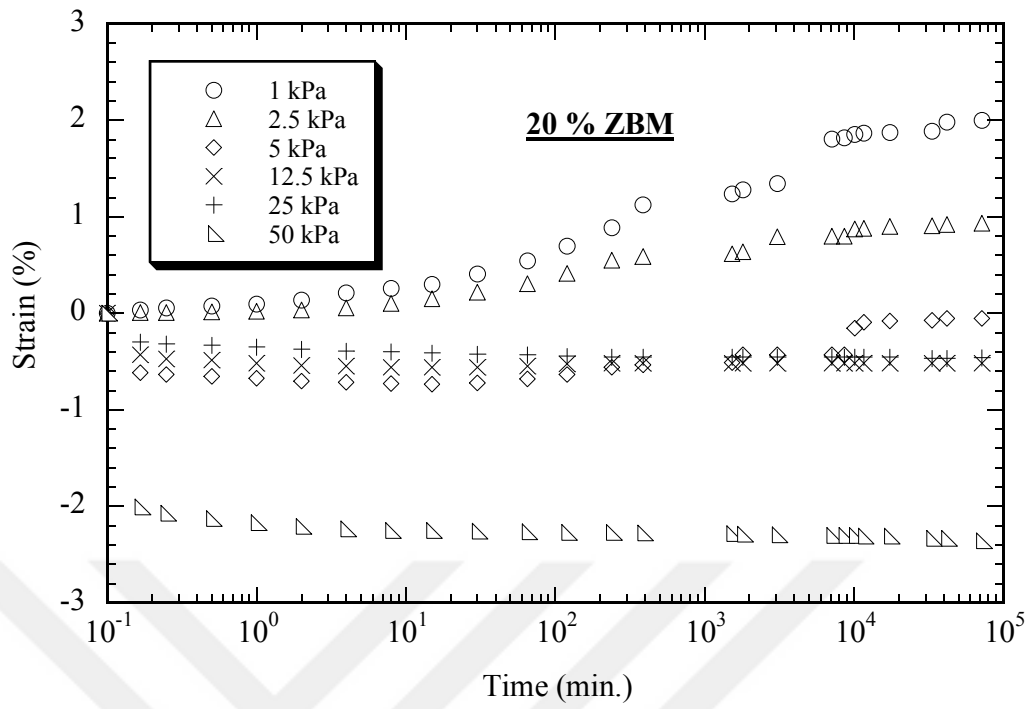
(a)
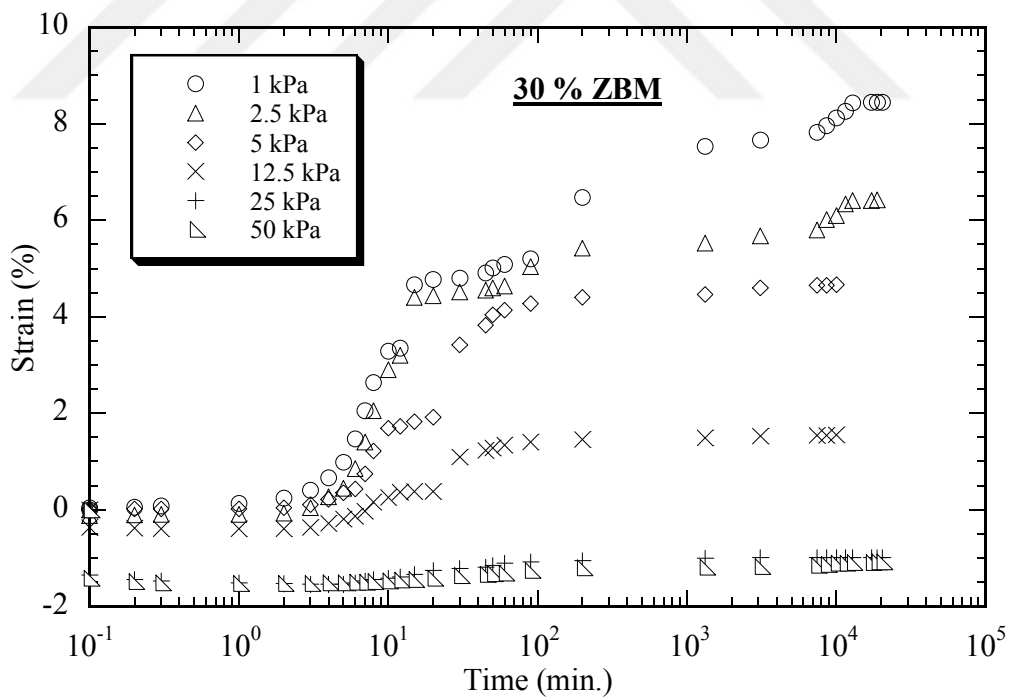
(b)

Figure B.1 Swelling strain-time relationship of ZBMs: a) 20% ZBM, b) 30% ZBM

1-) 20% ZBM under 1 kPa Effective Vertical Stress

Table B.1. 20% ZBM under 1 kPa effective vertical stress (dial readings and sample heights)

Time (min.)	Dial Reading	Height (mm)
0.1	2341.5	19.0000
0.167	2338	19.0070
0.25	2336	19.0110
0.5	2334	19.0150
1	2332.5	19.0180
2	2328.5	19.0260
4	2321.5	19.0400
6	2317	19.0490
8	2313	19.0570
15	2303	19.0770
30	2290	19.1030
60	2275	19.1330
120	2257	19.1690
240	2234.5	19.2140
323	2223	19.2370
360	2219.3	19.2444
420	2213	19.2570
1296	2169	19.3450
1403	2167	19.3490
1440	2164	19.3550
1505	2163	19.3570
1560	2162.3	19.3584
1680	2161	19.3610
2760	2152	19.3790
3000	2149.5	19.3840
3120	2148	19.3870
3180	2148	19.3870
3240	2148	19.3870
4500	2142	19.3990
6060	2139	19.4050
7200	2136	19.4110
9300	2128	19.4270
11760	2128	19.4270
17220	2123	19.4370
20400	2120.5	19.4420
32040	2117	19.4490
43560	2116	19.4510
50700	2115	19.4530
60840	2115	19.4530

Figure B.1. Swelling of 20% ZBM under 1 kPa effective vertical stress

2-) 20% ZBM under 2.5 kPa Effective Vertical Stress

Table B.2. 20% ZBM under 2.5 kPa effective vertical stress (dial readings and sample heights)

Time(min.)	Dial Reading	Height(mm)
0.1	1912	19
0.167	1911.5	19.001
0.25	1911	19.002
0.5	1910.5	19.003
1	1910	19.004
2	1908.8	19.0064
4	1906.5	19.011
8	1902.5	19.019
15	1898	19.028
30	1891.1	19.0418
60	1883	19.058
120	1872.5	19.079
240	1860	19.104
300	1856	19.112
360	1853	19.118

61

Table B.2. 20% ZBM under 2.5 kPa effective vertical stress (dial readings and sample heights) (continued)

Time (min.)	Dial Reading	Height (mm)
397	1851.5	19.121
1440	1836.5	19.151
1560	1836	19.152
1680	1835.8	19.1524
2760	1829	19.166
2980	1828	19.168
3090	1826	19.172
3150	1825.5	19.173
3210	1824	19.176
4480	1823	19.178
6030	1821.6	19.1808
7200	1820	19.184
9300	1819	19.186
11760	1817	19.19
17190	1817	19.19
20400	1817	19.19
32040	1817	19.19

Figure B.2. Swelling of 20% ZBM under 2.5 kPa effective vertical stress

3-) 20% ZBM under 5 kPa Effective Vertical Stress

Table B.3. 20% ZBM under 5 kPa effective vertical stress (dial readings and sample heights)

Time (min.)	Dial Reading	Height (mm)
0.1	2815	19.0000
0.167	2873	18.8840
0.25	2875	18.8800
0.5	2877	18.8760
1	2879	18.8720
2	2881.7	18.8666
4	2883	18.8640
8	2884	18.8620
15	2884.5	18.8610
30	2883.5	18.8630
60	2880	18.8700
120	2875	18.8800
240	2868	18.8940
300	2866	18.8980
360	2864	18.9020
1340	2856	18.9180
1475	2856	18.9180
1500	2856	18.9180
1590	2856	18.9180
1680	2830	18.9700
1720	2824	18.9820
1800	2823	18.9840
3080	2822	18.9860
4620	2820.5	18.9890
5760	2820	18.9900
7860	2819	18.9920
10320	2817.5	18.9950
15780	2816	18.9980
19080	2815.5	18.9990
30600	2815	19.0000
49320	2815	19.0000
42120	2815	19.0000
59400	2815	19.0000

Figure B.3. Swelling of 20% ZBM under 5 kPa effective vertical stress

4-) 20% ZBM under 12.5 kPa Effective Vertical Stress

Table B.4. 20% ZBM under 12.5 kPa effective vertical stress (dial readings and sample heights)

Time (min.)	Dial Reading	Height (mm)
0.1	3077	19
0.167	3118	18.918
0.333	3122	18.91
0.5	3123	18.908
1	3126.5	18.901
2	3128	18.898
4	3129	18.896
8	3130	18.894
15	3130	18.894
30	3129.8	18.8944
60	3128.8	18.8964
120	3127	18.9
240	3126	18.902
300	3126	18.902
360	3126	18.902
1320	3126	18.902
1440	3126	18.902

Table B.4. 20% ZBM under 12.5 kPa effective vertical stress (dial readings and sample heights) (continued)

Time (min.)	Dial Reading	Height (mm)
1500	3126	18.902
1560	3126	18.902
1710	3126	18.902
1770	3126	18.902
1785	3126	18.902
3060	3126	18.902
5760	3126	18.902
7860	3126	18.902
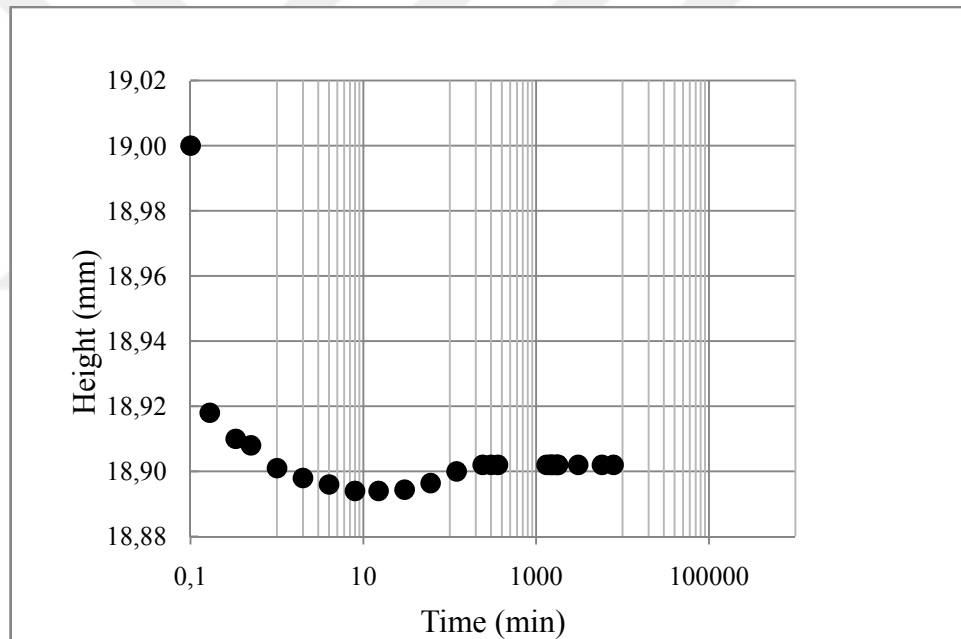
Figure B.4. Swelling of 20% ZBM under 12.5 kPa effective vertical stress

5-) 20% ZBM under 25 kPa Effective Vertical Stress

Table B.5. 20% ZBM under 25 kPa effective vertical stress (dial readings and sample heights)

Time (min.)	Dial Reading	Height (mm)
0.1	2300	19
0.167	2328	18.944
0.25	2330	18.94

Table B.5. 20% ZBM under 25 kPa effective vertical stress (dial readings and sample heights) (continued)

Time (min.)	Dial Reading	Height (mm)
0.5	2331	18.938
1	2333	18.934
2	2335	18.93
4	2337	18.926
8	2338	18.924
15	2339	18.922
30	2340.2	18.9196
60	2341.2	18.9176
120	2342	18.916
240	2342.5	18.915
360	2342.5	18.915
1346	2342.9	18.9142
1549	2342.9	18.9142
1819	2343.1	18.9138
2852	2343.1	18.9138
3017	2343.1	18.9138
4260	2343.2	18.9136
4590	2343.2	18.9136
8580	2343.2	18.9136
10020	2343.8	18.9124
10200	2343.8	18.9124
11515	2343.7	18.9126
11735	2343.7	18.9126
12960	2343.7	18.9126
13359	2343.6	18.9128
14259	2343.6	18.9128
14449	2343.5	18.913
18673	2343.2	18.9136
19119	2343.2	18.9136
22733	2344.1	18.9118
24383	2344.1	18.9118
28718	2344.1	18.9118
30188	2344.5	18.911

Table B.5. 20% ZBM under 25 kPa effective vertical stress (dial readings and sample heights) (continued)

Time (min.)	Dial Reading	Height (mm)
31680	2344.5	18.911
33120	2344.5	18.911
38880	2344.5	18.911
55080	2345.2	18.9096
63640	2345.2	18.9096
93620	2346.5	18.907

Figure B.5. Swelling of 20% ZBM under 25 kPa effective vertical stress

6-) 20% ZBM under 50 kPa Effective Vertical Stress

Table B.6. 20% ZBM under 50 kPa effective vertical stress (dial readings and sample heights)

Time (min.)	Dial Reading	Height (mm)
0.1	1645.1	19
0.167	1836	18.6182
0.25	1842	18.6062

Table B.6. 20% ZBM under 50 kPa effective vertical stress (dial readings and sample heights) (continued)

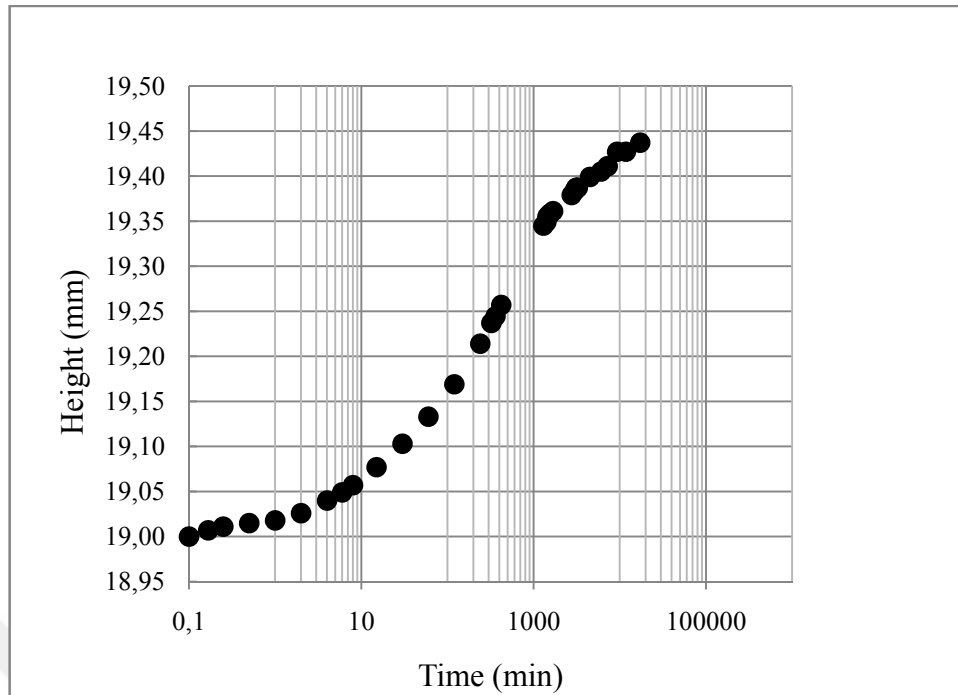| Time (min.)	Dial Reading	Height (mm)
0.5	1847	18.5962
1	1851	18.5882
2	1854.2	18.5818
4	1857.1	18.576
8	1858.1	18.574
15	1858.5	18.5732
30	1859.1	18.572
65	1859.6	18.571
120	1860	18.5702
240	1860.2	18.5698
387	1860.9	18.5684
1526	1861.5	18.5672
1817	1861.8	18.5666
3073	1862.5	18.5652
7104	1863	18.5642
8580	1863.1	18.564
10160	1863.5	18.5632
11600	1863.8	18.5626
17280	1864	18.5622
33420	1865.7	18.5588
42030	1866.1	18.558
71980	1868	18.5542

Figure B.6. Swelling of 20% ZBM under 50 kPa effective vertical stress

7-) 30% ZBM under 1 kPa Effective Vertical Stress

Table B.7. 30% ZBM under 1 kPa effective vertical stress (dial readings and sample heights)

Time (min.)	Dial Reading	Height (mm)
0.1	1878	19.0000
0.167	1874	19.0080
0.333	1872.5	19.0110
0.5	1870	19.0160
1	1865	19.0260
2	1854.5	19.0470
4	1839	19.0780
8	1815	19.1260
15	1783.5	19.1890
30	1737	19.2820
60	1681	19.3940
120	1624	19.5080
240	1562	19.6320
300	1555	19.6460
1320	1426	19.9040
1440	1415	19.9260
1470	1412	19.9320
1560	1402	19.9520
1650	1391	19.9740
1740	1384	19.9880
1860	1372	20.0120

3120	1245	20.2660
4600	1138.5	20.4790
5730	1125	20.5060
7800	1107	20.5420
10290	1094	20.5680
15780	1076.5	20.6030
19050	1064	20.6280
30600	1045	20.6660
42120	1044	20.6680
49260	1044	20.6680
59400	1044	20.6680
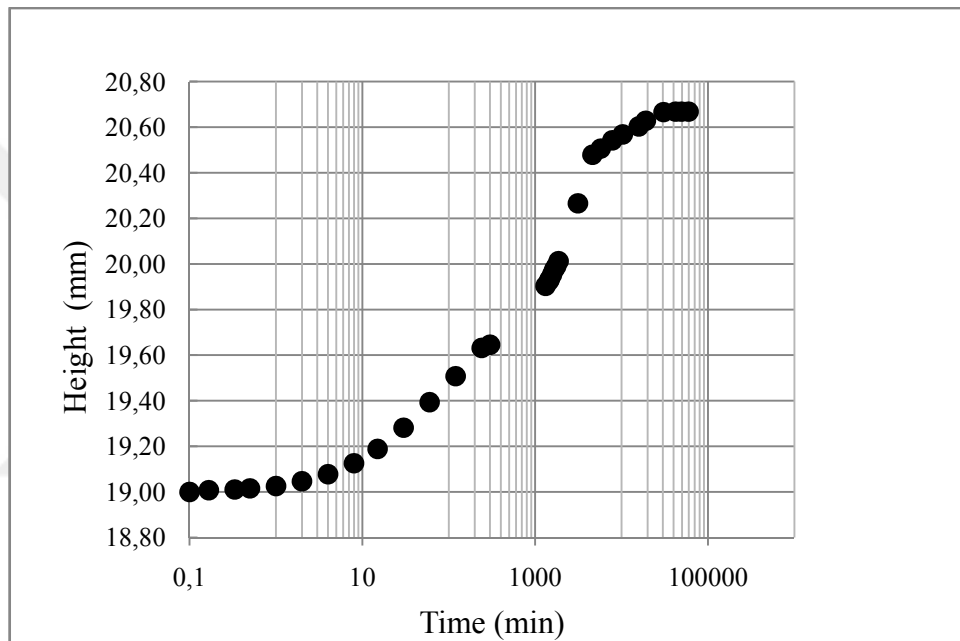
Figure B.7. Swelling of 30% ZBM under 1 kPa effective vertical stress

8-) 30% ZBM under 2.5 kPa Effective Vertical Stress

Table B.8. 30% ZBM under 2.5 kPa effective vertical stress (dial readings and sample heights)

Time (min.)	Dial Reading	Height (mm)
0.1	2380	19
0.167	2391	18.978
0.333	2390	18.98
0.5	2389.5	18.981
1	2389	18.982
2	2386	18.988
4	2376.5	19.007

Time	Dial Reading	Height
8	2354	19.052
15	2337	19.086
30	2299	19.162
60	2246	19.268
120	2183	19.394
240	2101	19.558
300	2071	19.618
1380	1953	19.854
1440	1951	19.858
1560	1943	19.874

Table B.8. 30% ZBM under 2.5 kPa effective vertical stress (dial readings and sample heights) (continued)

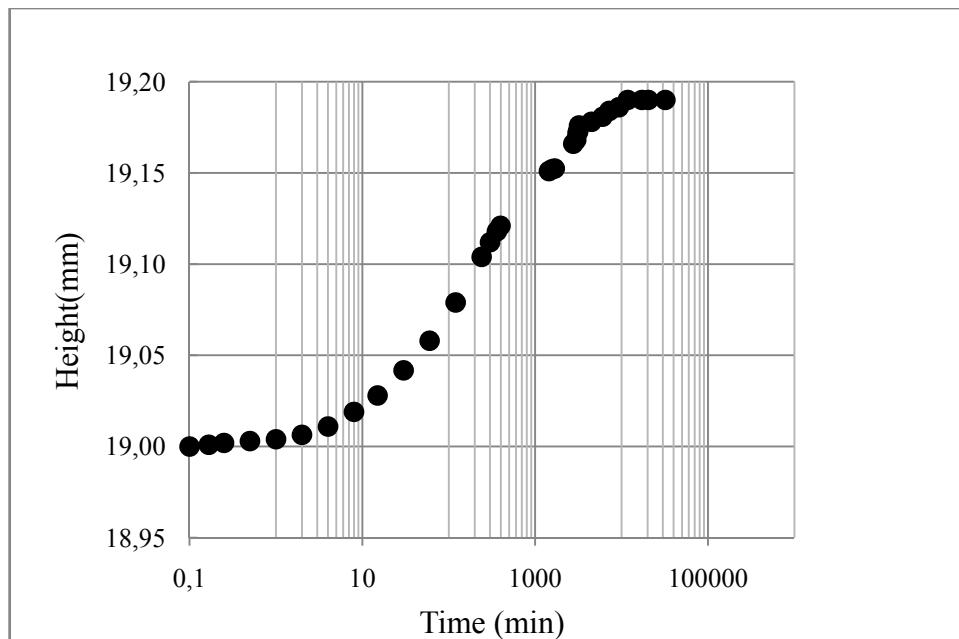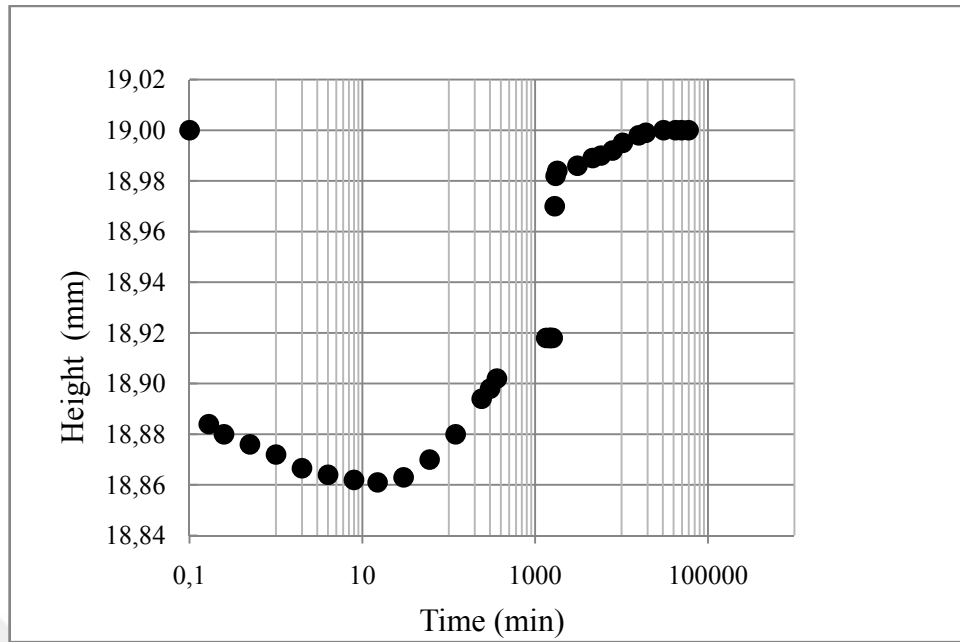| Time (min.)	Dial Reading	Height (mm)
1620	1939.5	19.881
1680	1935	19.89
1785	1931	19.898
3030	1890	19.98
4540	1852	20.056
5700	1842	20.076
7800	1826.5	20.107
10260	1815	20.13
15720	1793	20.174
19020	1784	20.192
30600	1760.5	20.239
42120	1753	20.254
49200	1753	20.254
59400	1752	20.256
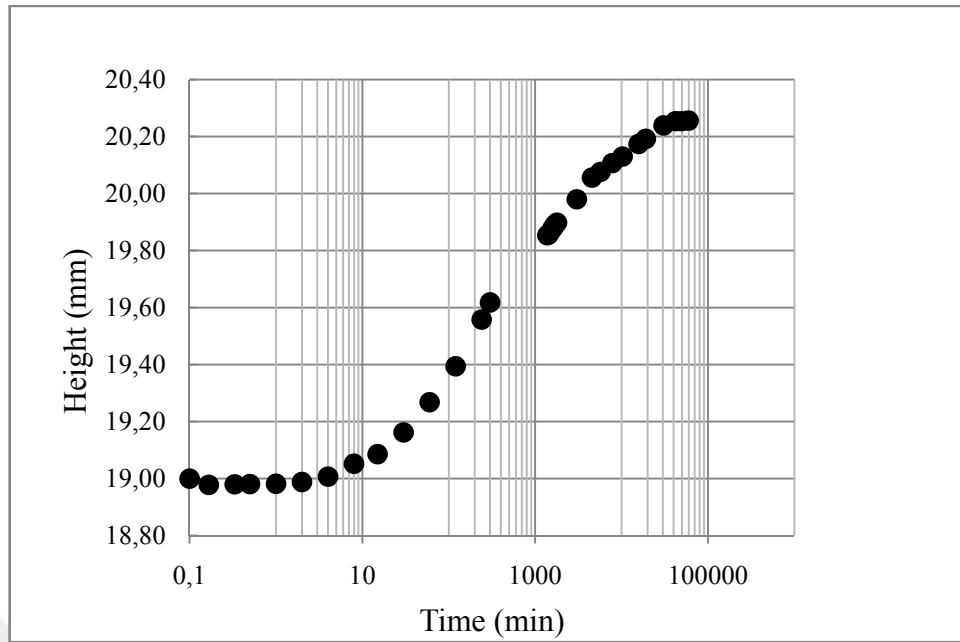
Figure B.8. Swelling of 30% ZBM under 2.5 kPa effective vertical stress

9-) 30% ZBM under 5 kPa Effective Vertical Stress

Table B.9. 30% ZBM under 5 kPa effective vertical stress (dial readings and sample heights)

Time (min.)	Dial Reading	Height (mm)
0.1	2388	19.0000
0.167	2386	19.0040
0.333	2386	19.0040
0.5	2386	19.0040
1	2386	19.0040
2	2383.5	19.0090
4	2378	19.0200
8	2367	19.0420
15	2354.5	19.0670
30	2347	19.0820
60	2316.5	19.1430
120	2272	19.2320
230	2226	19.3240
240	2222	19.3320
270	2213	19.3500
300	2204	19.3680
1510	2058.5	19.6590
3090	2019	19.7380
4320	1997.5	19.7810
6420	1988	19.8000
8820	1975	19.8260
14280	1962	19.8520

| 17580	1956	19.8640
29160	1942.5	19.8910
40620	1937.5	19.9010
47760	1937	19.9020
57960	1936	19.9040
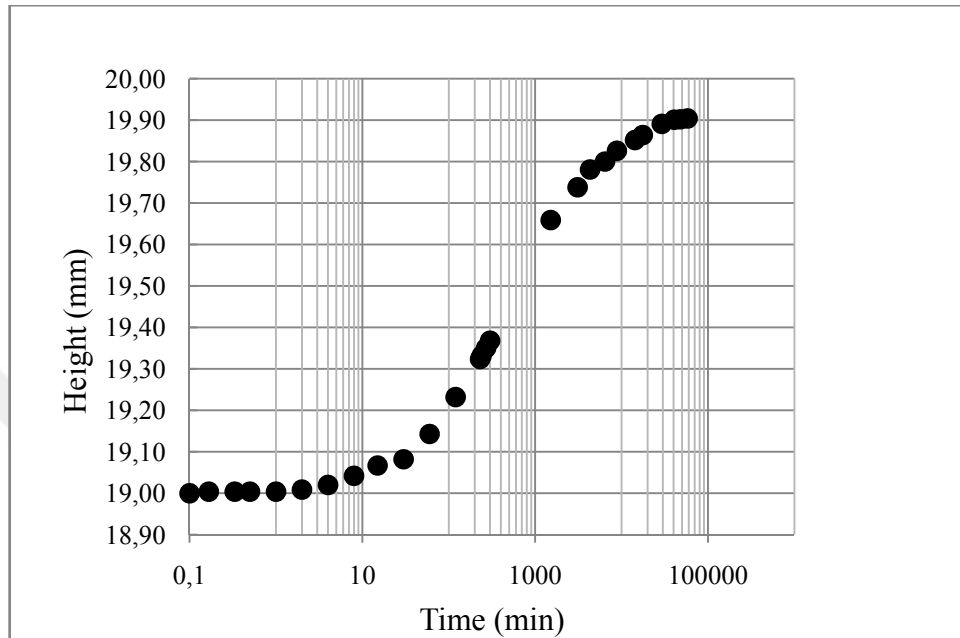
Figure B.9. Swelling of 30% ZBM under 5 kPa effective vertical stress

10-) 30% ZBM under 12.5 kPa Effective Vertical Stress

Table B.10. 30% ZBM under 12.5 kPa effective vertical stress (dial readings and sample heights)

Time (min.)	Dial Reading	Height (mm)
0.1	2258	19
0.167	2293	18.93
0.333	2294	18.928
0.5	2295	18.926
1	2295	18.926
2	2295	18.926
4	2292.5	18.931
8	2285.5	18.945
15	2275.5	18.965
30	2271	18.974
60	2261	18.994
120	2242	19.032

Table B.10. 30% ZBM under 12.5 kPa effective vertical stress (dial readings and sample heights) (continued)

Time (min.)	Dial Reading	Height (mm)
180	2234	19.048
240	2222.5	19.071
270	2222	19.072
306	2222	19.072
1580	2154	19.208
3100	2140.5	19.235
4320	2136	19.244
6420	2129.5	19.257
8820	2124	19.268
14280	2118.5	19.279
17580	2116	19.284
29160	2112	19.292
40620	2111	19.294
47760	2111	19.294
57960	2109	19.298
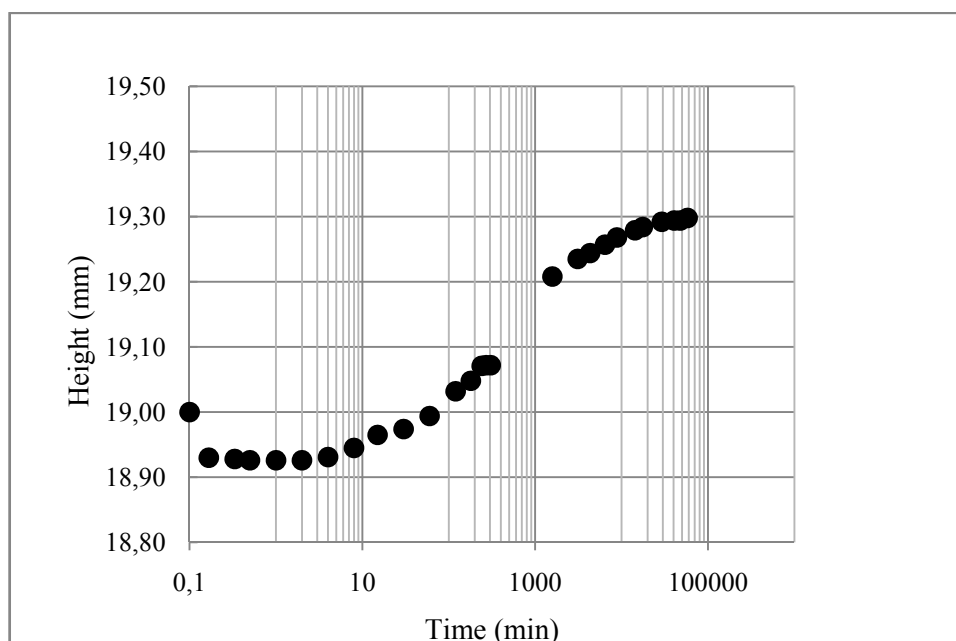
Figure B.10. Swelling of 30% ZBM under 12.5 kPa effective vertical stress

11-) 30% ZBM under 25 kPa Effective Vertical Stress

Table B.11. 30% ZBM under 25 kPa effective vertical stress (dial readings and sample heights)

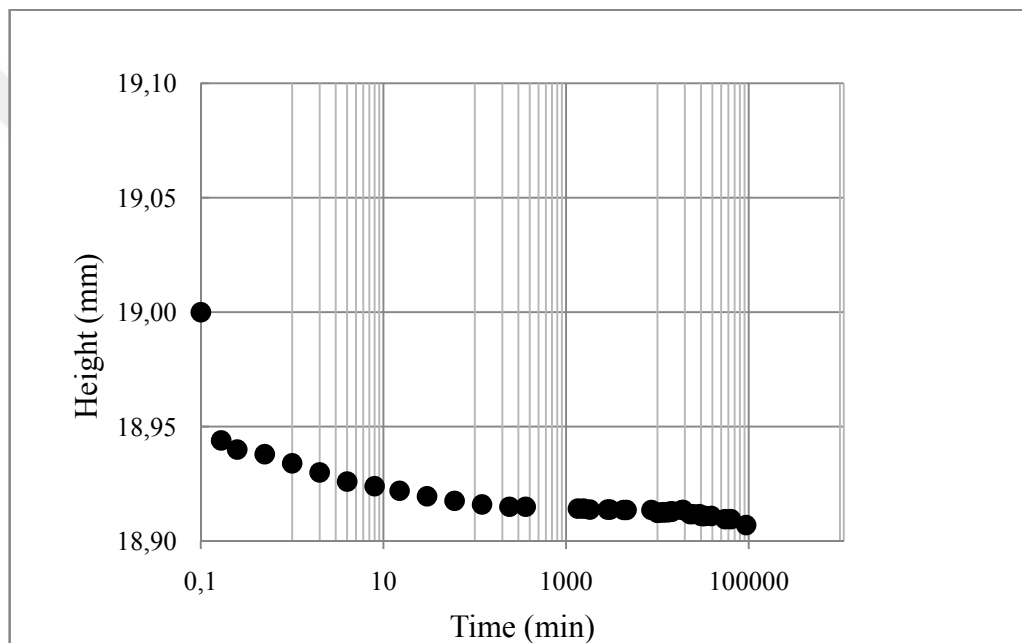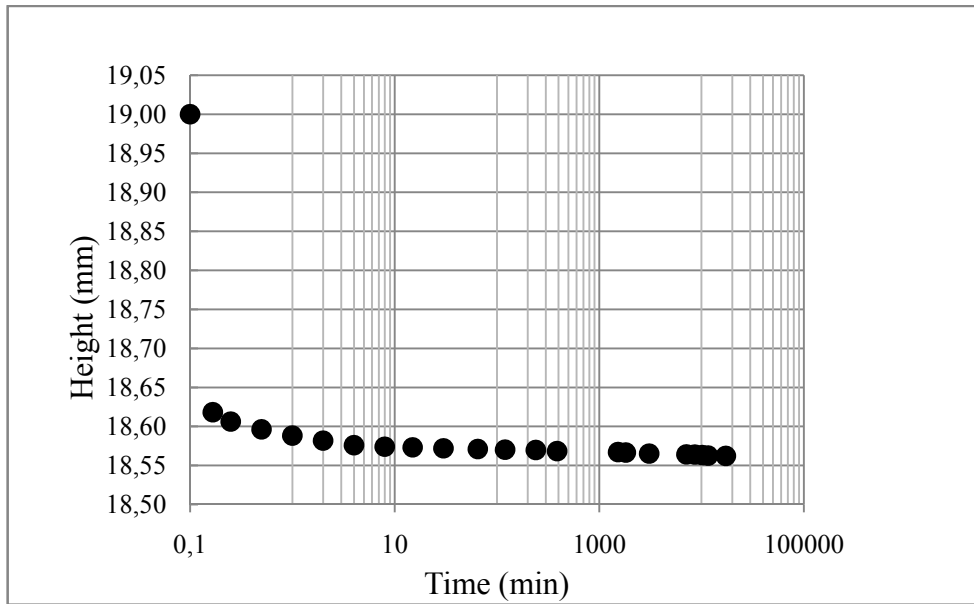| Time (min.)	Dial Reading	Height (mm)
0.1	950	19.0000
0.15	1078	18.7440
0.2	1087	18.7260
0.3	1090	18.7200
0.45	1093	18.7140
1	1094.5	18.7110
2	1096	18.7080
3	1096	18.7080
4	1095.5	18.7090
6	1093	18.7140
8	1090	18.7200
10	1087.5	18.7250
12	1085	18.7300
15	1081.5	18.7370
20	1077	18.7460
30	1070	18.7600
40	1065	18.7700
45	1063	18.7740
60	1059	18.7820
80	1055	18.7900
90	1053.2	18.7936
120	1050	18.8000
240	1045	18.8100
1380	1044	18.8120
3120	1044	18.8120
7440	1044	18.8120
8640	1044	18.8120
10080	1044	18.8120
11520	1044	18.8120
12870	1044	18.8120
17280	1044	18.8120
18840	1044	18.8120
20310	1044	18.8120
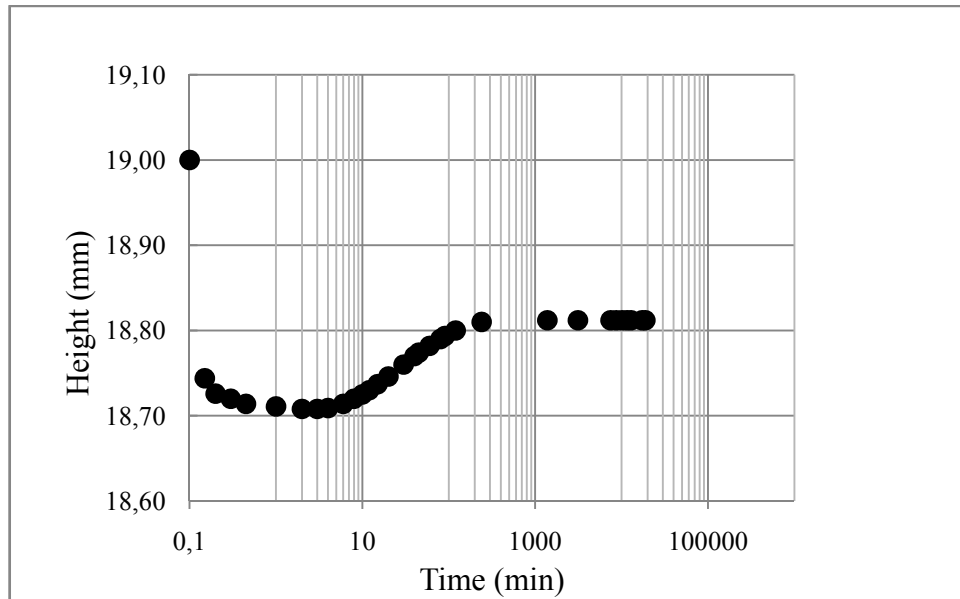
Figure B.11. Swelling of 30% ZBM under 25 kPa effective vertical stress

12-) 30% ZBM under 50 kPa Effective Vertical Stress

Table B.12. 30% ZBM under 50 kPa effective vertical stress (dial readings and sample heights)

Time (min.)	Dial Reading	Height (mm)
0.1	950	19
0.15	1085	18.73
0.2	1091	18.718
0.3	1093	18.714
0.45	1094.5	18.711
1	1094.5	18.711
2	1094.5	18.711
3	1094	18.712
4	1093	18.714
6	1092.5	18.715
7	1092	18.716
8	1091	18.718
10	1090	18.72
12	1088.5	18.723
15	1086.5	18.727
20	1084	18.732
30	1080	18.74

Table B.12. 30% ZBM under 50 kPa effective vertical stress (dial readings and sample heights) (continued)

Time (min.)	Dial Reading	Height (mm)
45	1076.5	18.747
50	1075.5	18.749
60	1074	18.752
90	1070	18.76
200	1065	18.77
1320	1063	18.774
3090	1062	18.776
7415	1059	18.782
8580	1058	18.784
10045	1056	18.788
11485	1055	18.79
12835	1054	18.792
17245	1053.5	18.793
18805	1053	18.794
20275	1052.5	18.795
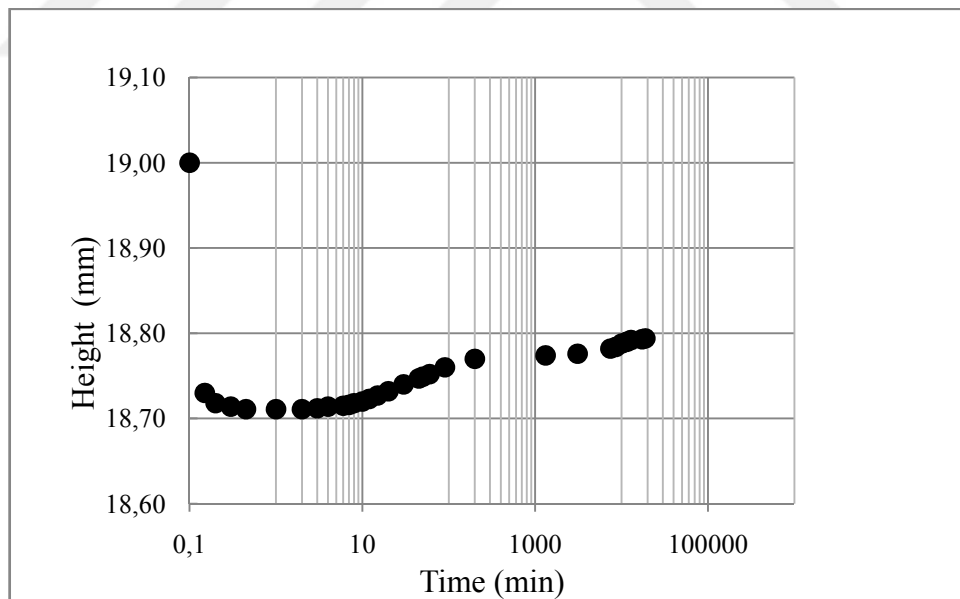
Figure B.12. Swelling of 30% ZBM under 25 kPa effective vertical stress

13-) 100% Bentonite Sample under 1 kPa Effective Vertical Stress for 10 and 25 Blows

Table B.13. 100% Bentonite Sample under 1 kPa Effective Vertical Stress for 10 Blows (dial readings and sample heights)

Time (min.)	Dial Reading	Height (mm)
0.01	5808	3.000
0.1	5822	2.972
0.25	5828	2.960
0.5	5826	2.964
0.75	5821	2.974
1	5818	2.980
2	5794	3.028
4	5745	3.126
6	5700	3.216
8	5656	3.304
12	5596	3.424
15	5537	3.542
30	5330	3.956
60	5032	4.552
135	4568	5.480
245	3893	6.830
435	3225	8.166
1560	1779	11.058
2910	1282	12.052
4320	1048	12.520
8640	893	12.830
10035	862	12.892
11445	841	12.934

Figure B.13. Swelling of 100% Bentonite Sample under 1 kPa effective vertical stress for 10 Blows

Table B.14. 100% Bentonite Sample under 1 kPa Effective Vertical Stress for 25 Blows (dial readings and sample heights)

Time (min.)	Dial Reading	Height (mm)
0.01	6112	3
0.1	6118	2.988
0.25	6113	2.998
0.75	6093	3.038
1	6081	3.062
2	6047	3.13
3	6020	3.184
4	5997	3.23
6	5952	3.32
8	5911	3.402
12	5837	3.55
15	5786	3.652
30	5560	4.104
60	5229	4.766
125	4716	5.792
210	4200	6.824
250	3968	7.288
320	3641	7.942
360	3475	8.274

Table B.14. 100% Bentonite Sample under 1 kPa Effective Vertical Stress for 25 Blows (dial readings and sample heights)   (continued)

Time (min.)	Dial Reading	Height (mm)
600	2724	9.776
1380	1700	11.824
1450	1645	11.934
1800	1423	12.378
2040	1309	12.606
2820	1056	13.112
3060	1008	13.208
3240	971	13.282
4340	832	13.56
7110	729	13.766
7270	719	13.786
8550	688.5	13.847
8840	679	13.866
10020	649	13.926
11460	625	13.974
12960	608	14.008
14400	596	14.032
16070	572	14.08
17220	558	14.108
17660	549	14.126
18660	546	14.132
18780	543	14.138
18930	540	14.144
20370	536	14.152
20550	532	14.16
21540	525	14.174
23060	515	14.194
23300	511	14.202
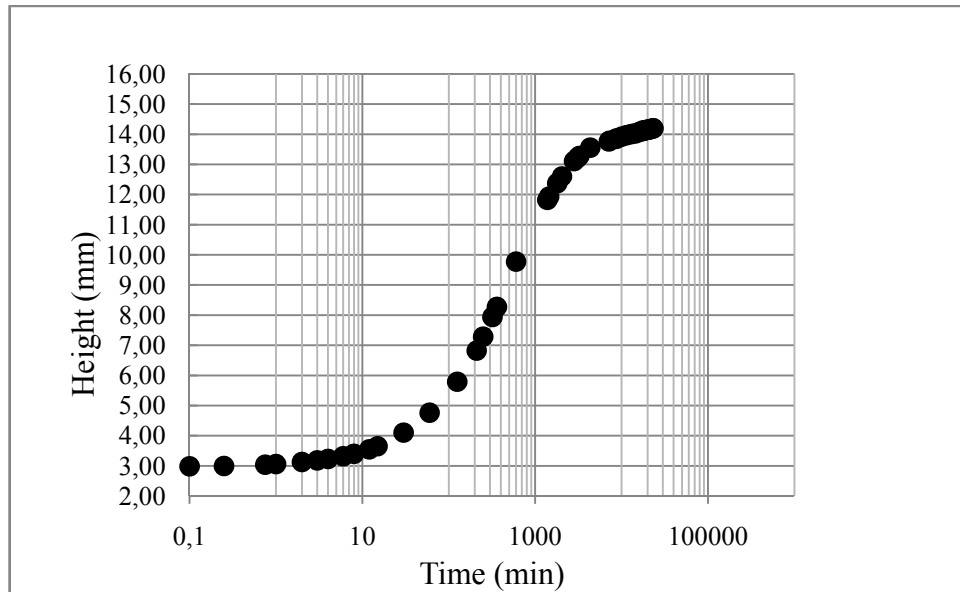
Figure B.14 Swelling of 100% Bentonite Sample under 1 kPa effective vertical stress for 25 Blows

14-) 100% Bentonite Sample under 2.5 kPa Effective Vertical Stress for 10 and 25 Blows

Table B.15. 100% Bentonite Sample under 2.5 kPa Effective Vertical Stress for 10 Blows (dial readings and sample heights)

Time (min.)	Dial Reading	Height (mm)
0.01	4740	3
0.1	4778	2.924
0.25	4783	2.914
0.75	4777	2.926
1	4772	2.936
2	4752	2.976
3	4733	3.014
4	4715	3.05
6	4681	3.118
8	4652	3.176
15	4565	3.35
30	4434	3.612
60	4240	4
110	4078	4.324
230	3469	5.542
300	3254	5.972
360	3103	6.274

Table B.15. 100% Bentonite Sample under 2.5 kPa Effective Vertical Stress for 10 Blows (dial readings and sample heights) (continued)

Time (min.)	Dial Reading	Height (mm)
630	2638	7.204
1350	2150	8.18
1380	2138	8.204
1440	2117	8.246
1500	2097	8.286
1560	2078	8.324
1680	2045	8.39
1800	2014	8.452
2820	1875	8.73
3300	1851	8.778
4340	1804	8.872
4800	1792	8.896
5670	1772	8.936
5760	1770	8.94
6030	1764	8.952
6150	1762	8.956
7110	1748	8.984
7230	1746	8.988
7350	1744	8.992
7500	1742	8.996
8580	1727	9.027
8700	1725	9.03
9000	1723	9.034
9180	1721	9.038
10020	1712	9.056

Figure B.15. Swelling of 100% Bentonite Sample under 2.5 kPa effective vertical stress for 10 Blows

Table B.16. 100% Bentonite Sample under 2.5 kPa Effective Vertical Stress for 25 Blows (dial readings and sample heights)

Time (min.)	Dial Reading	Height (mm)
0.01	6440	3
0.1	6455	2.97
0.25	6459	2.962
0.5	6461	2.958
1	6455	2.97
2	6434	3.012
3	6402	3.076
4	6370	3.14
6	6319	3.242
8	6263	3.354
15	6124	3.632
30	5900	4.08
60	5580	4.72
120	5112	5.656
240	4479	6.922
310	4234	7.412
360	4068	7.744
630	3488	8.904
1350	2832	10.216
1380	2818	10.244
1440	2790	10.3

Table B.16. 100% Bentonite Sample under 2.5 kPa Effective Vertical Stress for 25 Blows (dial readings and sample heights) (continued)

Time (min.)	Dial Reading	Height (mm)
1500	2762	10.356
1560	2738	10.404
1680	2690	10.5
1800	2652	10.576
2820	2478	10.924
3300	2441	10.998
4350	2369	11.142
4800	2355	11.17
5670	2337	11.206
5760	2330	11.22
6030	2329.5	11.221
6150	2329	11.222
7110	2315	11.25
7230	2312	11.256
7350	2309	11.262
7500	2308	11.264
8580	2288	11.304
8700	2286.5	11.307
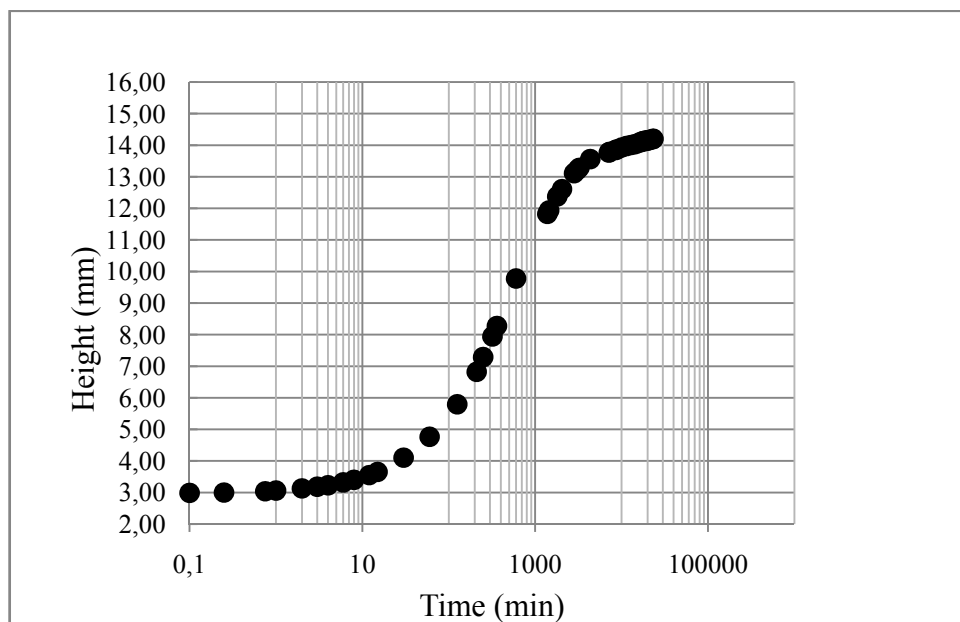
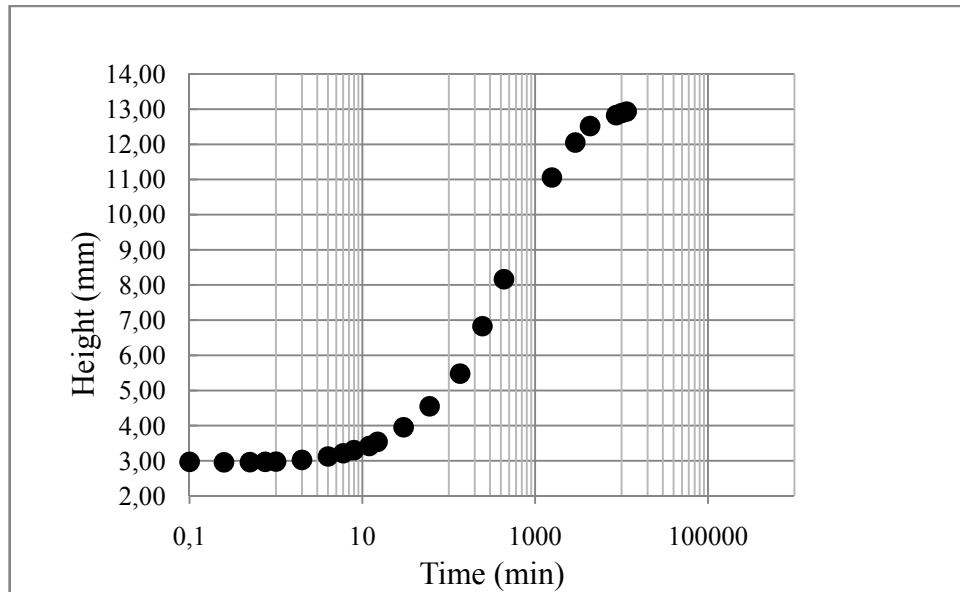Figure B.16. Swelling of 100% Bentonite Sample under 2.5 kPa effective vertical stress for 25 Blows

15-) 100% Bentonite Sample under 5 kPa Effective Vertical Stress for 10 and 25 Blows

Table B.17. 100% Bentonite Sample under 5 kPa Effective Vertical Stress for 10 Blows (dial readings and sample heights)

Time (min.)	Dial Reading	Height (mm)
0.01	5535	3
0.25	5598	2.874
0.5	5599	2.872
1	5596	2.878
2	5579	2.912
4	5541	2.988
5	5523	3.024
6	5506	3.058
8	5475	3.12
12	5421	3.228
15	5386	3.298
30	5335	3.4
60	5003	4.064
120	4672	4.726
250	4159	5.752
405	3762	6.546
1410	2970	8.13
1530	2828	8.414
1680	2783	8.504
2880	2572	8.926
3120	2548	8.974
3300	2535	9
4260	2487	9.096
5800	2451	9.168
6035	2446	9.178
10380	2382	9.306
12000	2363	9.344
13380	2347	9.376
14760	2332	9.406
16170	2317	9.436
20100	2286	9.498
20580	2282	9.506

Table B.17. 100% Bentonite Sample under 5 kPa Effective Vertical Stress for 10 Blows (dial readings and sample heights) (continued)

| Time (min.)	Dial Reading	Height (mm)
21570	2276	9.518
21810	2270	9.53
22080	2268	9.534
23220	2263	9.544
24540	2256	9.558
25960	2246	9.578
30270	2222	9.626
31680	2214	9.642
33090	2206	9.658
33160	2205	9.66

Figure B.17. Swelling of 100% Bentonite Sample under 5 kPa effective vertical stress for 10 Blows

Table B.18. 100% Bentonite Sample under 5 kPa Effective Vertical Stress for 25 Blows (dial readings and sample heights)

Time (min.)	Dial Reading	Height (mm)
0.01	3982	3
0.1	4064	2.836

Table B.18. 100% Bentonite Sample under 5 kPa Effective Vertical Stress for 25 Blows (dial readings and sample heights) (continued)

Time (min.)	Dial Reading	Height (mm)
0.25	4079	2.806
0.5	4085	2.794
0.75	4084	2.796
1	4080	2.804
2	4058	2.848
3	4038	2.888
4	4017	2.93
6	3981	3.002
8	3954	3.056
12	3888	3.188
15	3860	3.244
30	3716	3.532
45	3581	3.802
60	3461	4.042
120	3076	4.812
290	2398	6.168
300	2374	6.216
440	2077	6.81
1440	1364	8.236
1560	1330	8.304
1710	1290	8.384
2880	1140	8.684
3150	1123	8.718
3320	1112	8.74
4320	1074	8.816
5850	1045	8.874
6070	1040	8.884
10410	986	8.992
12030	974	9.016
13410	960	9.044
14790	945	9.074
16200	926	9.112
20140	912	9.14
20620	909.5	9.145
21610	909	9.146
21850	908.5	9.147

Table 18. 100% Bentonite Sample under 5 kPa Effective Vertical Stress for 25 Blows (dial readings and sample heights) (continued)

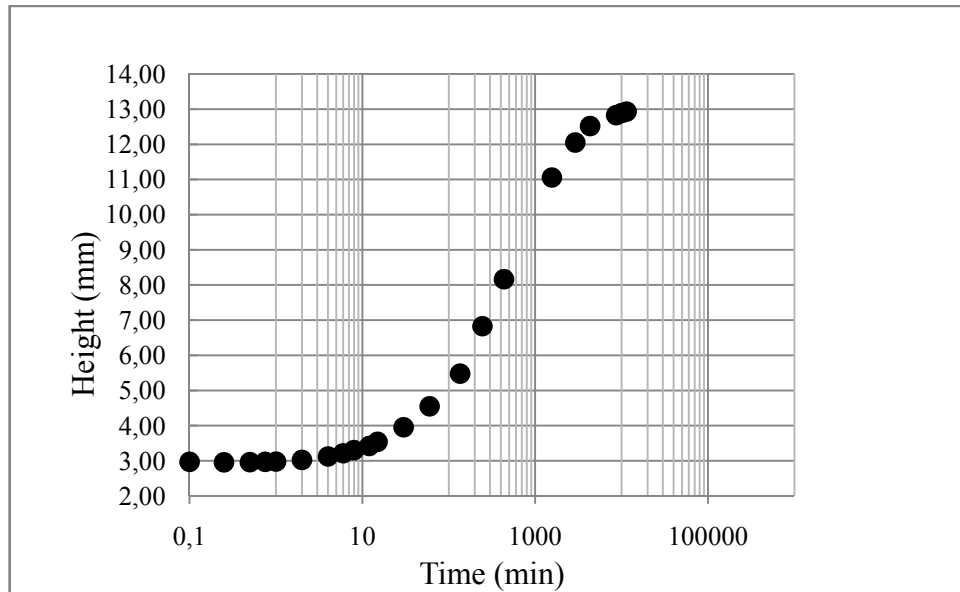| Time (min.)	Dial Reading	Height (mm)
23245	901.5	9.161
24575	894	9.176
25995	887	9.19
30310	874	9.216
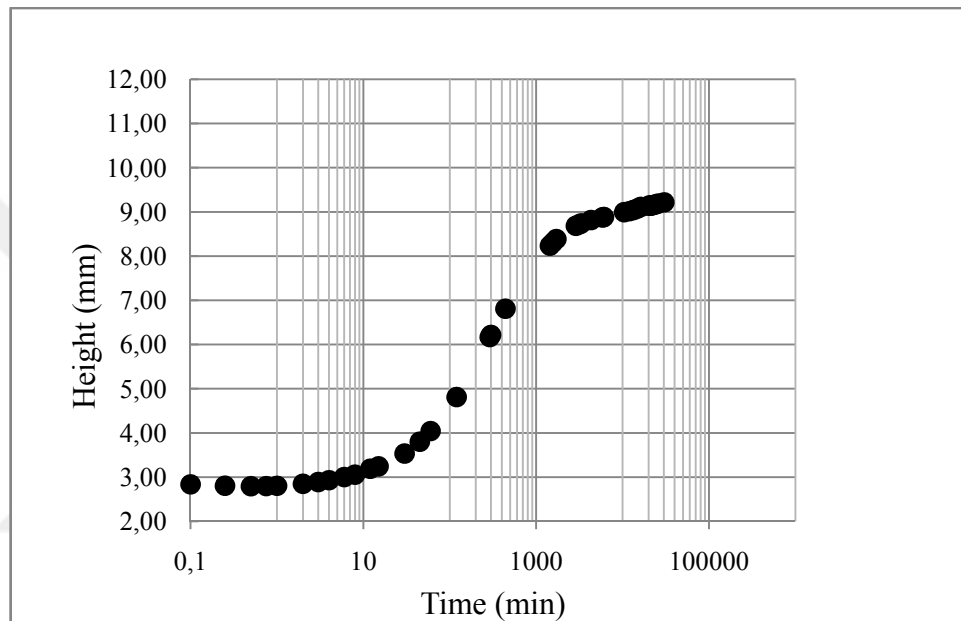
Figure B.18 Swelling of 100% Bentonite Sample under 5 kPa effective vertical stress for 25 Blows

16-) 100% Bentonite Sample under 12.5 kPa Effective Vertical Stress for 10 and 25 Blows

Table B.19. 100% Bentonite Sample under 12.5 kPa Effective Vertical Stress for 10 Blows (dial readings and sample heights)

Time(min.)	Dial Reading	Height(mm)
0.01	4260	3
0.1	4322	2.876
0.25	4323	2.874
0.5	4325	2.87
0.75	4321	2.878
1	4317	2.886

Table B.19. 100% Bentonite Sample under 12.5 kPa Effective Vertical Stress for 10 Blows (dial readings and sample heights) (continued)

| Time(min.)	Dial Reading	Height(mm)
2	4298	2.924
4	4261	2.998
6	4230	3.06
8	4209	3.102
10	4177	3.166
12	4155	3.21
15	4125	3.27
30	4000	3.52
60	3800	3.92
120	3480	4.56
160	3300	4.92
270	2955	5.61
450	2613	6.294
1580	2150	7.22
2925	1940	7.64
4340	1905	7.71
8660	1849	7.822
10060	1835	7.85
11460	1821	7.878

Figure B.19. Swelling of 100% Bentonite Sample under 12.5 kPa effective vertical stress for 10 Blows

Table B.20. 100% Bentonite Sample under 12.5 kPa Effective Vertical Stress for 25 Blows (dial readings and sample heights)

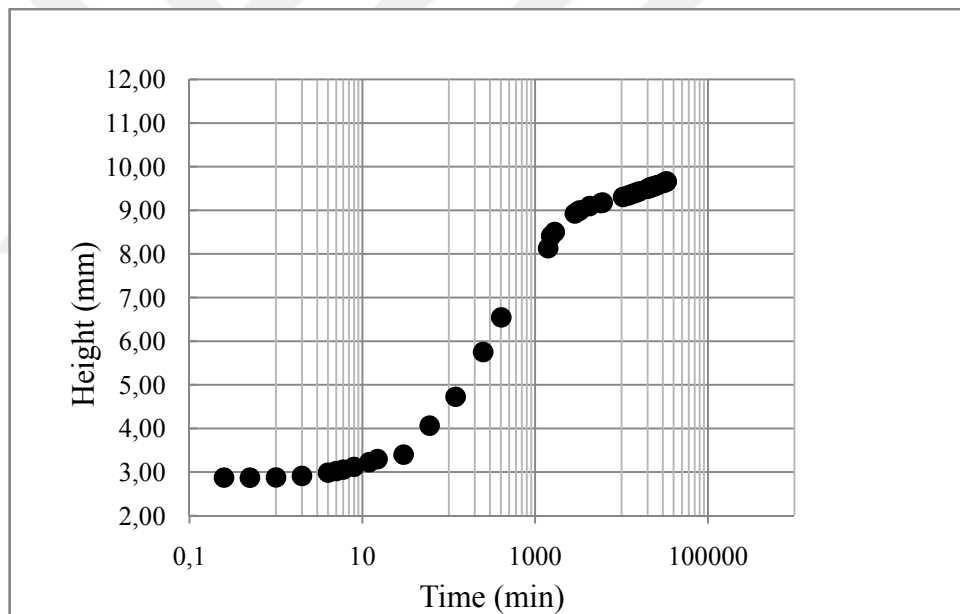| Time(min.)	Dial Reading	Height(mm)
0.01	3547	3.000
0.1	3650	2.794
0.25	3653	2.788
0.5	3654	2.786
1	3647	2.800
2	3628	2.838
3	3607	2.880
4	3586	2.922
5	3566	2.962
6.5	3539	3.016
8	3514	3.066
12	3454	3.186
15	3416	3.262
22	3336	3.422
30	3259	3.576
45.5	3132	3.830
60	3031	4.032
120	2710	4.674
180	2449	5.196
240	2223	5.648
280	2089	5.916
300	2030	6.034
360	1865	6.364
660	1318	7.458
1395	890	8.314
1480	856	8.382
1810	762	8.570
2070	712	8.670
2835	626	8.842
3090	606	8.882
3270	599	8.896
4365	548	8.998
7140	493	9.108
7300	490	9.114
8580	489.5	9.115
8850	485	9.124
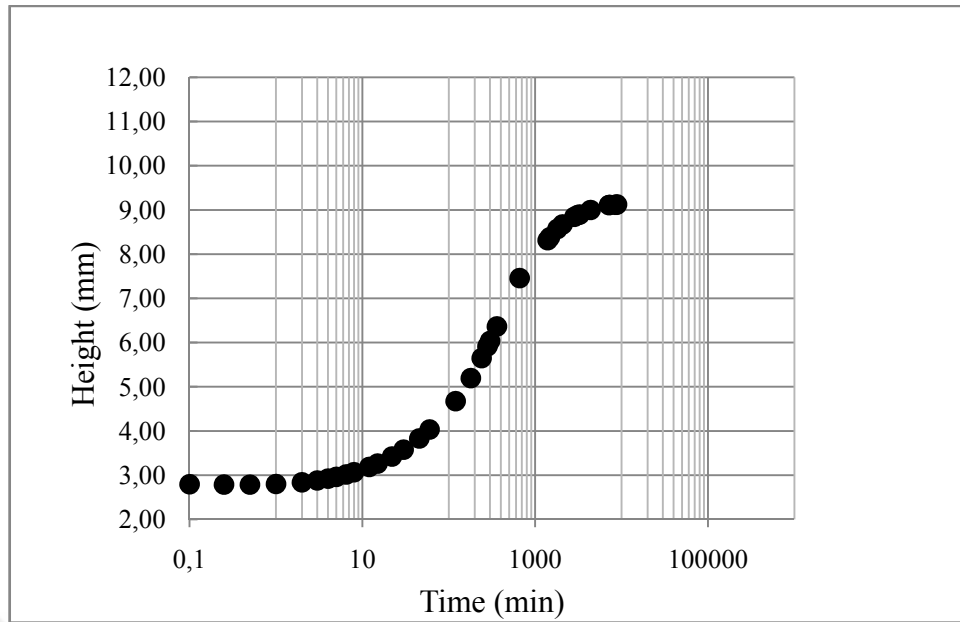
Figure B.20. Swelling of 100% Bentonite Sample under 12.5 kPa effective vertical stress for 25 Blows

17-) 100% Bentonite Sample under 25 kPa Effective Vertical Stress for 10 and 25 Blows

Table B.21. 100% Bentonite Sample under 25 kPa Effective Vertical Stress for 10 Blows (dial readings and sample heights)

Time(min.)	Dial Reading	Height(mm)
0.01	3105	3
0.1	3225	2.76
0.3	3490	2.23
0.45	3497	2.216
1	3499	2.212
2	3499	2.212
3	3493	2.224
4	3485	2.24
5	3478	2.254
6	3469	2.272
8	3452	2.306
12	3419	2.372
15	3395	2.42
30	3289	2.632
60	3118	2.974
120	2840	3.53
240	2460	4.29

Table B.21. 100% Bentonite Sample under 25 kPa Effective Vertical Stress for 10 Blows (dial readings and sample heights) (continued)

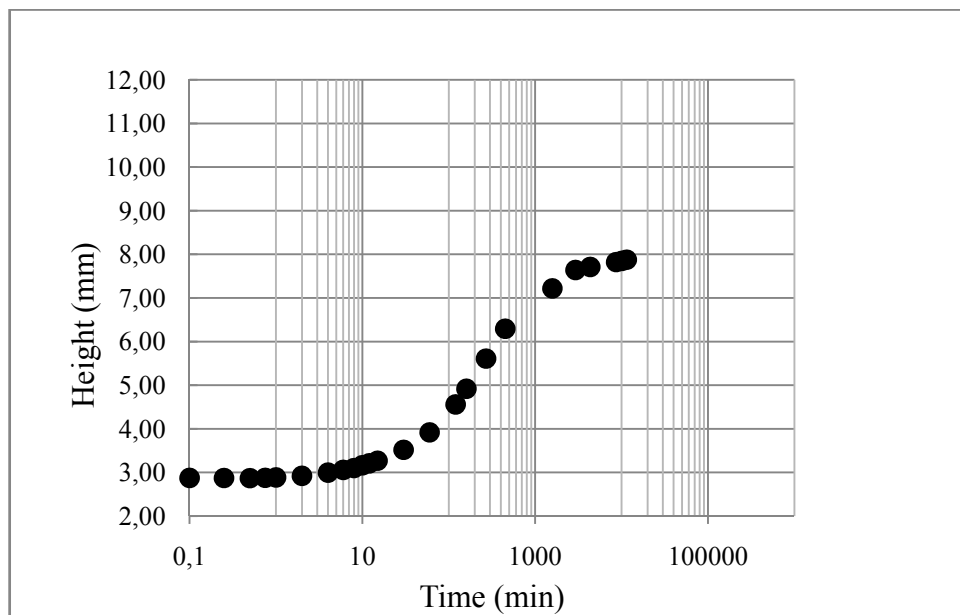| Time(min.)	Dial Reading	Height(mm)
390	2130	4.95
1520	1390	6.43
2870	1240	6.73
4275	1181	6.848
4305	1111	6.988
5729	1092	7.026
7135	1075	7.06
7555	1070	7.07
8635	1058	7.094
9025	1053	7.104
10255	1040	7.13
11545	1026.5	7.157
15956	986	7.238
17387	973	7.264
18767	962	7.286
24475	927	7.356
25915	921	7.368
27355	915	7.38
28799	908	7.394
30239	901	7.408
31709	883	7.444
33029	877	7.456
34529	870	7.47
34829	867	7.476
35965	863	7.484
37709	858	7.494
39149	847	7.516
40349	844	7.522
41789	840	7.53
43229	837	7.536
44579	836	7.538
46109	834	7.542
47669	832	7.546
49139	831.5	7.547

Figure B.21. Swelling of 100% Bentonite Sample under 25 kPa effective vertical stress for 10 Blows

Table B.22. 100% Bentonite Sample under 25 kPa Effective Vertical Stress for 25 Blows (dial readings and sample heights)

Time(min.)	Dial Reading	Height(mm)
0.01	4084	3
0.1	4154	2.86
0.25	4156	2.856
0.33	4158	2.852
0.5	4147	2.874
0.75	4135	2.898
1	4120	2.928
2	4106	2.956
3	4094	2.98
4	4081	3.006
5	4067	3.034
6	4053	3.062
7	4040	3.088
8	4027	3.114
12	3980	3.208
15	3950	3.268
20	3906	3.356
30	3832	3.504
60	3660	3.848

Table B.22. 100% Bentonite Sample under 25 kPa Effective Vertical Stress for 25 Blows (dial readings and sample heights) (continued)

| Time(min.)	Dial Reading	Height(mm)
120	3400	4.368
200	3124	4.92
240	2998	5.172
300	2823	5.522
330	2775	5.618
360	2677	5.814
600	2263	6.642
1350	1745	7.678
1440	1715	7.738
1770	1629	7.91
2040	1579	8.01
2790	1493	8.182
3060	1471	8.226
3240	1457	8.254
4320	1403	8.362
7095	1338	8.492
7260	1335	8.498
8535	1312	8.544
8820	1307.5	8.553
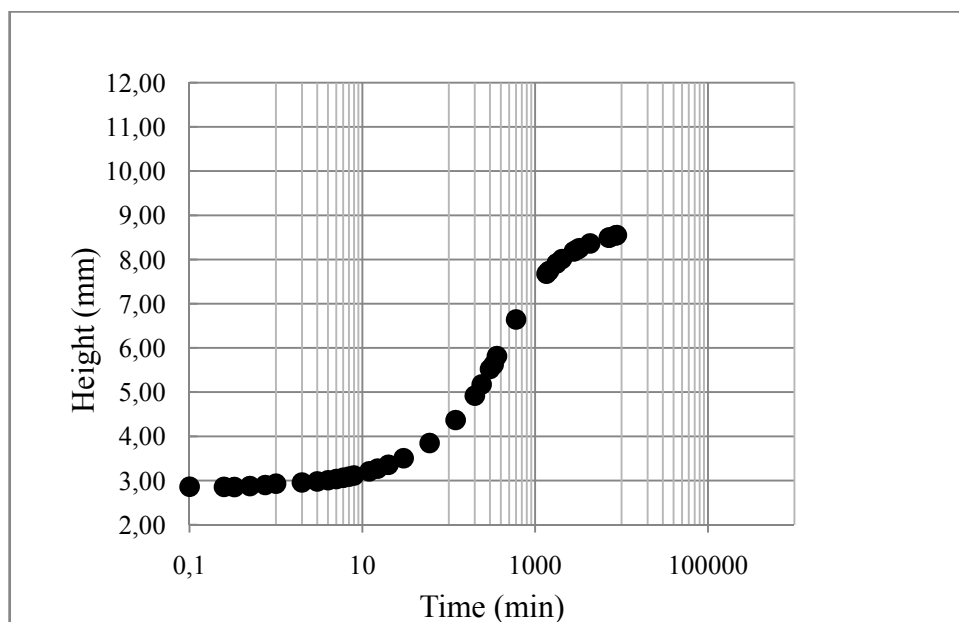
Figure B.22. Swelling of 100% Bentonite Sample under 25 kPa effective vertical stress for 25 Blows

18-) 100% Bentonite Sample under 50 kPa Effective Vertical Stress for 10 and 25 Blows

Table B.23. 100% Bentonite Sample under 50 kPa Effective Vertical Stress for 10 Blows (dial readings and sample heights)

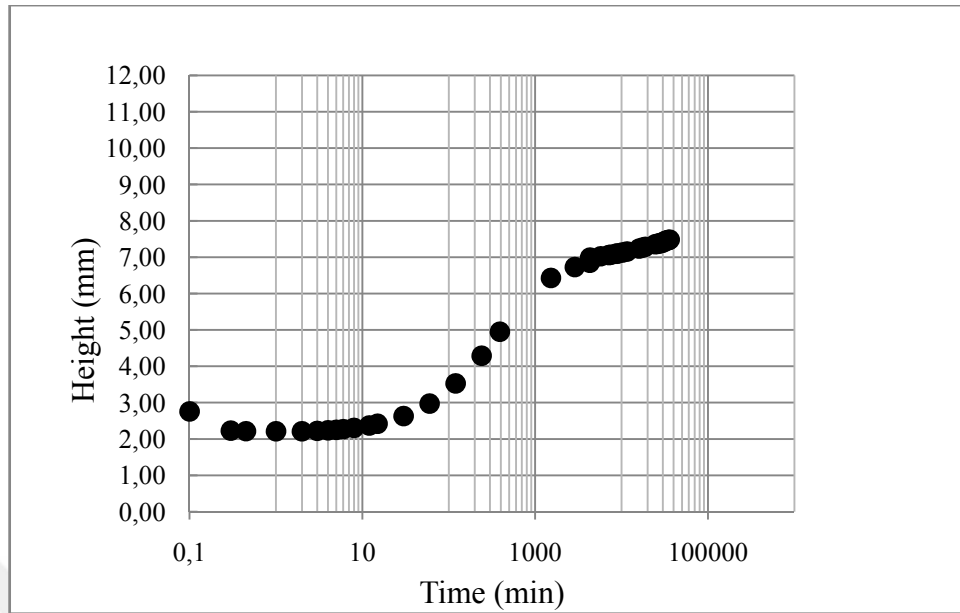| Time(min.)	Dial Reading	Height(mm)
0.01	2400	3.000
0.1	2733	2.334
0.15	2744	2.312
0.3	2751	2.298
1	2752	2.296
2	2743	2.314
3	2735	2.330
4	2726	2.348
5	2717	2.366
6	2708	2.384
7	2700	2.400
8	2692	2.416
9	2684	2.432
11	2672	2.456
12	2666	2.468
15	2648	2.504
25	2592	2.616
30	2566	2.668
45	2504	2.792
60	2444	2.912
150	2154	3.492
380	1809	4.182
1455	1526	4.748
1860	1496	4.808
3090	1470	4.860
4380	1464.5	4.871
8788	1449	4.902
10219	1444	4.912
11520	1439	4.922
17280	1423	4.954
18720	1420	4.960
20160	1417	4.966
21630	1413	4.974
23070	1409	4.982
27435	1401	4.998
28755	1398	5.004

Figure B.23. Swelling of 100% Bentonite Sample under 50 kPa effective vertical stress for 10 Blows

Table B.24. 100% Bentonite Sample under 50 kPa Effective Vertical Stress for 25 Blows (dial readings and sample heights)

Time(min.)	Dial Reading	Height(mm)
0.01	3137	3
0.25	3397	2.48
0.42	3431	2.412
1	3441	2.392
2	3431	2.412
3	3425	2.424
4	3415	2.444
5	3404	2.466
6	3394	2.486
8	3376	2.522
10	3359	2.556
12	3344	2.586
15	3323	2.628
21	3284	2.706
30	3233	2.808
45	3160	2.954
60	3098	3.078
120	2900	3.474
270	2621	4.032
425	2479	4.316

Table B.24. 100% Bentonite Sample under 50 kPa Effective Vertical Stress for 25 Blows (dial readings and sample heights) (continued)

| Time(min.)	Dial Reading	Height(mm)
1425	2264	4.746
1545	2255	4.764
1695	2245	4.784
2880	2193	4.888
3130	2186	4.902
3300	2182	4.91
4290	2166	4.942
5820	2151	4.972
6060	2150	4.974
10390	2118	5.038
12010	2107	5.06
13390	2098	5.078
14770	2088	5.098
16180	2080	5.114
20120	2062	5.15
20600	2060	5.154
21680	2056	5.162

Figure B.24. Swelling of 100% Bentonite Sample under 50 kPa effective vertical stress for 25 Blows

19-) 100% Bentonite Sample under 100 kPa Effective Vertical Stress for 10 and 25 Blows

Table B.25. 100% Bentonite Sample under 100 kPa Effective Vertical Stress for 10 Blows (dial readings and sample heights)

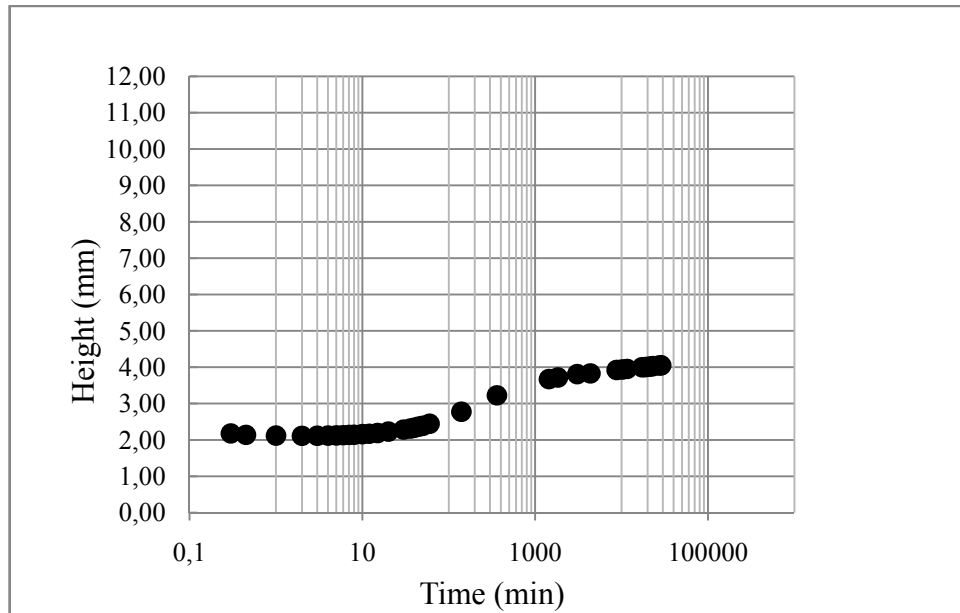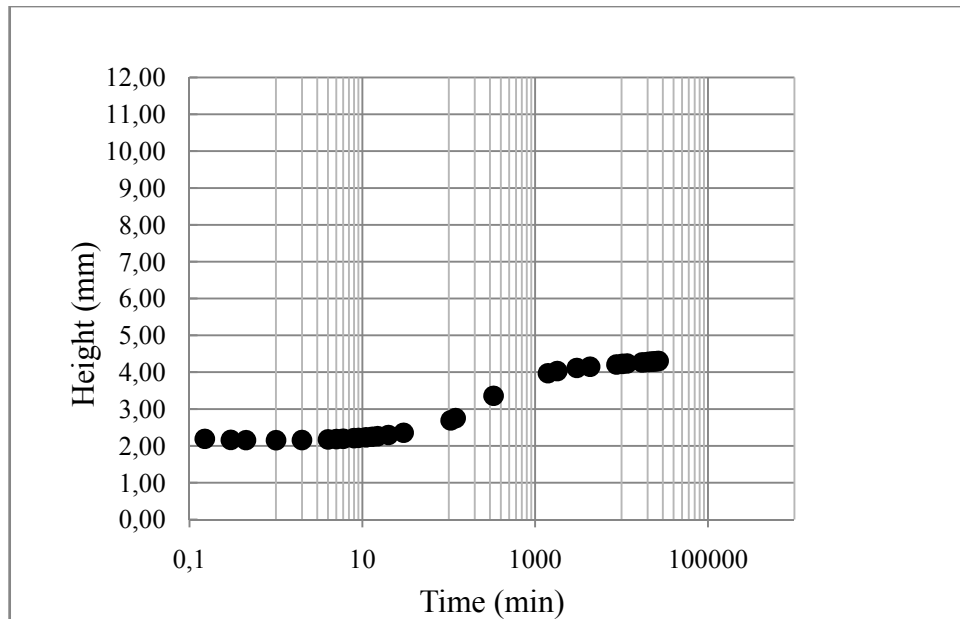| Time(min.)	Dial Reading	Height(mm)
0.01	1070	3.000
0.3	1480	2.180
0.45	1500	2.140
1	1510	2.120
2	1513	2.114
3	1512.5	2.115
4	1510	2.120
5	1508	2.124
6	1504	2.132
7	1500	2.140
8	1498	2.144
10	1490	2.160
12	1484	2.172
15	1474	2.192
20	1455	2.230
30	1427	2.286
36	1412.5	2.315
40	1402	2.336
45	1386	2.368
50	1375	2.390
60	1346	2.448
140	1181	2.778
360	956	3.228
1440	733	3.674
1830	710	3.720
3060	664	3.812
4350	654.5	3.831
8768	607	3.926
10198	600	3.940
11578	593	3.954
17278	570	4.000
18718	567	4.006
20158	564	4.012
21613	560	4.020
23053	555	4.030
27403	546	4.048
28738	543	4.054
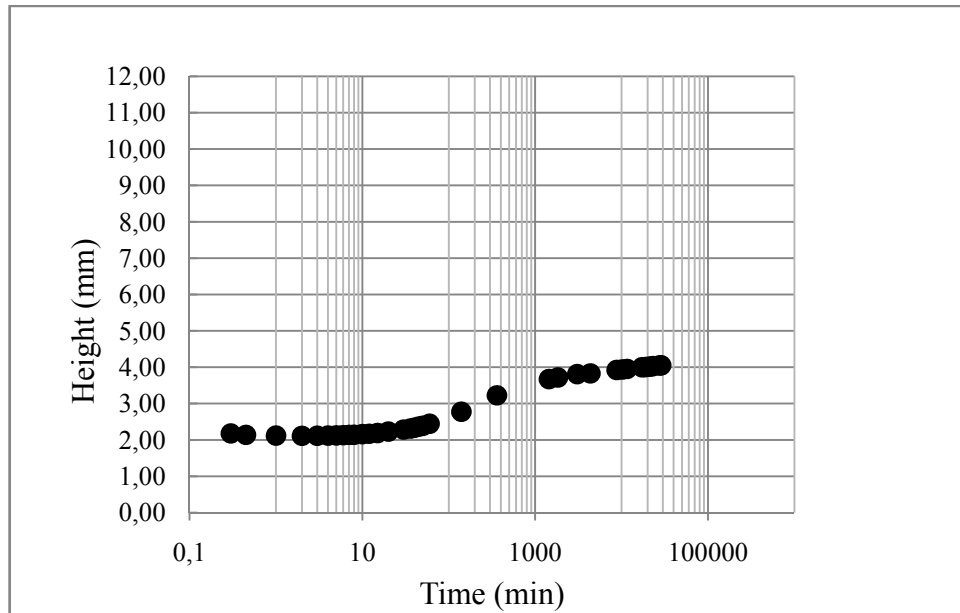
Figure B.25. Swelling of 100% Bentonite Sample under 100 kPa effective vertical stress for 10 Blows

Table B.26. 100% Bentonite Sample under 100 kPa Effective Vertical Stress for 25 Blows (dial readings and sample heights)

Time(min.)	Dial Reading	Height(mm)
0.01	3150	3
0.15	3555	2.19
0.3	3570	2.16
0.45	3573	2.154
1	3573.5	2.153
2	3571.5	2.157
4	3563	2.174
5	3558.5	2.183
6	3554	2.192
8	3546	2.208
9	3542	2.216
11	3534	2.232
13	3527	2.246
15	3519.5	2.261
20	3503	2.294
30	3473	2.354
105	3305	2.69
120	3274	2.752
330	2971	3.358
1405	2665	3.97
1800	2636	4.028

Table B.26. 100% Bentonite Sample under 100 kPa Effective Vertical Stress for 25 Blows (dial readings and sample heights) (continued)

Time(min.)	Dial Reading	Height(mm)
3030	2593	4.114
4320	2577	4.146
8735	2546	4.208
10166	2538	4.224
11546	2532	4.236
17280	2518	4.264
19720	2514	4.272
21160	2510	4.28
22600	2507.5	4.285
24040	2505	4.29
25510	2500	4.3
26830	2499	4.302
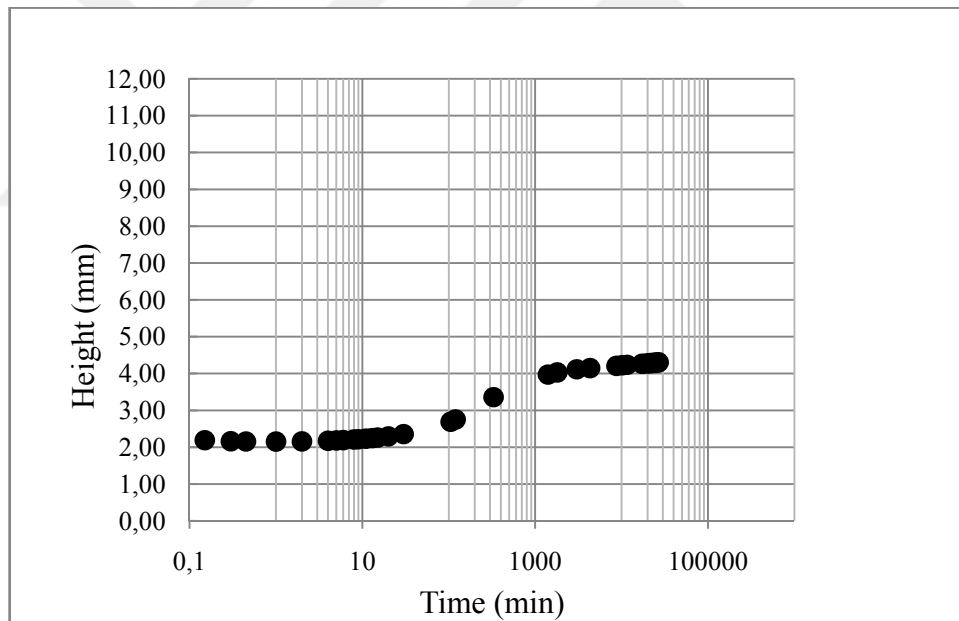
Figure B.26. Swelling of 100% Bentonite Sample under 100 kPa effective vertical stress for 25 Blows

Calculation of the initial and final dry density values and 100% bentonite final void ratios (e_f):

W_1= Wet weight before test, W_2=Dry weight before test, W_3= Wet weight after test

$$w_{INITIAL} = \frac{W_1 - W_2}{W_2} \, (\%) \tag{B-1}$$

$$w_{FINAL} = \frac{W_3 - W_2}{W_2} \, (\%) \tag{B-2}$$

$$V_{INITIAL} = A * H_0 \tag{B-3}$$

$$V_{FINAL} = A * H_F \tag{B-4}$$

A= Area of ring, H_0=height of sample before test, H_F=height of sample after test.

$$\gamma_{INITIAL} = \frac{W_1}{V_{INITIAL}} \tag{B-5}$$

$$\gamma_{DRY,INITIAL} = \frac{\gamma_{INITIAL}}{1 + w_{INITIAL}} \tag{B-6}$$

$$\gamma_{FINAL} = \frac{W_3}{V_{FINAL}} \tag{B-7}$$

$$\gamma_{DRY,FINAL} = \frac{\gamma_{FINAL}}{1 + w_{FINAL}} \tag{B-8}$$

$$\gamma_{DRY,FINAL} = \frac{G_{BENTONITE}}{1 + e_{FINAL}} \gamma_w \tag{B-9}$$

Calculation of the void ratio of smectite (e_m) of ZBMs:

The void ratio of smectite of the zeolite-bentonite mixtures can be calculated by using the following formulas. Water content, w, which is one of the basic factors, can be calculated as follows:

$$w = \frac{W_{WET} - W_{DRY}}{W_{DRY}} (\%) \tag{B-10}$$

Where; W_{WET} is the measured value after the test and W_{DRY} is the value measured after drying.

In order to calculate specific gravity of the mixture $Gs_{(mixture)}$; the percentages of zeolite and bentonite are multiplied by specific gravities as follows:

$$G_{S(MIXTURE)} = (20 - 30)\% G_{S(BENTONITE)} + (80 - 70)\% G_{S(ZEOLITE)} \tag{B-11}$$

H_0 is the initial height of the sample, whereas H_f is the final height measured after the test. Meanwhile H_s is the height of the solid part. H_s is obtained by using the following formula.

$$H_S = \frac{W_{DRY}}{A\gamma_w} (mm) \tag{B-12}$$

Final void ratio calculation

$$e_f = \frac{H_F - H_S}{H_S} \qquad \text{(B-13)}$$

For calculating the void ratio of smectite; smectite ratios included in zeolite and bentonite will be taken into account as follows:

$$e_m = \frac{e_f G_{S(BENTONITE)}}{(G_{S(MIXTURE)}(20 - 30\%)\,0.77 + G_{S(MIXTURE)}(80 - 70\%)\,0.01)} \qquad \text{(B-14)}$$

A formula has been developed in accordance with the ratios of zeolite and bentonite in the mixtures and smectite percentages. Smectite percentages are as follows: 77% in bentonite, 1% in zeolite.

APPENDIX C

TEST DATA
(20%-30% ZBMs and 100% BENTONITE SAMPLES)

Table C.1. Test data of ZBM samples

RING	ZBMs (%)	σ'_v (kPa)	RING WEIGHT (g)	WEIGHT OF RING+WET SAMPLE BEFORE TEST (g)	WET SAMPLE WEIGHT AFTER TEST W_{WET} (g)	DRY WEIGHT W_{DRY} (g)	WET SAMPLE WEIGHT BEFORE TEST W_{WET} (g)	WATER CONTENT BEFORE TEST (%)	WATER CONTENT AFTER TEST (%)	INITIAL DENSITY γ_i (g/cm³)	INITIAL DRY DENSITY $\gamma_{d,i}$ (g/cm³)	FINAL DENSITY γ_f (g/cm³)	FINAL DRY DENSITY $\gamma_{d,f}$ (g/cm³)	e_f	e_m
RING-1	20%	1	69.28	178.45	123.62	78.5	109.17	0.3907	0.5748	1.3188	0.9483	1.4585	0.9261	1.2611	9.1182
RING-2	20%	2.5	68.9	178.5	121.6	77.8	109.6	0.4087	0.5630	1.3240	0.9398	1.4544	0.9305	1.2506	9.0423
RING-3	20%	5	69.45	178.62	117.5	77.54	109.17	0.4079	0.5153	1.3188	0.9367	1.4194	0.9367	1.2358	8.9352
RING-4	20%	12.5	69.74	180	118	79	110.26	0.3957	0.4937	1.3320	0.9543	1.4327	0.9592	1.1829	8.5529
RING-2B	20%	25	79.42	189.27	117	72	109.85	0.5257	0.6250	1.3270	0.8698	1.4844	0.9135	1.2117	8.7612
RING-4B	20%	50	70	185	142	71	115	0.6197	1.0000	1.3707	0.8462	1.7332	0.8666	1.1987	8.6666
RING-5	30%	1	68.94	187	135	86	118.06	0.3728	0.5698	1.4262	1.0389	1.4992	0.9550	1.2254	5.9068
RING-6	30%	2.5	68.99	187	134.25	86	118.01	0.3722	0.5610	1.4256	1.0389	1.5212	0.9745	1.1813	5.6940
RING-7	30%	5	70.3	188.03	131.6	86	117.73	0.3690	0.5302	1.4222	1.0389	1.5175	0.9917	1.1425	5.5072
RING-8	30%	12.5	70.03	188.1	130.6	86.5	118.07	0.3650	0.5098	1.4263	1.0449	1.5533	1.0288	1.0779	5.1958
RING-1C	30%	25	69.78	179.14	194.99	80.56	109.36	0.3575	1.4204	1.3211	0.9732	2.3791	0.9829	1.1621	5.6018
RING-2C	30%	50	70.27	181.64	194.78	82.6	111.37	0.3483	1.3581	1.3454	0.9978	2.3786	1.0087	1.1063	5.3325

Table C.2. Test data of 100% bentonite samples

RING	NUMBER OF BLOWS	VERTICAL STRESS (kPa)	WEIGHT OF THE RING (g)	RING + WET SAMPLE BEFORE TEST (g)	RING + WET SAMPLE AFTER TEST (g)	Wwet AFTER TEST (g)	AFTER OVEN (g)	Wwet BEFORE TEST (g)	WATER CONTENT BEFORE TEST (%)	WATER CONTENT AFTER TEST (%)	INITIAL DENSITY γi (g/cm³)	INITIAL DRY DENSITY γd,i (g/cm³)	FINAL DENSITY γf (g/cm³)	FINAL DRY DENSITY γd,f (g/cm³)	ef
RİNG-1	25	2.5	69.93	84.54	125.99	56.06	12.2	14.61	19.75	359.51	1.27	1.06	1.28	0.28	8.56
RİNG-2	10	2.5	70.37	83.87	115.81	45.44	11.44	13.5	18.01	297.20	1.17	0.99	1,24	0.31	7.50
RİNG-3A	25	5	68.93	81.8	114.3	45.37	11	12.87	17.00	312.45	1.12	0.95	1.28	0.31	7.56
RİNG-3B	25	12.5	70.14	89.75	124.45	54.31	16.32	19.61	20.16	232.78	1.70	1.41	1.55	0.47	4.70
RİNG-4	25	1	70.05	86.77	140.65	70.6	13.94	16.72	19.94	406.46	1.45	1.21	1.29	0.26	9.42
RİNG-5	25	25	69.44	90.66	122.22	52.78	17.6	21.22	20.57	199.89	1.84	1.53	1.61	0.54	3.94
RİNG-6	25	50	70.27	85.5	104.05	33.78	12.8	15.23	18.98	163.91	1.32	1.11	1.72	0.65	3.08
RİNG-7	25	5	70.21	85.8	119.8	49.59	12.64	15.59	23.34	292.33	1.35	1.10	1.40	0.36	6.45
RİNG-8	10	5	69.72	86.2	121.04	51.32	13.18	16.48	25.04	289.38	1.43	1.14	1.38	0.35	6.53
RİNG-9	10	12.5	69.19	83.33	112.37	43.18	11.51	14.14	22.85	275.15	1.23	1.00	1.42	0.38	6.00
RİNG-11	10	1	69.11	85.45	137.4	68.29	13.15	16.34	24.26	419.32	1.42	1.14	1.32	0.25	9.50
RİNG-12	10	25	70.07	88.9	117.66	47.59	15.02	18.83	2537	216.84	1.63	1.30	1.65	0.52	4.11
RİNG-13	10	50	70.09	86.13	106.05	35.96	13.07	16.04	22.72	175.13	1.39	1.13	1.87	0.68	2.91
RİNG-14	10	100	70.17	87.61	104.21	34.04	14.07	17.44	23.95	141.93	1.51	1.22	2.21	0.91	1.91
RİNG-15	25	100	69.04	87.26	104.5	35.46	14.73	18.22	23.69	140.73	1.58	1.28	2.14	0.89	1.99